BRNO UNIVERSITY OF TECHNOLOGY
VYSOKÉ UČENÍ TECHNICKÉ V BRNĚ

FACULTY OF ELECTRICAL ENGINEERING AND COMMUNICATION
FAKULTA ELEKTROTECHNIKY A KOMUNIKAČNÍCH TECHNOLOGIÍ

DEPARTMENT OF ELECTRICAL POWER ENGINEERING
ÚSTAV ELEKTROENERGETIKY

DISTANCE PROTECTION FOR PARALLEL AND DOUBLE-CIRCUIT HV LINES

CHRÁNĚNÍ PARALELNÍCH A SOUBĚŽNÝCH VEDENÍ VVN DISTANČNÍ OCHRANOU

MASTER'S THESIS
DIPLOMOVÁ PRÁCE

AUTHOR — Bc. Obed Muhayimana
AUTOR PRÁCE

SUPERVISOR — doc. Ing. Jaroslava Orságová, Ph.D.
VEDOUCÍ PRÁCE

BRNO 2016

BRNO UNIVERSITY
OF TECHNOLOGY

Faculty of Electrical Engineering and
Communication

Department of Electrical Power Engineering

Diploma thesis

Master's study field
Power Electrical Engineering

Student: Bc. Obed Muhayimana *ID:* 171476
Year of study: 2 ***Academic year:*** 2015/16

TITLE OF THESIS:

Distance Protection for Parallel and Double-Circuit HV Lines

INSTRUCTION:

1. Problems of accurate fault location at parallel and double-circuit HV lines.
2. Current state of methods for accuracy improvement of fault locators.
3. The setting possibilities of digital distance protection for accurate fault location.
4. Range of fault location inaccuracies in case study of given HV line protected by digital distance protection.

REFERENCE:

according to instructions of the head of thesis

Assigment deadline: 8. 2. 2016 ***Submission deadline:*** 20. 5. 2016

Head of thesis: doc. Ing. Jaroslava Orságová, Ph.D.
Consultant:

doc. Ing. Petr Toman, Ph.D.
Subject Council chairman

WARNING:

Thesis Referencing:

MUHAYIMANA, O. Distance Protection for Parallel and Double-circuit HV Lines. Master's Thesis. Brno: Brno University of Technology, Faculty of Electrical Engineering and Communication, Department of Electrical Power Engineering, 2016, 75 pages.

Supervisor: doc. Ing. Jaroslava Orságová, Ph.D.

Jako autor uvedené diplomové práce dále prohlašuji, že v souvislosti s vytvořením této diplomové (bakalářské) práce jsem neporušil autorská práva třetích osob, zejména jsem nezasáhl nedovoleným způsobem do cizích autorských práv osobnostních a jsem si plně vědom následků porušení ustanovení § 11 a následujících autorského zákona č. 121/2000 Sb., včetně možných trestněprávních důsledků vyplývajících z ustanovení části druhé, hlavy VI. Díl 4 Trestního zákoníku č. 40/2009 Sb.

……

ABSTRACT

The protection of parallel and double-circuit lines is actually challenging due to the effect of mutual coupling impedance, fault resistance and the current reversal phenomenon which distort the single-phase fault impedance ‘’seen’’ by the distance protection. However, numerical distance protections currently used provide compensation functions which can be used for the characteristic correction and computation of distance-to-fault location, because of their locator characteristics with enough resistive reserve and the possibility of setting an adequate tripping mode.

This work explores the problems faced by the distance protection locator while measuring and calculating the location distance of a single-phase fault, and the current state of solutions adopted in solving those problems. Owing to the parameter calculations for the given transmission line, possible errors when localizing single-phase faults were evaluated, and a setting design was proposed for the effective line protection, including settings of parameters which compensate the above mentioned negative phenomena.

It was found that the earth-wire and the line transposition, improve the accuracy of the locators, because the least error was found in the transposed line with earth wire.

KEY WORDS: Protection of HV lines, parallel lines, double-circuit lines, distance protection, fault locator, line transposition, line parameters

ABSTRAKT

Chránění paralelních a souběžných vedení je skutečně problematické z důvodů účinku vzájemné indukčnosti vedení v souběhu, odporu poruchy nebo rozložení zpětného proudu poruchy, které zkreslují impedanci jednofázové poruchy „viděné“ distanční ochranou. Proto současné numerické distanční ochrany nabízí kompenzační funkce, které je možno použít pro korekci charakteristik a výpočtu vzdálenosti poruchy pomocí lokátorů její charakteristice s dostatečnou odporovou rezervou a možnosti nastavení odpovídajícího režimu vypnutí.

Tato práce se zabývá problémy, kterým čelí lokátor distanční ochrany při měření a výpočtu vzdálenosti místa jednofázové poruchy, a také mapuje současný stav řešení těchto problémů. Na základě výpočtu parametrů zadaného vedení bylo provedeno zhodnocení možných chyb při lokalizaci jednofázové poruchy a navrženo nastavení distanční ochrany určené k jeho chránění včetně nastavení parametrů určených pro kompenzaci výše uvedených negativních jevů.

Bylo zjištěno, že zemnící lana a transpozice vedení přispívají k přesnosti lokátorů, protože nejmenší chyba byla zjištěna v transponovaném vedení se zemním lanem.

KLÍČOVÁ SLOVA: chránění vedení vvn, paralelní vedení, souběžné vedení, distanční ochrana, lokátor poruch, transpozice vodičů, parametry vedení

CONTENTS

LIST OF FIGURES

LIST OF TABLES

LIST OF SYMBOLS AND ABBREVIATIONS

Symbol	Signification
MI	Measuring Input
IA	Input Amplifier
AD	Analogue-to- Digital converter
µC	Micro Computer
OA	Output Amplifier
I/O	Inputs/Outputs modules
LED	Light Emitting Diodes
LCD	Liquid Crystal Display
PC	Personal Computer
CT/CTs	Current Transformer/s
VT/VTs	Voltage Transformer/s
DP, D, D1, D_A	Distance Protection (in location 1 or A)
DDP	Digital Distance Protection
CB	Circuit Breaker
AR	Auto Reclosure
HV	High Voltage
$\bar{I}_i$	current in i^{th} phase conductor (A)
$\bar{E}_i$	electromotive force of the source at i^{th} location (A)
$\bar{S}_i$	apparent power of the source at i^{th} location (MVA)
$\bar{Z}_{\mathbf{F}}$	fault impedance (Ω)
$\bar{U}_{SC}$	short-circuit voltage (V)
$\bar{I}_{SC}$	short-circuit current (A)
$\bar{Z}_{\mathbf{sec}}, \bar{Z}_{\mathbf{prim}}$	secondary and primary transformer impedances(Ω)
$\bar{Z}_{\mathbf{abc}}$	impedance matrix
$\bar{Z}_{\mathbf{M}}$	modified impedance matrix
$\bar{Z}_{\mathbf{120}}$	impedance matrix in symmetrical components
$\bar{U}_{\mathbf{sec}}, \bar{U}_{\mathbf{prim}}$	secondary and primary transformer voltages (V)

$\bar{I}_{\text{sec}}, \bar{I}_{\text{prim}}$	secondary and primary transformer currents (A)
$R_{\mathbf{L}}, X_{\mathbf{L}}$	resistance and reactance of the short-circuited section of the line (Ω)
R_{F}	fault resistance or arc resistance (Ω)
l_{arc}	arc length (m)
$u(t)$	instantaneous voltage (V)
$i(t)$	instantaneous value of the current (A)
L_{L}	line inductance (H)
$\frac{di}{dt}$	variation of current with respect to time (A/s)
$l_{\mathbf{F}}$	distance to fault location (m)
$X_{\mathbf{F}}$	fault reactance (Ω)
X'	line reactance per unit length (Ω/km)
$\bar{U}_{\mathbf{A}}$	voltage measured at point A (V)
$\bar{Z}_{L}$	line impedance (Ω),
$\bar{Z}_{\mathbf{i}}$	impedance measured by the DP at i^{th} location (Ω).
$\bar{Z}_{\mathbf{D}}$	impedance measured by DP (Ω),
R_k	resistance per unit length of k^{th} conductor (Ω/km)
R_{1g}	earth resistance per unit length (Ω/km)
ξ	correcting factor (-)
r_k	radius of the k^{th} conductor (m)
d_{km}, d, $d+$, $d+'$	distance, or mean distance between the line conductors (m)
D_g	depth of fictive conductor (m)
ρ	specific resistance of earth in (Ω.m)
f	system frequency (Hz)
$\bar{Z}_{\mathbf{OM}}$	mutual coupling impedance in the zero-sequence system (Ω/m)
$\bar{Z}_{\mathbf{M}}$	mutual coupling impedance (Ω/km)
ω	angular frequency (S^{-1}),
δ	penetration depth (m),
$R_{\mathbf{E}'}$	resistance of ground (Ω/km).
$A_{\mathbf{L}}$	geometrical mean distance

$\overline{U}_1, \overline{U}_2, \overline{U}_0$	voltage in the positive-, negative- and zero-sequence system (V)
$\overline{I}_1, \overline{I}_2, \overline{I}_0$	current in the positive-, negative- and zero-sequence system (A)
$\overline{U}_{1F}, \overline{U}_{2F}, \overline{U}_{0F}$	fault voltage in the positive-, negative- and zero-sequence system (V)
$\overline{Z}_{1L}, \overline{Z}_{0L}$	line impedance in the positive- and zero-sequence system (Ω/km)
$\overline{Z}_{Lit}$	total impedance in the ith phase conductor (Ω)
$\overline{I}_{0p}$	current passing through the self-inductance of a double line (A)
$\overline{Z}_E, \overline{Z}_{EL}$	earth impedance (Ω/km)
$\overline{I}_{ph}$	phase current (A)
$\overline{K}_E, \overline{K}_{EM}$	residual and mutual compensation factor (-)
$\overline{I}_E$	earth current (A) for line 1 and line 2,
$\overline{I}_{Ep}$	earth current flowing through the self-inductance (A)
l	length of the protected line segment (m)
x	distance to fault location (m)
R_1, R_0	line positive- and zero-sequence resistance (Ω/km)
X_1, X_0	line positive- and zero-sequence reactance (Ω/km)
$\Delta\overline{U}_i$	voltage drop across the i^{th} phase (V)
R_M, X_M	mutual resistance and mutual reactance (Ω/km)
R_{0M}, X_{0M}	zero sequence mutual resistance (Ω/km)
$\overline{U}_{in}$	input phase values for line voltage (V)
$\overline{I}_{in}$	input phase values for line current (A)
$\overline{U}_{out}$	output phase values for line voltage (V)
$\overline{I}_{out}$	output phase values for line current (A)
$\overline{H}$	matrix describing the system
$\overline{Y}$	line admittance (S)

1 INTRODUCTION

Due to its sensitivity, rapidity, selectivity and the considerable economic and technical advantages it provides, distance protection forms the basis for network protection in transmission as well as interconnected distribution networks.

The distance protection is used not only as the main protection for the overhead lines and cables but also as backup protections for the other parts of the network, such as bus bars, transformers and further feeders. Its functioning principle is based on the measurement and the evaluation of short-circuited loop impedance due to the measured voltage and current by voltage and current transformers (VTs and CTs) and it is thus sometimes called Impedance Protection.

Numerical Distance Protection which is the object of this work is faster, more accurate and more selective than Over-current Protection. Its tripping time, according to [1], is approximately one to two cycles (20 to 40ms at 50Hz) in the first zone for faults within the first 80% to 90% of the line length. In the second zone for faults on the last 10% to 20% of the protected feeder, the tripping time is approximately 300 to 400ms. The way different zones overlap, and the fact that they are set with different tripping time enable them to ensure proper main protection and remote backup protection. It is less susceptible to changes in the relative source impedances and system conditions. This device can at the same time act as a protecting device fulfilling additional functions including operational measurements and disturbance recording. They are therefore multifunction and intelligent; they can store information and communicate with peripherals. In addition, numerical distance protection has the integrated fault location function and allows the operation with PC as well as the integration into the network control systems, via serial interfaces.

The present study will deal with the distance protection for parallel and double-circuit HV transmission lines, the configuration which is extensively used in modern power systems to enhance the reliability and the security of electrical energy transmission. However, parallel and double circuit lines are subject to the effect of mutual coupling, fault resistance as well as current reversal faults, which make their protection really challenging because the parameters in these types of lines are no longer homogeneous. This results in inaccurate fault location of protection locators and increase in measuring error range. Therefore, the main purpose of this work is to analyse the problems of accurate fault location in parallel and double-circuit HV lines, the identification of the current state of methods improving accuracy of fault locators, to determine the measuring error range in a given HV parallel and double-circuit transmission line as well as to design settings of the distance protection for effective and reliable protection of the line.

2 OVERVIEW OF DISTANCE PROTECTION

Different researchers state that the distance protection has been used in transmission line protection for decades from the beginning of the twentieth century. It has developed continuously from induction coil measuring elements to moving coil technology, then to analogue static relay with operational amplifiers up to the modern devices we have today, the numerical/digital relay, which are intelligent, able to store information and communicate with other peripherals. In Fig. 2.1 is shown an example of numerical distance relay.

Fig. 2.1 SIPROTEC 4 7SA522 numerical distance protection relays [6]

2.1 Basic Principles of Distance Protection

The functioning principle of the distance protection is based on impedance measuring. For this reason, it is also known as impedance protection. Using the value of the voltage provided by potential transformer, referred to as short-circuit voltage U_{sc} and the current value from the current transformer here considered as short-circuit current I_{sc}, distance relay computes the impedance according to Ohm's law as shown by equation. (2.1)

$$\overline{Z}_F = \frac{\overline{U}_{sc}}{\overline{I}_{sc}} \qquad (2.1)$$

The measured impedance is referred to as fault impedance $\overline{Z}_F$ and is then compared with the pre-set protected line impedance. If this impedance $\overline{Z}_F$ is smaller than the pre-set line impedance, it means that for a short-circuit that occurred at any point which is not at the end of the protected line, the current $\overline{I}_{sc}$ used while computing impedance was not flowing through the entire protected line but only through the short-circuited portion of it. So, an internal fault has occurred and therefore a trip command is issued to the circuit breaker. The Fig. 2.2 illustrates the fault impedance determination.

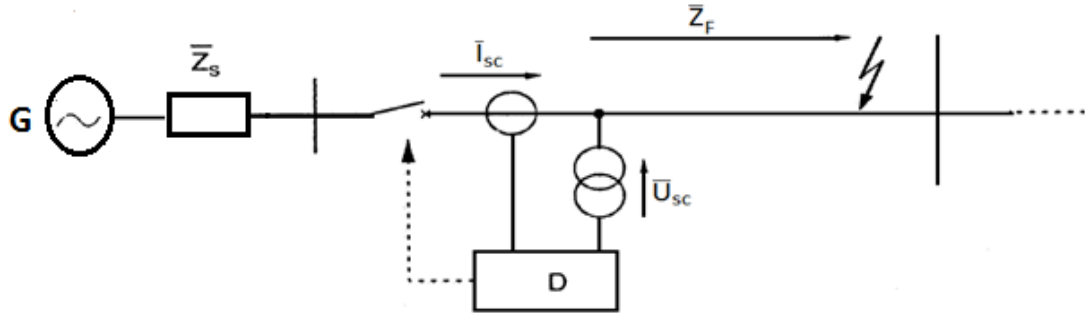

Fig. 2.2 Distance protection principle

When implementing the grading plan, primary impedances are used. But relay settings are always done using the secondary impedance because secondary signals are used. However, the distance protection relays are fed with the signals of voltages and currents from the lines through current transformers and voltage transformers. The relay therefore measures the secondary impedance which results from the transformation ratios of the CT and VT. It is given by the equation (2.2).

$$\bar{Z}_{\text{sec}} = \frac{\bar{I}_{\text{prim}} / \bar{I}_{\text{sec}}}{\bar{U}_{\text{prim}} / \bar{U}_{\text{sec}}} . \bar{Z}_{\text{prim}} \qquad (2.2)$$

2.2 Protection zones

The main purpose of the use of zones in the transmission line protection by distance protection, and the way these zones are made, is to ensure the proper selectivity of the distance protection in order to avoid unnecessary tripping on a non-faulted section (i.e. the actual impedance is smaller than the set impedance and the detected fault is actually located on an adjacent power line or elsewhere in the system), or tripping failures in case of faults, when real impedance is greater than the set one.

In order to ensure proper line protection of the entire line with high selectivity we cannot set the protection reach in the distance protection at 100% of the line impedance, because there are always possible errors in impedance computation due to either the inaccuracy of devices (DP, PTs, CTs) and the used algorithm, or impedance changes with temperature, spacing between wires, seasons or wind. Therefore the impedance relays are set to operate with setting between 80-90% mainly 85% of the protected line impedance, and this is known as zone 1 protection. The fault that may occur within the remaining 15% is cleared after a time delay in order to allow the adjacent line relay to trip first if fault was mistakenly detected and was in adjacent line, as shown in Figure 2.3. It is also clear that zones are set to over-reach into the other transmission lines and overlap to provide entire protection for the protected line and backup protection for adjacent lines.

Since DP is directional, another relay is set to the other end of the line protecting in opposite direction and all of them overlap to provide a pretty good protection scheme.

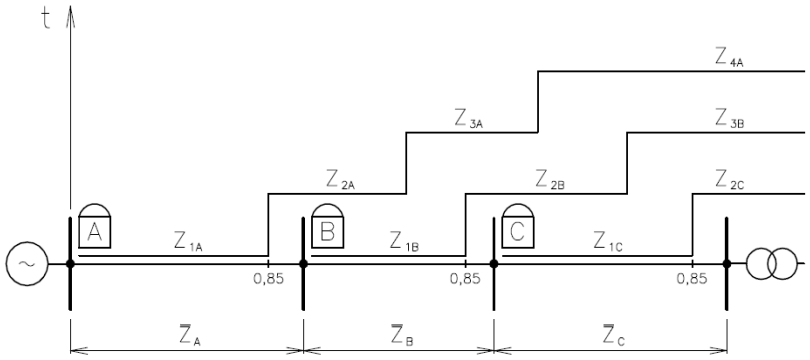

Fig. 2.3 Graded distance zones for distance protection [2]

2.3 Distance Relay Characteristic

2.3.1 Relay Characteristic and Impedance diagram

The distance relay characteristic is represented on the $R-X$ plane (resistance-reactance plane) (see Fig. 2.4) where the coordinate (0,0), i.e. $R=0$ and $X=0$ indicates the relay location. The measured line impedances or fault impedances in case of fault are found on the line OP. Those impedances are found in the proximity of (0,0) coordinate for faults which occur closer to the protecting relay and far from this coordinate for remote faults. Recall that in normal operating state either at load or at no load, the measured impedance corresponds to the entire line impedance which is always higher in both cases (at load and at no load) than the short-circuit impedance. When the short-circuit occurs this measured line impedance decreases rapidly and the measured values are referred to as the fault impedance or the short-circuit impedance that corresponds to the impedance between the distance relay location and the fault location, and it is given by the equation (2.3)

$$\overline{Z}_{\mathrm{F}} = R_{\mathrm{L}} + jX_{\mathrm{L}} \tag{2.3}$$

In case the arc resistance or the fault resistance is present to the fault location, an additional resistive component R_F will be considered and the equation (2.4) expresses the corresponding fault impedance.

$$\overline{Z}_{\mathrm{F}} = R_{\mathrm{L}} + R_{\mathrm{F}} + jX_{\mathrm{L}} \tag{2.4}$$

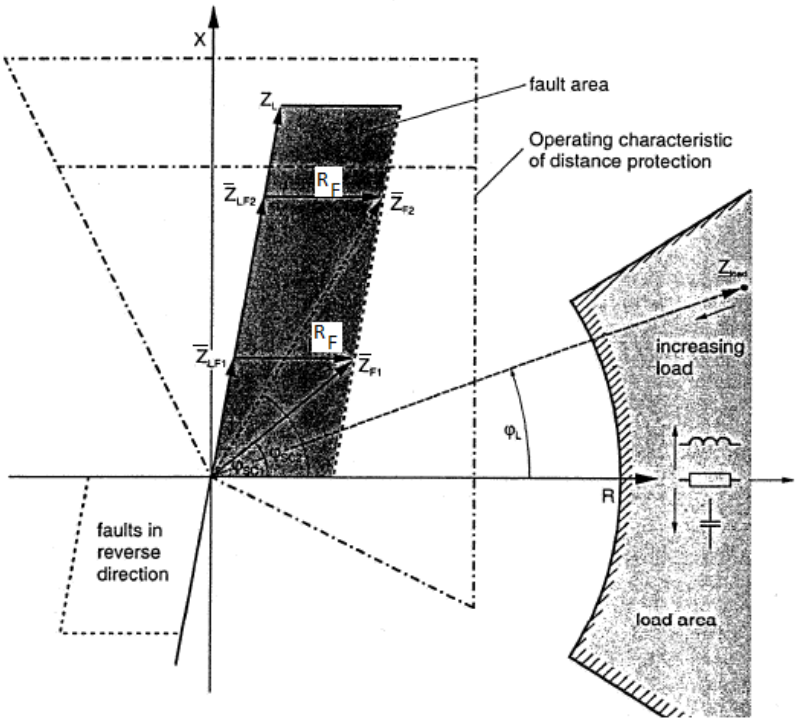

Fig. 2.4 Impedance diagram and distance protection characteristic [1]

Different ways are used to express the arc resistance or the fault resistance and they take into consideration different factors which have a given influence on it. According to [2] the Warrington equation for fault resistance considers the influence of the arc length and the intensity of the short-circuit current as seen in equation (2.5).

$$R_{\mathbf{F}} \approx \frac{28707 l_{\mathbf{arc}}}{\bar{I}_{\mathbf{sc}}^{1,4}} \tag{2.5}$$

2.3.2 Quadrilateral Characteristic

This characteristic is provided by modern distance relays, and their resistive and reactive reach can be adjusted independently. Its resistive coverage is better than for any mho-type characteristic for short lines. The impedance characteristic of most digital and numerical distance protections with this characteristic can be set with respect to the impedance of the load or the arc, in all of the zones (see Fig. 2.5). The quadrilateral characteristic is the most appropriate for the earth fault impedance measurement, where the arc resistances and fault resistance to earth increase the values of fault resistance. Polygonal impedance characteristics are highly flexible in terms of fault impedance coverage for both phase and earth faults. For this reason, today most digital relays offer this form of characteristic.

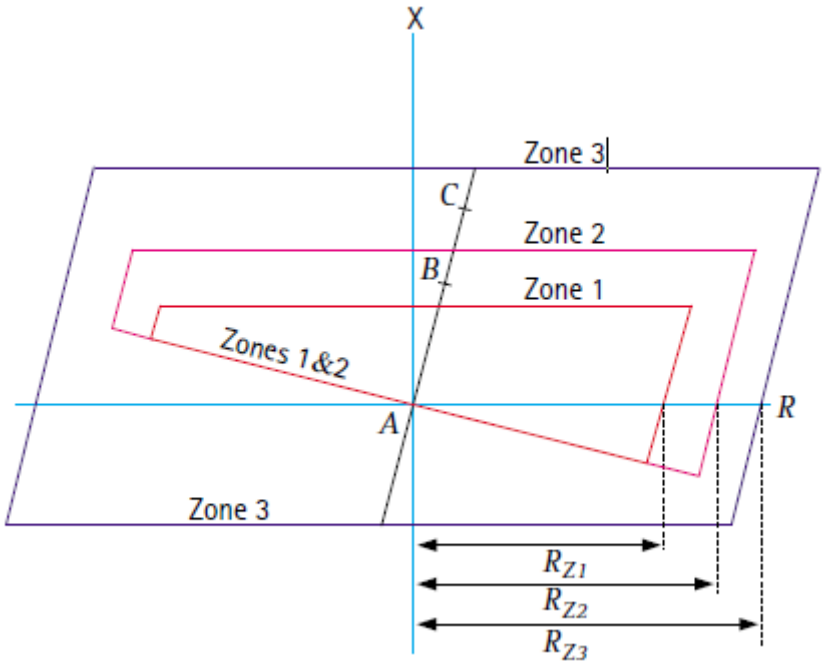

Fig. 2.5 Quadrilateral characteristic [5]

2.4 Distance to fault location

Any transmission line of electrical energy is characterized by its resistance and reactance per unit length, in other words its total impedance is proportional to its length distance.

When a fault occurs, the distance to fault location is computed by the fault locators which are integrated in the distance relays. These fault locators execute the measurement when the current passes by zero. This property helps them to eliminate not only the influence of the fault resistance but also the one of the line resistance. This is because in this very moment the instantaneous voltage does not depend on line and fault resistances but only on the line inductance as shown by the equations (2.6) and (2.7).

$$u(t) = (R_{\mathrm{L}} + R_{\mathrm{F}}).i(t) + L_{\mathrm{L}} \frac{di}{dt} \tag{2.6}$$

For $i(t) = 0$ then we have $u(t) = L_{\mathrm{L}} \frac{di}{dt}$ (2.7)

The measured distance is therefore proportional to the fault reactance (or line reactance) only as shown in the equation

$$l_{\mathrm{F}} = \frac{X_{\mathrm{F}}}{X'}, \tag{2.8}$$

where the fault reactance is given by the equation

$$X_{\mathrm{F}} = \frac{U_{\mathrm{sc}}}{I_{\mathrm{sc}}}.\sin\varphi_{\mathrm{sc}}. \tag{2.9}$$

The information about the distance to fault will be useful for efficient and faster fault locating process and a rapid restoration of normal conditions. However the locator needs longer time corresponding to the operating time of the protecting device plus the one of the circuit-breaker.

Thus, the fault locating accuracy may be improved by digital filtering and the compensation of the fault transient.

2.5 Factors Influencing the Fault Location accuracy

There are a number of factors that negatively influence the impedance measurement, thereby influencing the accuracy of the distance to fault locators for distance relay. They are fault resistance, intermediate in-feeds, parallel and double circuit line configurations, non-symmetry of the line, etc. In this paragraph we will briefly discuss each of the above mentioned factors except the effect of parallel and double circuit lines which will be the object of Chapter 3.

2.5.1 Fault resistance

When a phase-to-phase or phase-to-earth fault occurs in the line, accompanied with the production of the arc, there will be generated in the line a new impedance R_F with a resistive character which is in series with the line impedance. R_F is known as fault resistance or arc resistance.

In case the system is supplied from one end (single-ended in-feed), the distance protection located on the source side will correctly measure the fault distance because, according to the equation (2.4), the fault resistance R_F affects only the real part of impedance while the reactance on which depends the distance measurement, remains the same as discussed previously.

In case the line is supplied from both ends (double-ended in-feed) and the fault with arc occurs between the two sources (see Fig. 2.6), then there will be voltage drop caused by the short-circuit current from the other side in-feed through the fault resistance which has the same effect as an additional source and increases the measured fault resistance by $\frac{\bar{I}_B}{\bar{I}_A}.R_F$ according to the equations (2.10), (2.11), (2.12) and (2.13)

$$\bar{U}_A = \bar{I}_A.\bar{Z}_L + \left(\bar{I}_A + \bar{I}_B\right).R_F, \tag{2.10}$$

$$\bar{U}_A = \bar{I}_A.\left(\bar{Z}_L + \bar{R}_F\right) + \bar{I}_B.R_F, \tag{2.11}$$

$$\bar{Z}_A = \frac{\bar{U}_A}{I_A} = \bar{Z}_L + R_F + \frac{\bar{I}_B}{\bar{I}_A}.R_F, \tag{2.12}$$

$$\bar{Z}_A = \bar{Z}_L + R_F.\left(1 + \frac{\bar{I}_B}{\bar{I}_A}\right). \tag{2.13}$$

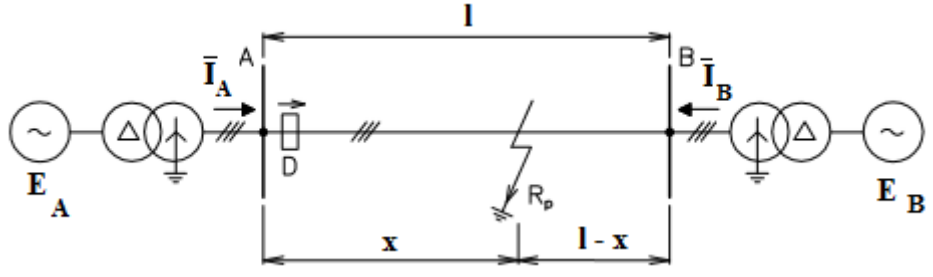

Fig. 2.6 System with double-sided in-feed and fault resistance [2]

This increase is on the fault resistance, i.e. on the real part of the impedance (on the axis R direction) and don't imply changes to the line reactance on which depends the fault distance measurement. Theoretically, the distance to fault location is correctly measured especially when E_A and E_B are in phase. However in practice according to [1] in case the system is supplied from both ends, the fault resistance influence on the measured distance to fault location exists particularly for long lines with strong power supply at the remote end. This influence increases as the fault location approaches the opposite line end.

In case there is a phase shift ϑ_L between E_A and E_B, it means that a real power is transmitted along the line with a transmission angle ϑ_L. Consequently the short-circuit currents from both sides are phase shifted by this angle because the ratio $\frac{\bar{I}_B}{\bar{I}_A}$ has also an imaginary part thus it not only increases the fault resistance value, but it also rotates it by the above mentioned angle as shown on Fig. 2.7. Therefore, distance protection situated on sending end, measures small reactance and tends to over-reach while the one located to the other end measure too high reactance with under-reaching tendency.

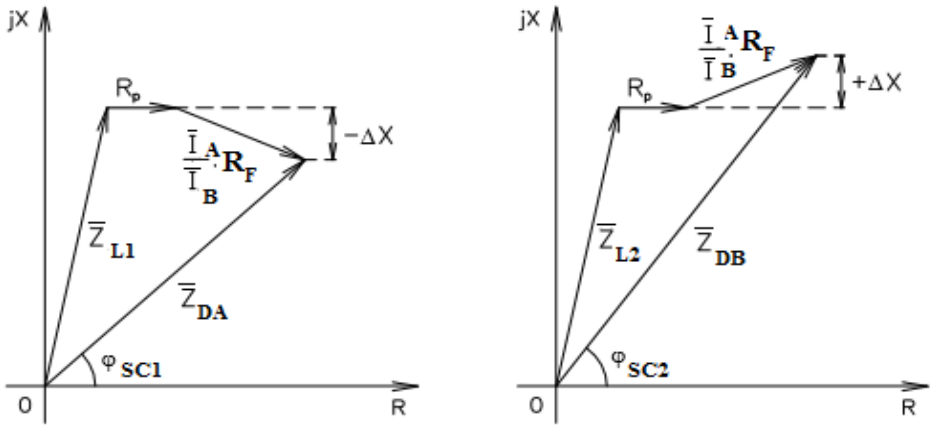

Fig. 2.7 Influence of fault resistance on distance measurement [2]

2.5.2 Intermediate Power Supply

We have seen in the previous section that an additional power supply to the other end of the line have an influence on the line impedance calculation, the influence exists even in the case of an intermediate in-feed as shown in Fig. 2.8.

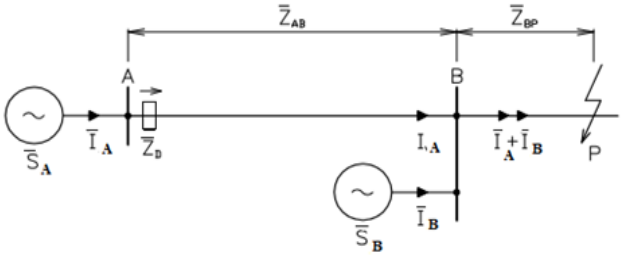

Fig. 2.8 Effect of intermediate in-feed on distance measurement

In case the power supply on B is not connected, and a fault with arc production occurs at the point P, the relay locator will calculate correctly the distance to fault location P according to the equation (2.14)

$$\overline{Z}_{\mathbf{D}} = \overline{Z}_{\mathbf{L}} + R_{\mathbf{F}}, \tag{2.14}$$

When the power supply at the point B in Fig. 2.8 is connected, the two currents I_A and I_B from respective sources sum up towards the fault location point P. The impedance Z_D measured by the distance protection is expressed by equation (2.15).

$$\overline{Z}_{\mathbf{A}} = \overline{Z}_{\mathbf{L}} + R_{\mathbf{F}}.\left(1+\frac{\overline{I}_{\mathbf{B}}}{\overline{I}_{\mathbf{A}}}\right) = \overline{Z}_{\mathbf{L}} + R_{\mathbf{F}}.\left(1+\frac{\overline{S}_{\mathbf{B}}}{\overline{S}_{\mathbf{A}}}\right), \tag{2.15}$$

In this case the protection sees the wrong impedance (distance to fault location) which has been increased of $R_{\mathbf{F}}.\left(1+\frac{\overline{I}_{\mathbf{B}}}{\overline{I}_{\mathbf{A}}}\right)$. Thus let's consider three possible extreme cases:

a. The generated power S_B by the generator connected at the point B is too low compared to the power S_A for the generator at point A In this case the ration $\frac{\overline{I}_{\mathbf{B}}}{\overline{I}_{\mathbf{A}}}$ tends to zero and the distance protection measures a correct distance to fault location.
b. (S_B=S_A), in this case there is an equilibrium of the powers for the two sources and their ratio is 1. The fault is considered by the protective relay to be at a doubled distance from the point B.
c. (S_A<<S_B) in this case the ration $\frac{\overline{I}_{\mathbf{B}}}{\overline{I}_{\mathbf{A}}}$ tends to infinity. This means that the fault location will be considered to be to the infinity and it is not possible to set the distance relay in a selective way.

2.5.2.1 Grounded transformers

In the zero sequence system grounded transformers can be considered as power supplies and represents a given influence on the accuracy of the distance to fault location measuring. This is due to the fact that in the zero-sequence system of the short-circuited loop, the transformer earth-currents produce additional voltage drops which lead to the increased measured fault impedance as illustrated in Fig. 2.9.

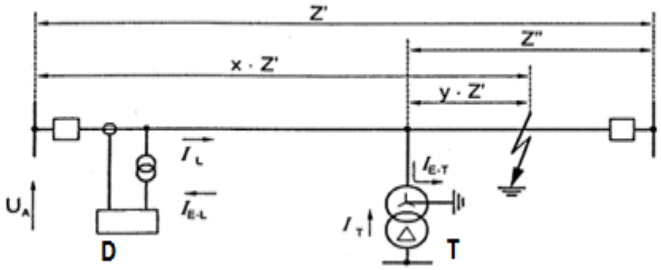

Fig. 2.9 Grounded transformer influence on distance measurement [1]

2.5.2.2 T-outgoing feeder

An outgoing feeder may be considered as a negative in-feed and thus, its influence will be opposite to the one of intermediate power supply and in this case the measured impedance will be decreased

and this will result in an over-reach. This is due to the presence of the parallel T-path with a short-circuit loop whose lengths are different as shown in Fig. 2.10.

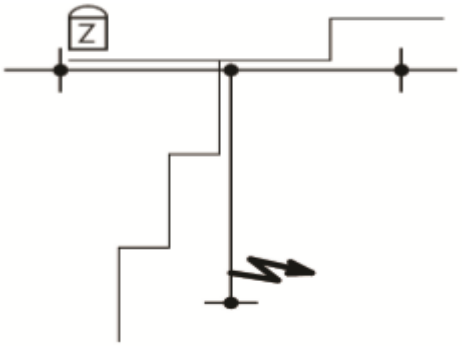

Fig. 2. 10 T-feeder influence on impedance measurement [2]

2.5.3 Non-symmetry of the line

Distance protections and fault locators are designed to work with the parameters of symmetric systems. It is then clear that the non-symmetric distribution of impedance in the line will affect the measurement results of distance protection and fault locators.

The non-symmetry of the line is mainly determined by:

- conductors configuration (suspension arrangement),
- distance between phase conductors,
- distance between phase conductors and the ground wire,
- conductor connections to the towers,
- presence or absence of the ground wire,
- conductivity of the used ground wires,
- soil characteristic for the zero-sequence impedances.

Normally a line longer than approximately 40km must be transposed in order to avoid negative sequence and earth currents.

3 ACCURACY PROBLEM ON FAULT LOCATION IN PARALLEL AND DOUBLE-CIRCUIT HV LINES.

Different researchers have worked on parallel and double circuit lines protection. However we noticed that the concept of parallel lines and double circuit lines were used differently by different authors whose publications were consulted. Some of them do not make any difference between parallel lines and double circuit lines [2], [12]. Others consider parallel lines as two or more lines operating in relatively close proximity but with different paths or right-of-way (single-circuit lines run in parallel), while double-circuit lines are considered as power lines which are mounted on the same tower along their entire length or just part of their length. In both cases (parallel and double-circuit lines), lines may be connected to the same substation at both ends of the line, to one end or to none of the ends [1], [5], [8], [10], [11]. This last approach in which the only difference between parallel lines and double circuit is based on the fact that they are either mount on the same tower/right-of-way or not, is the one we adopted in our work. In Fig. 3.1 parallel line is shown on a) and double circuit line on b).

Fig. 3.1 Parallel and double circuit lines

3.1 Possible configurations

Figure 3.2 illustrates the possible configurations for parallel and double circuit lines. The configuration on (a) is the most commonly used. The two lines are connected on the same buses at both ends. It is typical in double-circuit towers. Figure (b) shows a partial parallel trajectory for a distance d. The lines are connected on the same bus only at one end. Figures (c) and (d) illustrate independent lines running in parallel for a distance d.

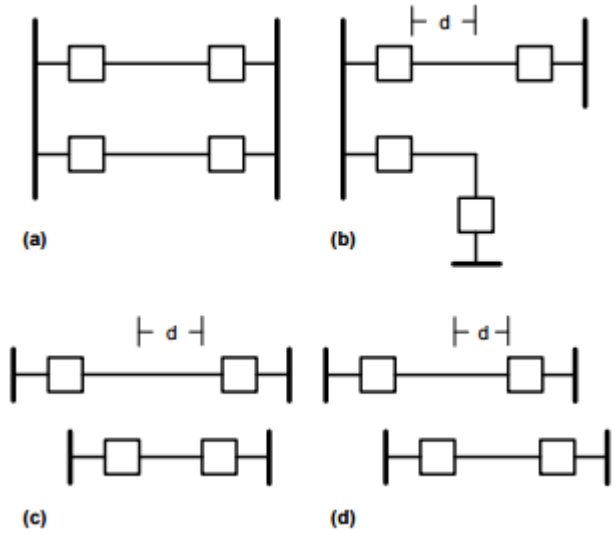

Fig. 3.2 Possible configurations of parallel lines [12]

3.2 Impedance matrix for parallel and double circuit transmission lines

We consider the double-circuit transmission line represented in Fig. 3.3 where two overhead lines are on the same tower with indices a, b and c corresponding respectively to the phase L1, L2 and L3 for the first line and indices A, B and C for the second line.

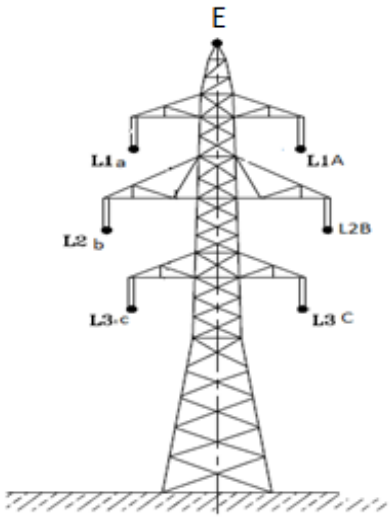

Fig. 3.3 Double-circuit line tower [2]

The impedance matrix will be obtained from the equation of the voltage drops in every phase conductor as well as in the earth wire as given by the equation (3.1)

$$\begin{bmatrix} \Delta\overline{U}_{\mathbf{a}} \\ \Delta\overline{U}_{\mathbf{b}} \\ \Delta\overline{U}_{\mathbf{c}} \\ \Delta\overline{U}_{\mathbf{A}} \\ \Delta\overline{U}_{\mathbf{B}} \\ \Delta\overline{U}_{\mathbf{C}} \\ \Delta\overline{U}_{\mathbf{E}} \end{bmatrix} = \begin{bmatrix} \overline{Z}_{\mathbf{aa}} & \overline{Z}_{\mathbf{ab}} & \overline{Z}_{\mathbf{ac}} & \overline{Z}_{\mathbf{aA}} & \overline{Z}_{\mathbf{aB}} & \overline{Z}_{\mathbf{aC}} & \overline{Z}_{\mathbf{aE}} \\ \overline{Z}_{\mathbf{ba}} & \overline{Z}_{\mathbf{bb}} & \overline{Z}_{\mathbf{bc}} & \overline{Z}_{\mathbf{bA}} & \overline{Z}_{\mathbf{bB}} & \overline{Z}_{\mathbf{bC}} & \overline{Z}_{\mathbf{bE}} \\ \overline{Z}_{\mathbf{ca}} & \overline{Z}_{\mathbf{cb}} & \overline{Z}_{\mathbf{cc}} & \overline{Z}_{\mathbf{cA}} & \overline{Z}_{\mathbf{cB}} & \overline{Z}_{\mathbf{cC}} & \overline{Z}_{\mathbf{cE}} \\ \overline{Z}_{\mathbf{Aa}} & \overline{Z}_{\mathbf{Ab}} & \overline{Z}_{\mathbf{Ac}} & \overline{Z}_{\mathbf{AA}} & \overline{Z}_{\mathbf{AB}} & \overline{Z}_{\mathbf{AC}} & \overline{Z}_{\mathbf{AE}} \\ \overline{Z}_{\mathbf{Ba}} & \overline{Z}_{\mathbf{Bb}} & \overline{Z}_{\mathbf{Bc}} & \overline{Z}_{\mathbf{BA}} & \overline{Z}_{\mathbf{BB}} & \overline{Z}_{\mathbf{BC}} & \overline{Z}_{\mathbf{BE}} \\ \overline{Z}_{\mathbf{Ca}} & \overline{Z}_{\mathbf{Cb}} & \overline{Z}_{\mathbf{Cc}} & \overline{Z}_{\mathbf{CA}} & \overline{Z}_{\mathbf{CB}} & \overline{Z}_{\mathbf{CC}} & \overline{Z}_{\mathbf{CE}} \\ \overline{Z}_{\mathbf{Ea}} & \overline{Z}_{\mathbf{Eb}} & \overline{Z}_{\mathbf{Ec}} & \overline{Z}_{\mathbf{EA}} & \overline{Z}_{\mathbf{EB}} & \overline{Z}_{\mathbf{EC}} & \overline{Z}_{\mathbf{EE}} \end{bmatrix} \cdot \begin{bmatrix} \overline{I}_{\mathbf{a}} \\ \overline{I}_{\mathbf{b}} \\ \overline{I}_{\mathbf{c}} \\ \overline{I}_{\mathbf{A}} \\ \overline{I}_{\mathbf{B}} \\ \overline{I}_{\mathbf{C}} \\ \overline{I}_{\mathbf{E}} \end{bmatrix} \tag{3.1}$$

$$\Rightarrow \begin{bmatrix} [\Delta U_{\mathbf{v}}] \\ [\Delta U_{\mathbf{V}}] \\ [\Delta U_{\mathbf{E}}] \end{bmatrix} = \begin{bmatrix} [\overline{Z}_{\mathbf{vv}}] & [\overline{Z}_{\mathbf{vV}}] & [\overline{Z}_{\mathbf{vE}}] \\ [\overline{Z}_{\mathbf{Vv}}] & [\overline{Z}_{\mathbf{VV}}] & [\overline{Z}_{\mathbf{VE}}] \\ [\overline{Z}_{\mathbf{Ev}}] & [\overline{Z}_{\mathbf{EV}}] & [\overline{Z}_{\mathbf{EE}}] \end{bmatrix} \tag{3.2}$$

$$\Rightarrow [\Delta\overline{U}] = [\overline{Z}][\overline{I}] \tag{3.3}$$

where $[\Delta\overline{U}]$ stands for voltage drops across individual phase conductors and the earth-wire, $[\overline{Z}]$ stands for impedance matrix and $[\overline{I}]$ for the current flowing in different phase conductors and earth-wire.

Diagonal elements of the impedance matrix represent the self-impedance of individual line whereas the elements out of the diagonal represent the mutual impedance between different phase conductors and the one between phase conductors and the earth-wire.

The values of different elements of the above matrix will be determined according to the following equations:

$$\overline{Z}_{kk} = R_{kk} + j\omega L_{kk} = R_k + R_{\mathbf{1g}} + j0{,}1445\log\frac{D_{\mathbf{g}}}{\xi.r_k} \tag{3.4}$$

$$\overline{Z}_{km} = R_{km} + j\omega L_{km} = \overline{Z}_{mk} = R_{\mathbf{1g}} + j0{,}1445\log\frac{D_{\mathbf{g}}}{d_{km}} \tag{3.5}$$

$$R_{1g} = \pi^2.f.10^{-7}\ (\Omega/\text{m}),\ \text{thus}\ R_{1g} = \pi^2.f.10^{-4} \tag{3.6}$$

for $f = 50$ Hz, $R_{1g} = 0{,}0495\,\Omega$/km.

D_g is the depth of fictive conductor which is given by the equation (3.7) and illustrated in Fig. 3.4

$$D_{\mathbf{g}} = \frac{0{,}178.\sqrt{\rho.10^7}}{\sqrt{f}} \tag{3.7}$$

For the case of system frequency of 50Hz and specific earth resistance of 100Ω.m which is consider as typical earth resistance, D_g =796,04m.

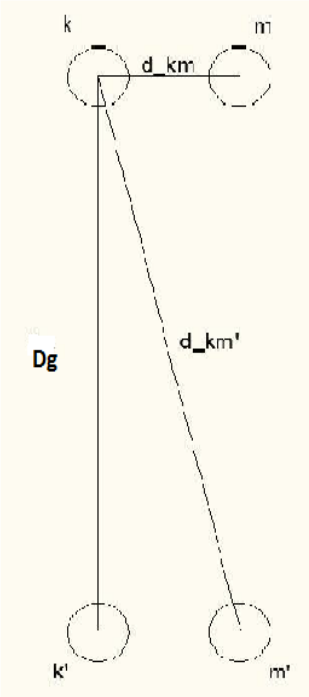

Fig. 3.4 Depth of fictive conductor [22]

The correction factor ξ depends on the factor α which considers differences in current distribution on the cross-sectional area of the conductor, as well as on the permeability of the conductor material μ_{rc} for ferromagnetic material as given in Table 3.1.

Table 3.1 *Correction factor* ξ [22]

Type of Conductor			ξ
Massive conductor with a circular section			0,779
Wire from single material	Number of conductor elements	Number of layers	
	7		0,726
	19		0,758
	37		0,768
	61		0,772
	91		0,774
	127		0,776
Wire AlFe	26	2	0,809
	30	2	0,826
	54	3	0,810
Wire with one layer of Al conductor			0,55-0,7
Cuboid conductor with sides a,b			0,223 (a+b)

The conductor radius r_k and resistance R_k are determined depending on the type of conductor and its nominal cross-sectional area according to Table 3.2

Table 3.2 *Parameters for AlFe 6 conductor* [13]

Conductor AlFe 6			
Nominal cross-sectional area of the cable (mm^2)	Conductor diameter (mm)	Mass per 1km (kg)	Highest resistance per 1km (Ω)
16	5,40	62,5	1,882
25	6,75	97,6	1,205
35	8,10	140,5	0,837
50	9,60	197,3	0,596
70	11,55	277,1	0,434
95	13,35	370,9	0,319
120	15,65	509,2	0,234
150	17,25	619,4	0,193
185	19,20	765,5	0,156
210	20,43	868,7	0,137
240	21,70	979,2	0,122
300	24,20	1217,2	0,097

3.2.1 Modified impedance matrix

In this case we consider an impedance matrix for a transmission line without the earth-wire, or simply for simplification we consider that the earth-wire is grounded not only on the towers but also along the entire length of the transmission line. Thus

$$\Delta\overline{U}_{\mathbf{E}} = 0 \Rightarrow \left[\Delta\overline{U}_{\mathbf{E}}\right] = [0] \tag{3.7}$$

Considering the equation (3.3) and the above assumption in equation (3.7), we can introduce it as system of three equations:

$$\left[\Delta\overline{U}_{\mathbf{v}}\right] = \left[\overline{Z}_{\mathbf{vv}}\right].\left[\overline{I}_{\mathbf{v}}\right] + \left[\overline{Z}_{\mathbf{vV}}\right].\left[\overline{I}_{\mathbf{V}}\right] + \left[\overline{Z}_{\mathbf{vE}}\right].\left[\overline{I}_{\mathbf{E}}\right] \tag{3.8}$$

$$\left[\Delta\overline{U}_{\mathbf{V}}\right] = \left[\overline{Z}_{\mathbf{Vv}}\right].\left[\overline{I}_{\mathbf{v}}\right] + \left[\overline{Z}_{\mathbf{VV}}\right].\left[\overline{I}_{\mathbf{V}}\right] + \left[\overline{Z}_{\mathbf{VE}}\right].\left[\overline{I}_{\mathbf{E}}\right] \tag{3.9}$$

$$\left[\Delta\overline{U}_{\mathbf{E}}\right] = \left[\overline{Z}_{\mathbf{Ev}}\right].\left[\overline{I}_{\mathbf{v}}\right] + \left[\overline{Z}_{\mathbf{EV}}\right].\left[\overline{I}_{\mathbf{V}}\right] + \left[\overline{Z}_{\mathbf{EE}}\right].\left[\overline{I}_{\mathbf{E}}\right] = 0 \tag{3.10}$$

From equation (3.10) we can determine the current flowing the earth conductor as follows:

$$\left[\overline{I}_{\mathbf{E}}\right] = -\left[\overline{Z}_{\mathbf{EE}}\right]^{-1}.\left(\left[\overline{Z}_{\mathbf{Ev}}\right].\left[\overline{I}_{\mathbf{v}}\right] + \left[\overline{Z}_{\mathbf{EV}}\right].\left[\overline{I}_{\mathbf{V}}\right]\right) \tag{3.11}$$

Replacing equation (3.11) in (3.8) and (3.9), we get the line modification expressed as follows:

$$\left[\Delta\overline{U}_{\mathbf{v}}\right] = \left(\left[\overline{Z}_{\mathbf{vv}}\right] - \left[\overline{Z}_{\mathbf{vE}}\right].\left[\overline{Z}_{\mathbf{EE}}\right]^{-1}.\left[\overline{Z}_{\mathbf{Ev}}\right]\right).\left[\overline{I}_{\mathbf{v}}\right] + \left(\left[\overline{Z}_{\mathbf{vV}}\right] - \left[\overline{Z}_{\mathbf{vE}}\right].\left[\overline{Z}_{\mathbf{EE}}\right]^{-1}.\left[\overline{Z}_{\mathbf{EV}}\right]\right).\left[\overline{I}_{\mathbf{V}}\right] \tag{3.12}$$

$$\left[\Delta\overline{U}_{\mathbf{V}}\right] = \left(\left[\overline{Z}_{\mathbf{Vv}}\right] - \left[\overline{Z}_{\mathbf{VE}}\right].\left[\overline{Z}_{\mathbf{EE}}\right]^{-1}.\left[\overline{Z}_{\mathbf{Ev}}\right]\right).\left[\overline{I}_{\mathbf{v}}\right] + \left(\left[\overline{Z}_{\mathbf{VV}}\right] - \left[\overline{Z}_{\mathbf{VE}}\right].\left[\overline{Z}_{\mathbf{EE}}\right]^{-1}.\left[\overline{Z}_{\mathbf{EV}}\right]\right).\left[\overline{I}_{\mathbf{V}}\right] \tag{3.13}$$

and thus:

$$\begin{aligned}
\left[\overline{Z}_{\mathbf{vv}}\right] &= \left[\overline{Z}_{\mathbf{vv}}\right] - \left[\overline{Z}_{\mathbf{vE}}\right].\left[\overline{Z}_{\mathbf{EE}}\right]^{-1}.\left[\overline{Z}_{\mathbf{Ev}}\right] \\
\left[\overline{Z}_{\mathbf{vv}}\right] &= \left[\overline{Z}_{\mathbf{vV}}\right] - \left[\overline{Z}_{\mathbf{vE}}\right].\left[\overline{Z}_{\mathbf{EE}}\right]^{-1}.\left[\overline{Z}_{\mathbf{Ev}}\right] \\
\left[\overline{Z}_{\mathbf{vv}}\right] &= \left[\overline{Z}_{\mathbf{Vv}}\right] - \left[\overline{Z}_{\mathbf{VE}}\right].\left[\overline{Z}_{\mathbf{EE}}\right]^{-1}.\left[\overline{\mathbf{Z}}_{\mathbf{Ev}}\right] \\
\left[\overline{Z}_{\mathbf{vv}}\right] &= \left[\overline{Z}_{\mathbf{VV}}\right] - \left[\overline{Z}_{\mathbf{VE}}\right].\left[\overline{Z}_{\mathbf{EE}}\right]^{-1}.\left[\overline{Z}_{\mathbf{Ev}}\right]
\end{aligned} \qquad (3.14)$$

The modified impedance matrix $\left[\overline{Z}_{\mathbf{M}}\right]$ will therefore be given by equation (3.15)

$$\left[\overline{Z}_{\mathbf{M}}\right] = \begin{bmatrix} \left[\overline{Z}_{\mathbf{vvM}}\right] & \left[\overline{Z}_{\mathbf{vVM}}\right] \\ \left[\overline{Z}_{\mathbf{VvM}}\right] & \left[\overline{Z}_{\mathbf{VVM}}\right] \end{bmatrix} = \begin{bmatrix} \overline{Z}_{\mathbf{aaM}} & \overline{Z}_{\mathbf{abM}} & \overline{Z}_{\mathbf{acM}} & \overline{Z}_{\mathbf{aAM}} & \overline{Z}_{\mathbf{aBM}} & \overline{Z}_{\mathbf{aCM}} \\ \overline{Z}_{\mathbf{baM}} & \overline{Z}_{\mathbf{bbM}} & \overline{Z}_{\mathbf{bcM}} & \overline{Z}_{\mathbf{bAM}} & \overline{Z}_{\mathbf{bBM}} & \overline{Z}_{\mathbf{bCM}} \\ \overline{Z}_{\mathbf{caM}} & \overline{Z}_{\mathbf{cbM}} & \overline{Z}_{\mathbf{ccM}} & \overline{Z}_{\mathbf{cAM}} & \overline{Z}_{\mathbf{cBM}} & \overline{Z}_{\mathbf{cCM}} \\ \overline{Z}_{\mathbf{AaM}} & \overline{Z}_{\mathbf{AbM}} & \overline{Z}_{\mathbf{AcM}} & \overline{Z}_{\mathbf{AAM}} & \overline{Z}_{\mathbf{ABM}} & \overline{Z}_{\mathbf{ACM}} \\ \overline{Z}_{\mathbf{BaM}} & \overline{Z}_{\mathbf{BbM}} & \overline{Z}_{\mathbf{BcM}} & \overline{Z}_{\mathbf{BAM}} & \overline{Z}_{\mathbf{BBM}} & \overline{Z}_{\mathbf{BCM}} \\ \overline{Z}_{\mathbf{CaM}} & \overline{Z}_{\mathbf{CbM}} & \overline{Z}_{\mathbf{CcM}} & \overline{Z}_{\mathbf{CAM}} & \overline{Z}_{\mathbf{CBM}} & \overline{Z}_{\mathbf{CCM}} \end{bmatrix} \qquad (3.15)$$

3.3 Fault Location Problem in Parallel and Double-circuit HV Lines

3.3.1 Mutual coupling impedance between lines

Two or more overhead lines running in close proximity to each other, cannot be considered as working independently of each other because the current flowing through one line induces voltage drop in the other line and consequently a mutual inductance and capacitance are generated between them. For transposed and more symmetric lines, the effect of mutual coupling impedance in the positive and negative sequence system is too small and may be neglected. However, this is not the case for the zero sequence system when a single phase to ground faults or faults with ground involved occur, because zero-sequence currents will be flowing in the line and the mutual coupling impedance will be high.

The operating impedance for each phase of anyone of the two lines at one kilometre length is given by the equations (3.16), (3.17) and (3.18)

$$\overline{Z}_{\mathbf{a}} = \frac{\overline{Z}_{\mathbf{aa}} I_{\mathbf{a}} + \overline{Z}_{\mathbf{ab}} I_{\mathbf{b}} + \overline{Z}_{\mathbf{ac}} I_{\mathbf{c}}}{I_{\mathbf{a}}} = \frac{\left(\overline{Z}_{\mathbf{aa}} + \overline{a}^{2}\overline{Z}_{\mathbf{ab}} + \overline{a}\overline{Z}_{\mathbf{ac}}\right) I_{\mathbf{a}}}{\overline{I}_{\mathbf{a}}} = \overline{Z}_{\mathbf{aa}} + \overline{a}^{2}\overline{Z}_{\mathbf{ab}} + \overline{a}\overline{Z}_{\mathbf{ac}}, \qquad (3.16)$$

$$\overline{Z}_{\mathbf{b}} = \frac{\overline{Z}_{\mathbf{ba}} I_{\mathbf{a}} + \overline{Z}_{\mathbf{bb}} I_{\mathbf{b}} + \overline{Z}_{\mathbf{bc}} I_{\mathbf{c}}}{I_{\mathbf{b}}} = \frac{\left(\overline{Z}_{\mathbf{ba}} + \overline{a}^{2}\overline{Z}_{\mathbf{bb}} + \overline{a}\overline{Z}_{\mathbf{bc}}\right) I_{\mathbf{a}}}{\overline{a}^{2}\overline{I}_{\mathbf{a}}} = \frac{\overline{Z}_{\mathbf{ba}} + \overline{a}^{2}\overline{Z}_{\mathbf{bb}} + \overline{a}\overline{Z}_{\mathbf{bc}}}{\overline{a}^{2}}, \qquad (3.17)$$

$$\overline{Z}_{\mathbf{c}} = \frac{\overline{Z}_{\mathbf{ca}} I_{\mathbf{a}} + \overline{Z}_{\mathbf{cb}} I_{\mathbf{b}} + \overline{Z}_{\mathbf{cc}} I_{\mathbf{c}}}{I_{\mathbf{c}}} = \frac{\left(\overline{Z}_{\mathbf{ca}} + \overline{a}^{2}\overline{Z}_{\mathbf{cb}} + \overline{a}\overline{Z}_{\mathbf{cc}}\right) I_{\mathbf{a}}}{\overline{a}\overline{I}_{\mathbf{a}}} = \frac{\overline{Z}_{\mathbf{ca}} + \overline{a}^{2}\overline{Z}_{\mathbf{cb}} + \overline{a}\overline{Z}_{\mathbf{cc}}}{\overline{a}}, \qquad (3.18)$$

considering $\overline{I}_{\mathrm{a}} = \overline{I}_{\mathrm{a}}; \overline{I}_{\mathrm{b}} = \overline{a}^{2}\overline{I}_{\mathrm{a}}; \overline{I}_{c} = \overline{a}\overline{I}_{\mathrm{a}}$,

where $\overline{a}^{2} = -\frac{1}{2} - j\frac{\sqrt{3}}{2}$ and $\overline{a} = -\frac{1}{2} + j\frac{\sqrt{3}}{2}$.

3.3.1.1 Symmetrical Component and Mutual coupling impedances

Impedance symmetrical components are very important in line protection analysis because it is the positive- and the zero-sequences that characterize a transmission line. In previous paragraphs we have seen that:

$$\left[\Delta\overline{U}_{\mathbf{abc}}\right]=\left[\overline{Z}_{\mathbf{abc}}\right]\left[\overline{I}_{\mathbf{abc}}\right] \tag{3.19}$$

We can convert the phase voltages and currents in equation (3.19) by appropriate symmetrical components voltages and currents by means of the symmetrical component matrix to obtain the equation (3.20)

$$\begin{bmatrix}\begin{bmatrix}1 & 1 & 1\\ 1 & \overline{a}^{2} & \overline{a}\\ 1 & \overline{a} & \overline{a}^{2}\end{bmatrix} & 0\\ 0 & \begin{bmatrix}1 & 1 & 1\\ 1 & \overline{a}^{2} & \overline{a}\\ 1 & \overline{a} & \overline{a}^{2}\end{bmatrix}\end{bmatrix}.\left[\Delta\overline{U}_{012}\right]=\left[\overline{Z}_{\mathbf{abc}}\right].\begin{bmatrix}\begin{bmatrix}1 & 1 & 1\\ 1 & \overline{a}^{2} & \overline{a}\\ 1 & \overline{a} & \overline{a}^{2}\end{bmatrix} & 0\\ 0 & \begin{bmatrix}1 & 1 & 1\\ 1 & \overline{a}^{2} & \overline{a}\\ 1 & \overline{a} & \overline{a}^{2}\end{bmatrix}\end{bmatrix}.\left[\overline{I}_{012}\right] \tag{3.20}$$

The impedance symmetrical component will therefore be given by:

$$\left[\overline{Z}_{012}\right]=\frac{\left[\Delta\overline{U}_{012}\right]}{\left[\overline{I}_{012}\right]}=\begin{bmatrix}\begin{bmatrix}1 & 1 & 1\\ 1 & \overline{a}^{2} & \overline{a}\\ 1 & \overline{a} & \overline{a}^{2}\end{bmatrix} & 0\\ 0 & \begin{bmatrix}1 & 1 & 1\\ 1 & \overline{a}^{2} & \overline{a}\\ 1 & \overline{a} & \overline{a}^{2}\end{bmatrix}\end{bmatrix}^{-1}.\left[\overline{Z}_{\mathbf{abc}}\right]\begin{bmatrix}\begin{bmatrix}1 & 1 & 1\\ 1 & \overline{a}^{2} & \overline{a}\\ 1 & \overline{a} & \overline{a}^{2}\end{bmatrix} & 0\\ 0 & \begin{bmatrix}1 & 1 & 1\\ 1 & \overline{a}^{2} & \overline{a}\\ 1 & \overline{a} & \overline{a}^{2}\end{bmatrix}\end{bmatrix} \tag{3.2}$$

This gives a 6x6 matrix whose diagonal elements respectively zero-, positive- and negative-sequence for both parallel lines and the elements $\overline{Z}_{14}$ and $\overline{Z}_{41}$ of this matrix represent the mutual coupling impedance between the two lines.

3.3.1.2 Transposed parallel lines

The transposition of the transmission line which consist of rearranging line conductors such that their positions are exchanged at regular intervals, having divided the line segment into three sub-segment of the same length such that each of the phases a, b and c occupy each of positions 1,2 and 3 in the entire segment as shown in Fig. 4.1.

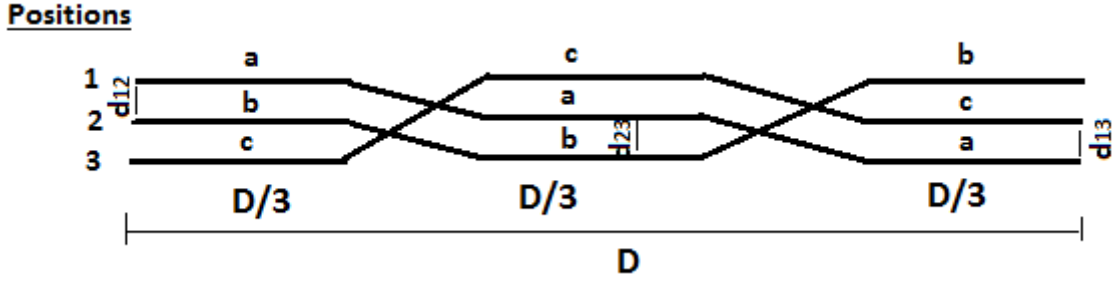

Fig. 3.5 Transmission line transposition

This procedure helps to restore the balanced nature of the line and the line-inductance operating in the segment D.

Impedance matrix for a transposed transmission line

According to [22], the voltage drop across 1km of the transposed transmission line will be given by the equation (3.22)

$$\begin{bmatrix} \Delta\overline{U}_{\mathbf{a}} \\ \Delta\overline{U}_{\mathbf{b}} \\ \Delta\overline{U}_{\mathbf{c}} \end{bmatrix} = \frac{1}{3}\left(\begin{bmatrix} \overline{Z}_{11} & \overline{Z}_{12} & \overline{Z}_{13} \\ \overline{Z}_{12} & \overline{Z}_{22} & \overline{Z}_{23} \\ \overline{Z}_{13} & \overline{Z}_{23} & \overline{Z}_{33} \end{bmatrix} + \begin{bmatrix} \overline{Z}_{33} & \overline{Z}_{13} & \overline{Z}_{23} \\ \overline{Z}_{13} & \overline{Z}_{11} & \overline{Z}_{12} \\ \overline{Z}_{23} & \overline{Z}_{12} & \overline{Z}_{22} \end{bmatrix} + \begin{bmatrix} \overline{Z}_{22} & \overline{Z}_{23} & \overline{Z}_{12} \\ \overline{Z}_{23} & \overline{Z}_{33} & \overline{Z}_{13} \\ \overline{Z}_{12} & \overline{Z}_{13} & \overline{Z}_{11} \end{bmatrix}\right).\begin{bmatrix} \overline{I}_{\mathbf{a}} \\ \overline{I}_{\mathbf{b}} \\ \overline{I}_{\mathbf{c}} \end{bmatrix} \tag{3.22}$$

$$\Rightarrow \begin{bmatrix} \Delta\overline{U}_{\mathbf{a}} \\ \Delta\overline{U}_{\mathbf{b}} \\ \Delta\overline{U}_{\mathbf{c}} \end{bmatrix} = \begin{bmatrix} \overline{Z} & \overline{Z}' & \overline{Z}' \\ \overline{Z}' & \overline{Z} & \overline{Z}' \\ \overline{Z}' & \overline{Z}' & \overline{Z} \end{bmatrix} \tag{3.23}$$

Where $\overline{Z}$ represents diagonal elements of the matrix and is given by equation (3.24)

$$\overline{Z} = \frac{1}{3}\left(\overline{Z}_{11} + \overline{Z}_{22} + \overline{Z}_{33}\right) = R_1 + R_{1\mathbf{g}} + j0{,}1445.\log\frac{D_{\mathbf{g}}}{\xi r}, \tag{3.24}$$

$\overline{Z}'$ represents the elements out of the diagonal and is given by equation (3.25)

$$\overline{Z}' = \frac{1}{3}\left(\overline{Z}_{12} + \overline{Z}_{13} + \overline{Z}_{23}\right) = R_{1\mathbf{g}} + j0{,}1445.\log\frac{D_{\mathbf{g}}}{d} \tag{3.25}$$

where d is the mean distance between conductors and is given by $d = \sqrt[3]{d_{12}d_{13}d_{23}}$.

In case of impedance in the ground wire the mean distance will be $d_{\mathbf{E}} = \sqrt[3]{d_{\mathbf{E1}}d_{\mathbf{E2}}d_{\mathbf{E3}}}$

The symmetrical components impedances are given in a matrix where the diagonal elements represent zero-, positive- and negative-sequence for both lines and due to the fact that the system is perfectly symmetric, all mutual impedances are equal to zero except the mutual coupling impedance as shown by the equation (3.26).

$$\left[\overline{Z}_{012}\right] = \begin{bmatrix} \overline{Z}_{00} & 0 & 0 & \overline{Z}_{\mathbf{00m}} & 0 & 0 \\ 0 & \overline{Z}_{11} & 0 & 0 & 0 & 0 \\ 0 & 0 & \overline{Z}_{22} & 0 & 0 & 0 \\ \overline{Z}_{\mathbf{00m}} & 0 & 0 & \overline{Z}'_{00} & 0 & 0 \\ 0 & 0 & 0 & 0 & \overline{Z}'_{11} & 0 \\ 0 & 0 & 0 & 0 & 0 & \overline{Z}'_{22} \end{bmatrix} \tag{3.26}$$

This matrix is obtained the same way as in equation (3.20) and (3.21).

In case of a perfect transposition, there are practically no inductive influences between different conductors and the operating impedance of each phase is given by the equation (3.25).

In case of a compromise transposition the mutual inductance influence is not totally eliminated thus the operating impedance for one phase of each line at one kilometre length is given by equation (3.27)

$$\overline{Z}_1 = R_{\mathbf{lg}} + j0{,}1445\log\frac{d.d^{+'}}{\xi r d^{+}} \tag{3.27}$$

where $d^{+} = \sqrt[3]{d_{\mathbf{aA}} d_{\mathbf{bB}} d_{\mathbf{cC}}}$ and $d^{+'} = \sqrt[3]{d_{\mathbf{aB}} d_{\mathbf{aC}} d_{\mathbf{bC}}}$

3.3.1.3 The other way to calculate the mutual coupling impedance

According to [1] the current in the zero-sequence system equals to the portion of the summated current relating to one phase, i.e. one-third of the earth current ($I_0 = I_E/3$). This means that the zero sequence impedance equal to three times the substitute conductor-earth impedance. Therefore, the coupling impedance between the zero-sequence systems of two lines without earth-wire is given by equation (3.28)

$$\overline{Z}_{\mathbf{OM}} = \left(3.R_{\mathbf{E}'} + j\omega.6.\ln\frac{\delta}{A_{\mathbf{L}}}\right).10^{-4}, \tag{3.28}$$

where

$$\omega = 2\pi f \tag{3.29}$$

$$\delta = 1650.\sqrt{\frac{\rho}{\omega}} \tag{3.30}$$

$$R_{\mathbf{E}'} = \frac{\pi}{2}.\omega.10^{-4} \tag{3.31}$$

$A_{\mathbf{L}}$ is the geometrical mean distance of the conductors of both three phases systems and corresponds approximately to the distance between the towers of the two lines.

Examples 1:

We determine the zero sequence mutual impedance, between conductors of two parallel lines, separated by 12m of distance in a system frequency of 50Hz and specific resistance of earth is 100Ω.m. Assuming that the distance between the two lines can vary taking any value between 0 and 500m, we determine graphically the variation of the zero sequence mutual impedance with respect to the distance separating the two parallel lines.

Solution:

The mutual coupling impedance is given by:

$$\overline{Z}_{OM} = \left(3.R_{\mathrm{E}'} + j\omega.6.\ln\frac{\delta}{A_{\mathrm{L}}}\right).10^{-4}$$

Calculation of ground resistance:

$$R_{\mathrm{E}'} = \frac{\pi}{2}.\omega.10^{-4} = \frac{3{,}14}{2}.2.3{,}14.50.10^{-4} = 0{,}0493\Omega$$

Calculation of penetration depth:

$$\delta = 1650.\sqrt{\frac{\rho}{\omega}} = 1650.\sqrt{\frac{100}{2.3,14.50}} = 931,15\text{m}$$

$$\overline{Z}_{OM} = \left(3.R_{E'} + j\omega.6.\ln\frac{\delta}{A_L}\right).10^{-4} = \left(3.0,0493 + j2.3,14.50.6.\ln\frac{931,15}{12}\right)$$

$$= (0,148 + j8198,25).10^{-4}\,\Omega/\text{km} = 0,8198\angle 89,999°\,\Omega/\text{km}$$

The mutual impedance of $0,82\,\Omega/\text{km}$ exists between two parallel lines separated by 12m of distance. The variation of the zero sequence mutual impedance with respect to line spacing is illustrated in Tab. 3.3

Table 3.3 *Variation of Z_{0M} with respect to distance between lines*

Distance(m)	Z_{0M} [Ωkm^{-1}]	Module Z_{0M} [Ωkm^{-1}]
5	(0.148+j9847.635).10^{-4}	0.985
10	(0.148+j8541,75) .10^{-4}	0.854
50	(0.148+j5509.565).10^{-4}	0.551
100	(0.148+j4203.675).10^{-4}	0.4204
150	(0.148+j3439.78).10^{-4}	0.344
200	(0.148+j2897.786).10^{-4}	0.2898
250	(0.148+j2477.3836).10^{-4}	0.2477
300	(0.148+j2133.89).10^{-4}	0.2134
350	(0.148+j1843.47).10^{-4}	0.1843
400	(0.148+j1591897).10^{-4}	0.1592
450	(0.148+j1369.99).10^{-4}	0.137
500	(0.148+j1171.49).10^{-4}	0.117

Graphic representation

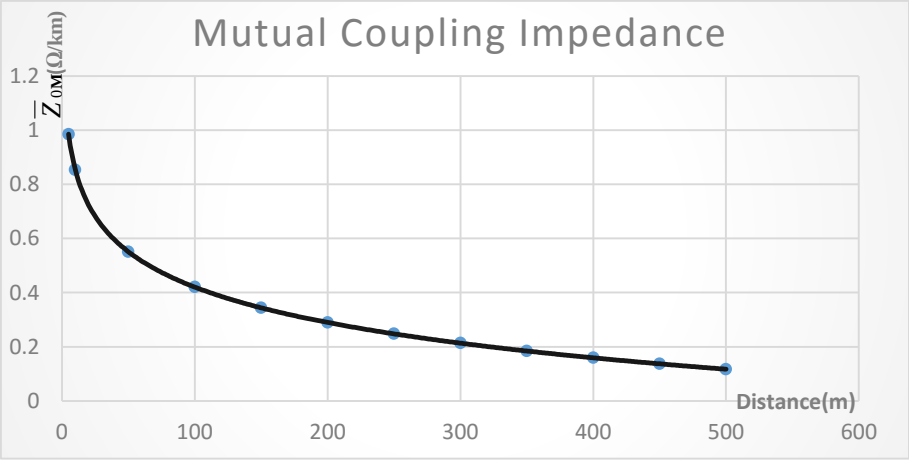

Fig. 3.6 Variation of $\overline{Z}_{0M}$ with respect to distance between parallel lines

Since the mutual impedance has a logarithmic relationship, it decreases relatively slowly with an increase in line spacing Fig. 3.6 shows that even with fairly large distance between the lines, mutual coupling is still present. This impedance is too high when the two lines have no ground

wire and decreases when only one line has the earth-wire and it has the smallest value when there is a ground-wire on both of the lines

3.3.2 Determination of measuring error due to the effect of the mutual coupling impedance

As shown in the previous paragraph, when a fault/short-circuit occurs on one of the parallel lines, earth-currents induce additional voltages in the fault loop of the measured line, and change the short circuit voltage measured by voltage transformer at the relay location. This results in impedance measuring error and thus in inaccurate fault location.

Consider the following symmetrical component equivalent circuit for the case of single ended in-feed:

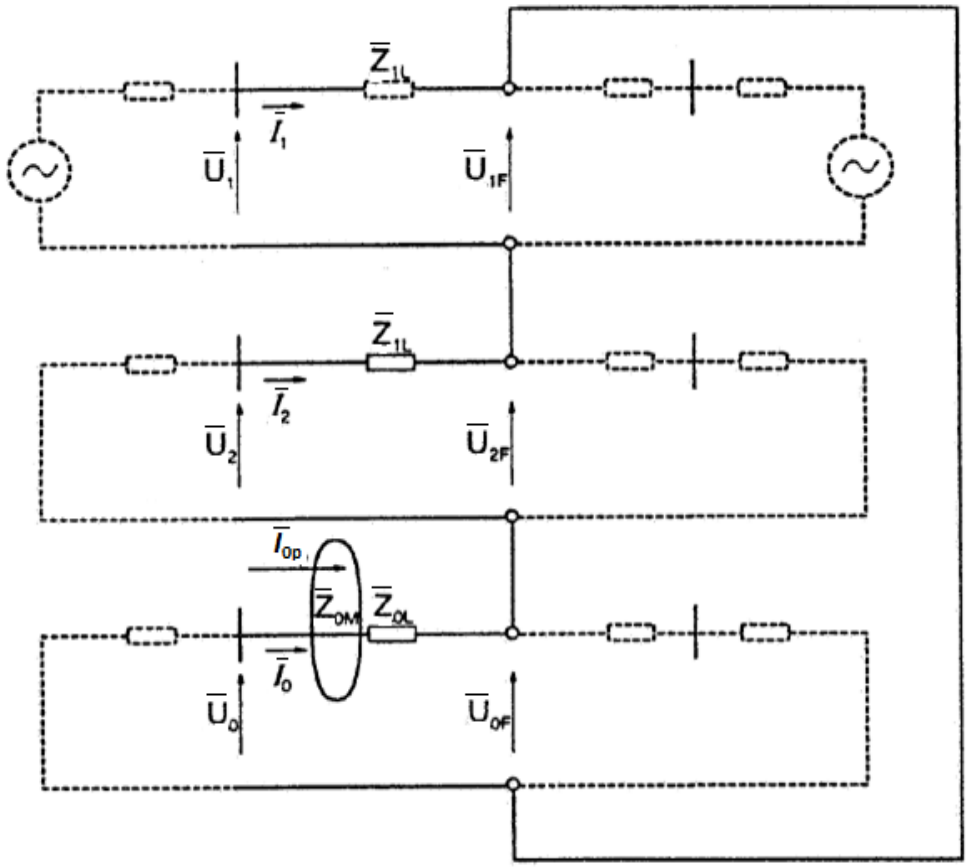

Fig. 3.7 Symmetrical component line impedance equivalent circuit [1]

From the above equivalent circuit, the following equations can be derived

$$\bar{U}_1 = \bar{Z}_{1L}.\bar{I}_1 + \bar{U}_{1F}, \tag{3.32}$$

$$\bar{U}_2 = \bar{Z}_{1L}.\bar{I}_2 + \bar{U}_{2F}, \tag{3.33}$$

$$\bar{U}_0 = \bar{Z}_{0L}.\bar{I}_0 + \bar{Z}_{0M}.\bar{I}_{0p} + \bar{U}_{0F}. \tag{3.34}$$

If these equations are added together and taking into consideration the equations (3.35) and (3.36)

$$\bar{U}_1 + \bar{U}_2 + \bar{U}_0 = \bar{U}_A, \tag{3.35}$$

$$\overline{U}_{1F} + \overline{U}_{2F} + \overline{U}_{0} = 0, \tag{3.36}$$

then the result is

$$\overline{U}_{A} = \overline{Z}_{1L}.\left(\overline{I}_{1} + \overline{I}_{2}\right) + \overline{Z}_{0L}.\overline{I}_{0} + \overline{Z}_{0M}.\overline{I}_{0p}, \tag{3.37}$$

$$\overline{U}_{A} = \overline{Z}_{1L}.\left(\overline{I}_{1} + \overline{I}_{2} + \overline{I}_{0}\right) + \left(\overline{Z}_{0L} - Z_{1L}\right)\overline{I}_{0} + \overline{Z}_{0M}.\overline{I}_{0p}. \tag{3.38}$$

Since the current in the zero sequence system equals the portion of the summated current relating to one phase as shown in equation (3.39)

$$\overline{I}_{0} = \frac{1}{3}\overline{I}_{E}, \tag{3.39}$$

which implies that

$$\overline{I}_{E} = 3\overline{I}_{0} \tag{3.40}$$

and similarly

$$\overline{I}_{EP} = 3\overline{I}_{0P} \tag{3.41}$$

and the corresponding zero sequence impedance is therefore three times the conductor-earth impedance

$$\overline{Z}_{E} = \frac{\overline{Z}_{0L} - Z_{1L}}{3}. \tag{3.42}$$

Considering that

$$\overline{I}_{1} + \overline{I}_{2} + \overline{I}_{0} = \overline{I}_{ph}, \tag{3.43}$$

the equation (3.38) becomes as shown in equation (3.44)

$$\overline{U}_{A} = \overline{Z}_{1L}.\overline{I}_{ph} + \frac{\overline{Z}_{0L} - Z_{1L}}{3}.\overline{I}_{E} + \frac{\overline{Z}_{0M}}{3}.\overline{I}_{Ep}. \tag{3.44}$$

The short circuit voltage at the relay location is therefore given by

$$\overline{U}_{A} = \overline{Z}_{1L}.\left[\overline{I}_{ph} + \frac{\overline{Z}_{EL}}{\overline{Z}_{1L}}.\overline{I}_{E} + \frac{\overline{Z}_{0M}}{3\overline{Z}_{1L}}.\overline{I}_{Ep}\right] \tag{3.45}$$

The measured impedance may now be calculated by using the following equation

$$\overline{Z}_{A} = \frac{\overline{U}_{A}}{\overline{I}_{ph} + \overline{K}_{E}.\overline{I}_{E}}, \tag{3.46}$$

where $\overline{K}_{E} = \dfrac{\overline{Z}_{EL}}{\overline{Z}_{1L}}$ and $\overline{K}_{EM} = \dfrac{\overline{Z}_{0M}}{3.\overline{Z}_{1L}}$ are residual and mutual compensation factors

$$\overline{Z}_{A} = \frac{\overline{Z}_{1L}.\left[\overline{I}_{ph} + \dfrac{\overline{Z}_{EL}}{\overline{Z}_{1L}}.\overline{I}_{E} + \dfrac{\overline{Z}_{0M}}{3\overline{Z}_{1L}}.\overline{I}_{Ep}\right]}{\overline{I}_{ph} + \overline{K}_{E}.\overline{I}_{E}}. \tag{3.47}$$

The final equation will be

$$\overline{Z}_{A} = \overline{Z}_{1L}\left[1+\frac{\frac{\overline{Z}_{0M}}{3.\overline{Z}_{1L}}.\overline{I}_{Ep}}{\overline{I}_{ph}+\frac{\overline{Z}_{EL}}{\overline{Z}_{1L}}.\overline{I}_{E}}\right]. \tag{3.48}$$

measuring error

Equation (3.48) illustrates the measured impedance in a transposed transmission line where the mutual coupling impedance in the positive- and negative-sequence is too low and neglected. However this is not the case in non-transposed line because the mutual impedance is important and must be taken into consideration. Applying the same analogy, the measured impedance by the DP in phase A of a non-transposed transmission line is given by equation (3.49)

$$\overline{Z}_{A} = \left(\overline{Z}_{1L}+\overline{Z}_{M}\right)\left[1+\frac{\frac{\overline{Z}_{0M}}{3.\left(\overline{Z}_{1L}+\overline{Z}_{M}\right)}.\overline{I}_{Ep}}{\overline{I}_{ph}+\frac{\overline{Z}_{EL}}{\left(\overline{Z}_{1L}+\overline{Z}_{M}\right)}.\overline{I}_{E}}\right], \tag{3.49}$$

where

$$\overline{Z}_{EL} = \frac{\overline{Z}_{0L}-\overline{Z}_{1L}-\overline{Z}_{M}}{3}, \tag{3.50}$$

$$\overline{K}_{E} = \frac{\overline{Z}_{EL}}{\overline{Z}_{1L}+\overline{Z}_{M}}, \tag{3.51}$$

$$\overline{K}_{EM} = \frac{Z_{0M}}{3.\left(\overline{Z}_{1L}+\overline{Z}_{M}\right)}. \tag{3.52}$$

To determine the error caused by the effect of mutual coupling impedance when an earth fault occurs, let's represent our system as shown in Fig 3.8

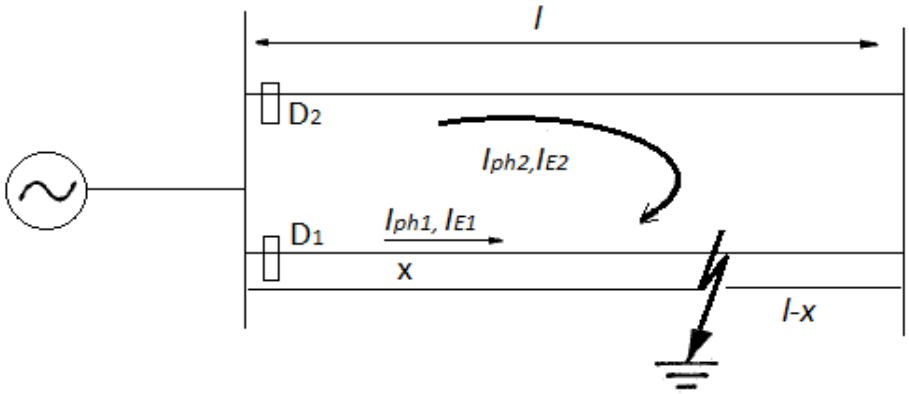

Fig. 3.8 Parallel line with earth-fault

In this case the following relationships can apply:

$$\overline{I}_{ph1} = \overline{I}_{E1} = \overline{I}_{Ep}, \tag{3.53}$$

$$\overline{I}_{ph2} = \overline{I}_{E2} = \frac{x}{2l-x}.\overline{I}_{E1}, \tag{3.54}$$

where $\bar{I}_{ph1}, \bar{I}_{ph2}$ are phase currents for line 1 and line 2, $\bar{I}_{E1}, \bar{I}_{E2}$ are the earth currents for line 1 and line 2, $\bar{I}_{Ep}$ is the earth current flowing through the self-inductance of the parallel line, l is the length of the protected line segment and x the distance to fault location.

According to the equation (3.48), the impedance measured by the distance protection D_1 on the faulted transposed line will be given by

$$\bar{Z}_1 = \frac{x}{l}\bar{Z}_{1L} + \frac{x}{l}\bar{Z}_{1L}.\frac{\frac{\bar{Z}_{0M}}{3.\bar{Z}_{1L}}.\bar{I}_{Ep}}{\bar{I}_{ph} + \frac{\bar{Z}_{EL}}{\bar{Z}_{1L}}.\bar{I}_E} = \frac{x}{l}\bar{Z}_{1L} + \frac{x}{l}\bar{Z}_{1L}.\frac{\frac{\bar{Z}_{0M}}{3.\bar{Z}_{1L}}.\bar{I}_{Ep}}{\left(\frac{\bar{I}_{ph}}{\bar{I}_E} + \frac{\bar{Z}_{EL}}{\bar{Z}_{1L}}\right).\bar{I}_E} = \frac{x}{l}\bar{Z}_{1L} + \frac{x}{l}\bar{Z}_{1L}.\frac{\frac{\bar{Z}_{0M}}{3.\bar{Z}_{1L}}.\frac{\bar{I}_{Ep}}{\bar{I}_E}}{1+\frac{\bar{Z}_{EL}}{\bar{Z}_{1L}}},$$

$$\bar{Z}_1 = \frac{x}{l}\bar{Z}_{1L} + \frac{x}{l}\bar{Z}_{1L}.\underbrace{\frac{\frac{\bar{Z}_{0M}}{3.\bar{Z}_{1L}}.\frac{x}{2l-x}}{1+\frac{\bar{Z}_{EL}}{\bar{Z}_{1L}}}}_{\text{Measuring error}} = \frac{x}{l}\bar{Z}_{1L}\left[1+\frac{\frac{\bar{Z}_{0M}}{3.\bar{Z}_{1L}}.\frac{x}{2l-x}}{1+\frac{\bar{Z}_{EL}}{\bar{Z}_{1L}}.}\right] \qquad (3.55)$$

In case of the non-transposed line, the impedance measured by the D1 will be given by equation (3.56)

$$\bar{Z}_1 = \frac{x}{l}\left(\bar{Z}_{1L} + \bar{Z}_M\right)\left[1+\frac{\frac{\bar{Z}_{0M}}{3.\left(\bar{Z}_{1L}+\bar{Z}_M\right)}.\frac{x}{2l-x}}{1+\frac{\bar{Z}_{EL}}{\bar{Z}_{1L}+\bar{Z}_M}}\right] \qquad (3.56)$$

When the parallel is supplied from both ends (double ended in-feed) two short-circuit currents $\bar{I}_a$ and $\bar{I}_b$ which are the current contributions from both sources, will be taken into consideration as shown in Fig. 3.9.

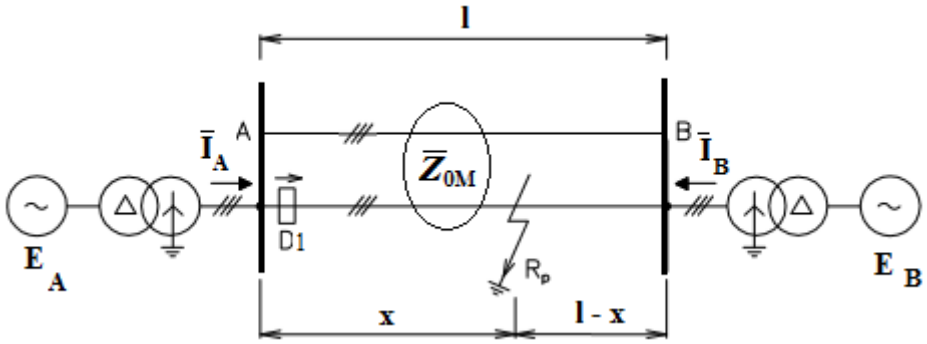

Fig. 3.9 Double sided in-feed for a parallel line [2]

Considering the distance protection D1, located on the faulted line on the side of the substation A, the measuring error will be negative for faults in the portion of the line where the parallel line earth current flows in opposite direction. In other words when $\bar{I}_{E1}$ and $\bar{I}_{E2}$ have opposite signs. The measuring error has its maximum negative value when the fault occur at the relay location or $x = 0$, it increases as x increases to reach its maximum positive value for fault occurring at the remote end of the protected line or $x = l$. This depends on the ration $\bar{I}_b / \bar{I}_a$ and Fig. 3.10 illustrates

the case of $\bar{I}_b = 0, \bar{I}_b = \bar{I}_a$ and $\bar{I}_b = 4\bar{I}_a$ where the measuring error varies between -29.29 to 43.93 for the last case.

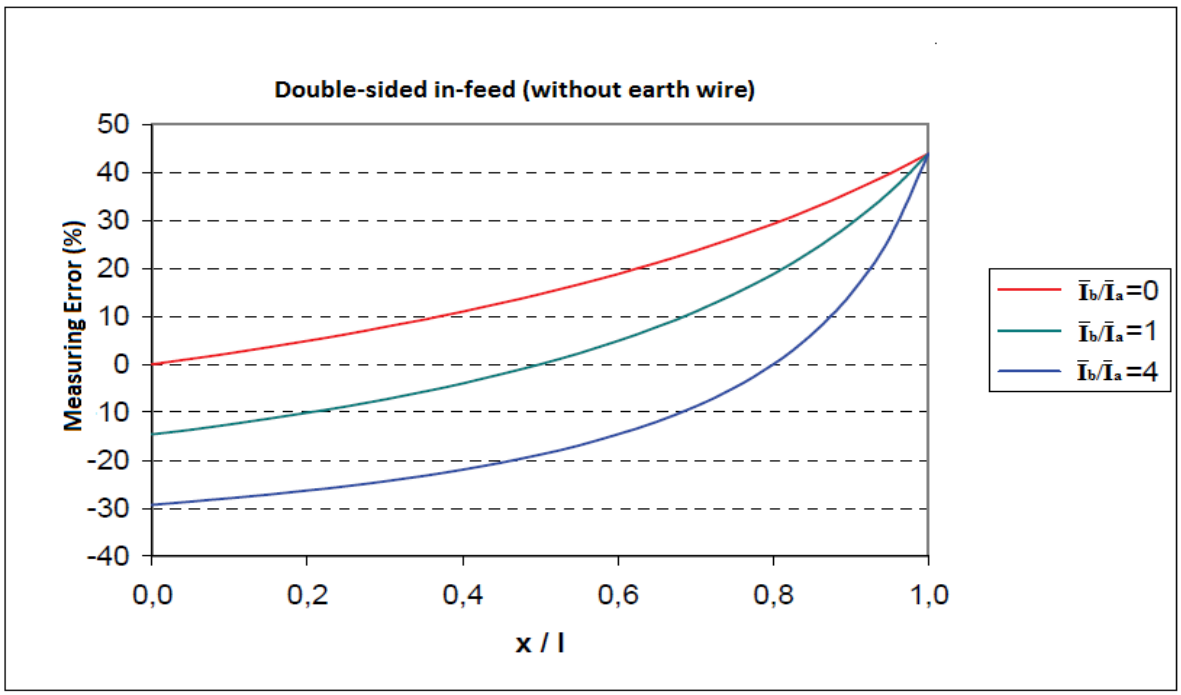

Fig. 3.10 Measuring error in parallel line with double sided in-feed [2]

3.4 Other Reasons for Inaccurate Fault Location in parallel lines

3.4.1 Parallel line out of service and grounded

Due to the grounding at both ends of the open parallel line, when there is an earth fault on the operating feeder as it can be seen on Fig. 3.11, currents are induced in the earth loop of the earthed feeder, causing a misleading mutual compensation signal. Therefore fault locator will not determine the distance to fault location correctly.

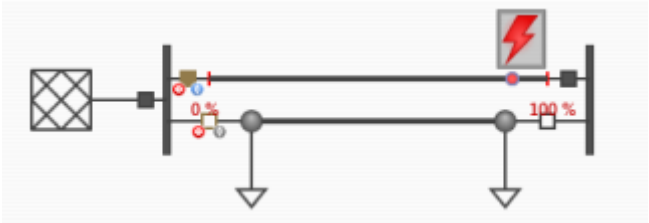

Fig. 3.11 Parallel line open and grounded at both ends [11]

In this case a considerable overreach of the impedance measurement is possible.

According to [13] the calculation with simulation for a given line with real values will give the overreach of around 17,5%.

3.4.2 Current reversal

Due to several reasons, for example due to the slight differences of protection devices tripping time or because the circuit breaker's durations to open a pole are also different (even depending on the fault inception angle), it is possible that when the fault is cleared sequentially on one circuit of

a double circuit line with generation sources at both ends of the circuit, the current in the healthy line can reverse for a period of time.

Unwanted tripping of circuit breakers on the healthy line can then occur. Figures 3.12a) and 3.12b) show how the situation can arise.

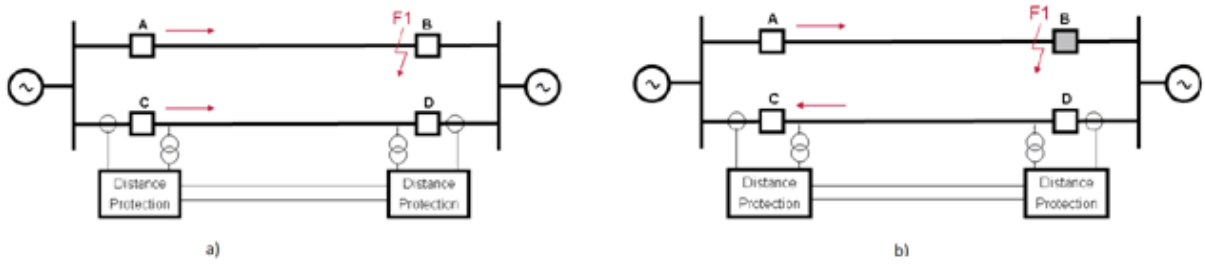

Fig. 3.12 Current reversal [5]

The protecting relay B clears the fault faster than the relay A. Once circuit breaker *B* opens, the relay element at *C* starts to reset, while the forward looking elements at *D* pick up (due to current reversal) (Fig. 3.12b) and initiate tripping. If the reset times of the forward-looking elements of the relay at *C* are longer than the operating time of the forward looking elements at *D*, the relays will trip the healthy line.

4 CURRENT STATE OF METHODS TO IMPROVE ACCURACY FOR FAULT LOCATORS

In the previous chapters we have discussed different factors that negatively influence the accurate fault location determination by distance protection locators, in the transmission lines in general and specially in parallel and double circuit lines. In this chapter we are going to discuss different solutions adopted to address all those problems faced by the locators and particularly the current states of methods used to ensure their accuracy. We will first analyse general methods and solutions to individual problem mentioned in the previous chapter, and lastly we will focus on some specific methods, techniques and algorithms used today and their input into the measuring accuracy improvement.

4.1 Solution to improve accuracy in fault location determination

4.1.1 Solution to fault resistance

In paragraph 2.5.1 we have seen that the fault resistance R_F has no influence on the measured impedance of lines with power supply on one side, because the line reactance, on which depend the determination of distance to the fault location, is not affected by the presence of R_F. This arc resistance results in increase of line resistance (only in *R*-direction). However, for very long line and for lines with power supplies on their both ends, the influence exists.

The adjustment of the relay settings, taking into consideration the possible presence of the fault resistance, and the use of an adequate distance relay with enough resistive reserve (reserve in *R*-direction), are enough to solve the problem. The distance protection with a quadrilateral characteristic is particularly suitable.

4.1.2 Solution to the effect of Intermediate power supply

The intermediate power supply as well as the earthed transformer and the T-outgoing feeder behaving like a negative in-feed, have relatively the same influence on distance measurement as the power supplies on both ends of the power line. Therefore the under-reach (or over-reach) caused can be corrected by properly adjusting the compensation factor K_E as expressed in paragraph 4.1.4.3, while setting the distance protection.

4.1.3 Solution to the non-symmetry of the line

This problem and its negative impact was discussed in paragraph 2.4.3. In order to avoid the non-symmetry effect, long power lines must be transposed. This enables us to avoid negative-sequence and earth currents in the line.

4.1.3.1 Line transposition

Even if the transmission line may be operating under balanced conditions, if the distance between its phase conductors differ, voltage drops are created across the conductors due to unsymmetrical mutual inductance between them. This affects enormously the impedance measurement and thus undermines the accurate computation of distance to fault location, the process of which depends on the line reactance.

4.1.4 Solution to the mutual coupling effect

4.1.4.1 Line transposition effect

The transmission line transposition discussed in the previous paragraph is one of the techniques that helps to reduce the impedance mutual coupling effects in the lines. When a transmission line is transposed, the effect of mutual impedance coupling in the positive and negative sequence system is very small and negligible. Normally mutual inductance is less than 5% of the self-inductance in the line. Thus in the transposed line this effect is considered only in the zero sequence system.

4.1.4.2 Ground/earth-wire

Another factor that contributes to the reduction of the effect of mutual coupling impedance is the current flowing in the ground-wire and its resulting magnetic flux. The magnetic flux produced by the current flowing in the ground wire in case of non-symmetric fault, acts against the magnetic flux produced by the line-conductor currents. These fluxes subtract each other. This explains the importance of the ground-wire in limiting the mutual coupling influence and thus improving the fault location determination accuracy. The lower is the earth-wire impedance, the higher is the current flowing through it and the higher will be the resultant magnetic flux. Therefore, the magnetic flux produced by the ground-wire decreases the mutual zero sequence reactance X_{0M}. Fig. 4.1 shows the percentage of the current that flows through the earth-wire, in case of a single phase to earth fault, and the corresponding mutual zero sequence reactance X_{0M} for different types of ground wires with different cross-sectional areas and consequently with different conductivity. The current flowing in the phase conductor is considered to be 100%.

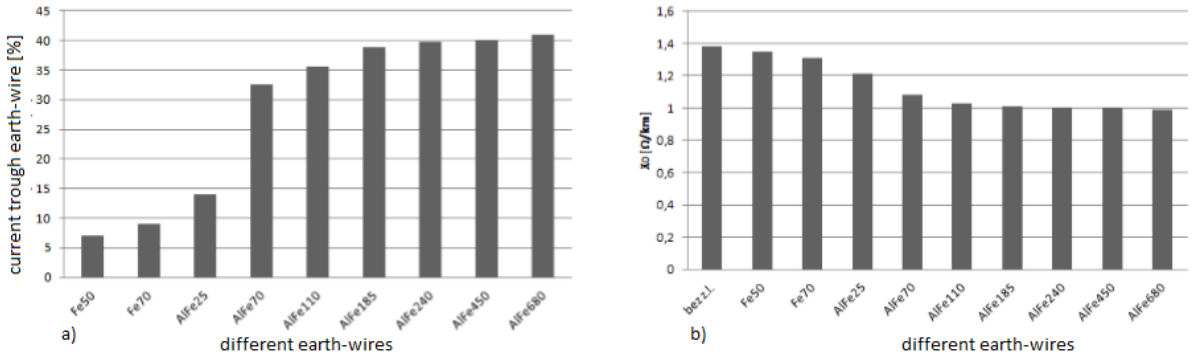

Fig. 4.1 The current and mutual reactance for different earth-wire types [16]

4.1.4.3 Earth Impedance compensation

This setting is very important for the accurate measurement of the distance to fault location by a distance protection when earth faults occur. The realization of this compensation is achieved either by setting resistance and reactance ratios R_E/R_L and X_E/X_L or by entering the complex earth (residual) compensation factor $\overline{K}_E$.

- **Earth Impedance Compensation by Scalar factors R_E/R_L *and* X_E/X_L**

Ratios R_E/R_L and X_E/X_L are entered in the DP, separately calculated and do not correspond to the real and imaginary parts of Z_E/Z_L. Thus the calculation with complex numbers is not necessary and the ratios are determined according to the equations (4.1) and (4.2)

$$\frac{R_{\mathbf{E}}}{R_{\mathbf{L}}} = \frac{1}{3}.\left(\frac{R_0}{R_1} - 1\right) \text{ and } \frac{X_{\mathbf{E}}}{X_{\mathbf{L}}} = \frac{1}{3}.\left(\frac{X_0}{X_1} - 1\right) \qquad (4.1), (4.2)$$

- **Earth Compensation with Magnitude and Angle ($\overline{K}_{\mathbf{E}}$ factor)**

In case the complex compensation factor $\overline{K}_{\mathbf{E}}$ is set in the distance protection. The line angle which is given in equation (4.3) will be needed to determine the compensation components from $\overline{K}_{\mathbf{E}}$.

$$\varphi = \arctan\frac{X_{\mathbf{L}}}{R_{\mathbf{L}}} \qquad (4.3)$$

The earth impedance compensation factor will be given by the equation (4.4)

$$\overline{K}_E = \frac{\overline{Z}_E}{\overline{Z}_L} = \frac{1}{3}.\left(\frac{\overline{Z}_0}{\overline{Z}_1} - 1\right) \qquad (4.4)$$

The quadrant of the result must be taken into consideration when determining the angle. This specifies the sign and angle range as shown by Tab. 4-1

Table 4.1 Quadrant and range of angle $K_{\mathbf{E}}$ [23]

Real part	Imaginary part	tan φ ($K_{\mathbf{E}}$)	Quadrant/range	Calculation
+	+	+	I 0° … +90°	arc tan (|Im| / |Re|)
+	-	-	IV -90° … 0°	-arc tan (|Im| / |Re|)
-	-	+	III -90° … 180°	arc tan (|Im| / |Re|)-180°
-	+	-	II -90° … 180°	arc tan (|Im| /|Re|)+180°

4.1.4.4 Parallel Line Mutual Impedance Compensation

Since the distance protections are also used in protecting the parallel and double circuit lines, the mutual coupling impedance is taken into consideration. The mutual coupling compensation factors set in the DP are determined according to equations (4.5) and (4.6)

$$\frac{R_{\mathbf{M}}}{R_{\mathbf{L}}} = \frac{1}{3}.\left(\frac{R_{0\mathbf{M}}}{R_1} - 1\right) \text{and } \frac{X_{\mathbf{M}}}{X_{\mathbf{L}}} = \frac{1}{3}.\left(\frac{X_{0\mathbf{M}}}{X_1} - 1\right) \qquad (4.5), (4.6)$$

The parallel compensation ratio which determines the earth current ratio $I_{\mathbf{E}} / I_{\mathbf{EP}}$ which must be exceeded for the compensation to take place, is normally set a 85%. But in case of a system with very low coupling factor ($X_{\mathbf{M}} / X_{\mathbf{L}} < 0.4$) or system with high asymmetry, lower setting can be used.

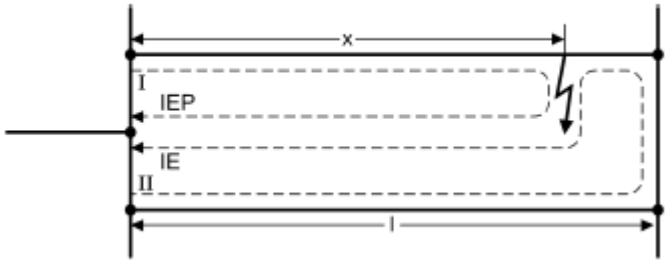

Fig. 4.2 *Distance with parallel line compensation at II* [23]

This ratio is calculated from the desired distance of the parallel line compensation as shown by equation (4.7) and illustrated in Fig. 4.2 where the considered DP location is II.

$$\frac{I_E}{I_{EP}} = \frac{x/l}{2 - x/l} \quad \text{or} \quad \frac{x}{l} = \frac{2}{1 + \dfrac{1}{I_E / I_{EP}}} \tag{4.7}$$

4.1.4.5 H parameters method

Since the classical approaches of fault location do not always lead to the correct determination of the distance to fault location, especially for multiple long lines, some improved methods based on the present technology advancement are developed and can help in improving remarkably the accuracy of fault localisation. This technology provides the possibility of the synchronous measurements of desired parameters in the system, and also the comparison and the evaluation of their transmission. For time synchronisation, the signal received from the satellite system GPS (Global Positions System) is used. The measured data can be used for network calculation, estimation and control, and are particularly useful for the protection and the computation of distance to fault location.

The description of the line impedance Z and admittance Y is currently a key-tool in network calculation. That is why the use of H parameters provides more accurate fault location.

4.1.4.6 Principles of H parameters method

In order to explain the principle of H parameter for distance to fault location determination in a protected system, we will consider a single-phase power line in an equivalent T-circuit as shown in Fig. 4.3.

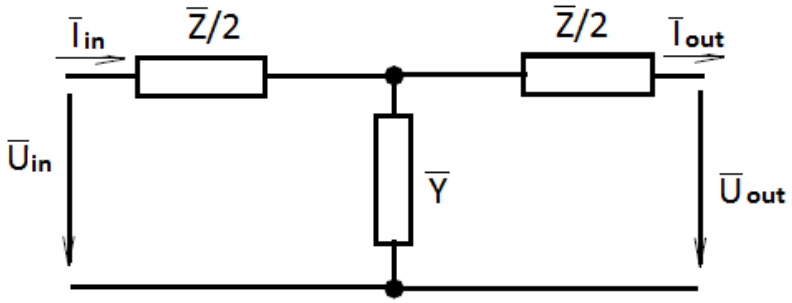

Fig. 4.3 The equivalent T-circuit for power line

When the details about element parameters inside the system are not required while calculating the network in the steady state, it is possible to determine inputs values with respect to output values as given by the equation (4.8)

$$\begin{bmatrix} \overline{U}_{out} \\ \overline{I}_{out} \end{bmatrix} = \overline{H} \begin{bmatrix} \overline{U}_{in} \\ \overline{I}_{in} \end{bmatrix}, \tag{4.8}$$

$$\overline{H} = \begin{bmatrix} \overline{A} & \overline{B} \\ \overline{C} & \overline{D} \end{bmatrix} \tag{4.9}$$

$\overline{A}$, $\overline{B}$, $\overline{C}$ and $\overline{D}$ are known as Blondel's constants and are given by:

$$\overline{A} = \overline{D} = 1 + \frac{\overline{Y}.\overline{Z}}{2}, \tag{4.10}$$

$$\overline{B} = Z + \frac{\overline{Y}.\overline{Z}^2}{4} \quad , \tag{4.11}$$

$$\overline{C} = \overline{Y} \tag{4.12}$$

For better and simpler description the power line can also be represented by a model shown in Fig. 4.4.

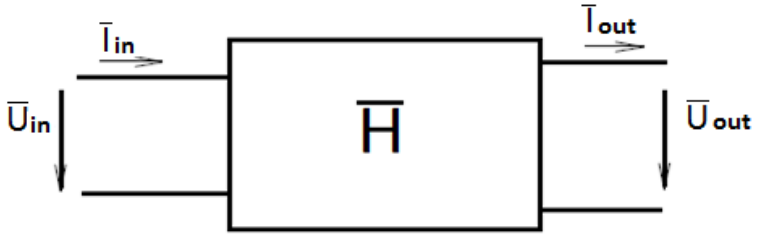

Fig. 4.4 Power line model

The use of H parameters relies on the simplicity of handling line parameters while calculating the system with lines or line-segments in cascade. If we consider a cascade arrangement of n line segments, the matrix $\overline{H}_s$ for the whole system will be given by the product of matrices of individual line-segments as shown by the equation (4.13)

$$\overline{H}_s = \overline{H}_1.\overline{H}_2.\overline{H}_3.....\overline{H}_n = \prod_{i=1}^{n} \overline{H}_i \tag{4.13}$$

$\overline{H}_i$ is the matrix describing ith line segment.

The relationship between input and output values for line voltage and current is given by the equation (78)

$$\begin{bmatrix} \overline{U}_{n+1} \\ \overline{I}_{n+1} \end{bmatrix} = \prod_{i=1}^{n} \overline{H}_i \begin{bmatrix} \overline{U}_1 \\ \overline{I}_1 \end{bmatrix} \tag{4.14}$$

In case the cascade line segments have the same parameters, the matrix $\overline{H}_s$ for n segments in cascade will be given by equation (4.15)

$$\overline{H}_s = \overline{H}^n \tag{4.15}$$

where $\overline{H} = H_1 = H_2 = ... = H_n$

The relationship between input and output values for line voltage and current is given by the equation (80)

$$\begin{bmatrix} \overline{U}_{n+1} \\ \overline{I}_{n+1} \end{bmatrix} = \overline{H}^n \begin{bmatrix} \overline{U}_1 \\ \overline{I}_1 \end{bmatrix} \tag{4.16}$$

For this method of H parameters we will consider a cascade arrangement of n line-segments and a the fault that occurs at the $(m+1)^{th}$ segment as shown in Fig. 4.5

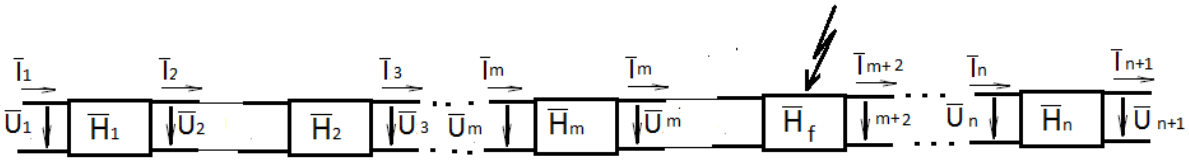

Fig. 4.5 Cascade arrangement of n line-segments

Considering $\overline{H}_s$ as the matrix describing the whole system, and $\overline{H}_f$ as the matrix for faulted line-segment (in our case $(m+1)^{th}$ segment), the relationship between the input and output values will be given by the equation (4.17)

$$\begin{bmatrix} \overline{U}_{n+1} \\ \overline{I}_{n+1} \end{bmatrix} = H_s . \begin{bmatrix} \overline{U}_1 \\ \overline{I}_1 \end{bmatrix} = \prod_{i=1}^{m} \overline{H}_i . \overline{H}_f . \prod_{j=1}^{n-m-1} \overline{H}_i \begin{bmatrix} \overline{U}_1 \\ \overline{I}_1 \end{bmatrix} \tag{4.17}$$

In case we assume that the parameters are the same for all segments, the relationship between the input and output values will be given by the equation (4.18)

$$\begin{bmatrix} \overline{U}_{n+1} \\ \overline{I}_{n+1} \end{bmatrix} = H_s . \begin{bmatrix} \overline{U}_1 \\ \overline{I}_1 \end{bmatrix} = \overline{H}^m . \overline{H}_f . \overline{H}^{n-m-1} . \begin{bmatrix} \overline{U}_1 \\ \overline{I}_1 \end{bmatrix} \tag{4.18}$$

Therefore

$$\overline{H}_s = \overline{H}^m . \overline{H}_f . \overline{H}^{n-m-1} \text{ or} \tag{4.19}$$

$$\overline{H}_s = \prod_{i=1}^{m} \overline{H}_i . \overline{H}_f . \prod_{j=1}^{n-m-1} \overline{H}_i \ .$$

Since the multiplication of the matrices is not commutative, equation (4.18) and (4.19) allow the determination of the index m for a defined type of fault and consequently the matrix $\overline{H}_f$. The method becomes easier when the matrix $\overline{H}_f$ is known but this is not always the case. We will therefore need to apply the method of getting the minimum function according to the equation (4.20) and (4.21)

$$\overline{H}_f = \overline{H}_f\left(\overline{Y}_f\right) = \overline{H}_f\left(\mathrm{Re}\left(\overline{Y}_f\right) + j.\mathrm{Im}\left(\overline{Y}_f\right)\right) \text{ and then} \tag{4.20}$$

$$\begin{bmatrix} \overline{U}_{n+1}\left(m, \overline{Y}_f\right) \\ \overline{I}_{n+1}\left(m, \overline{Y}_f\right) \end{bmatrix} = H_s\left(m, \overline{Y}_f\right) . \begin{bmatrix} \overline{U}_1 \\ \overline{I}_1 \end{bmatrix} = \overline{H}^m . \overline{H}_f\left(\overline{Y}_f\right) . \overline{H}^{n-m-1} . \begin{bmatrix} \overline{U}_1 \\ \overline{I}_1 \end{bmatrix} \tag{4.21}$$

Considering differences between phasors measured at the end of the line and the ones measured when the fault occurs in m[th] line-segment, obviously for real and positive numbers a and b, these differences are the function of distance to fault location as shown by the equation (4.22).

$$\Delta\left(m,\overline{Y}_{\mathbf{f}}\right)=a.\left|\overline{U}_{n}\left(m,\overline{Y}_{\mathbf{f}}\right)-\overline{U}_{\mathbf{nmeasured}}\right|+b.\left|\overline{I}_{n}\left(m,\overline{Y}_{f}\right)-\overline{I}_{\mathbf{nmeasured}}\right| \quad (4.22)$$

The distance to fault location is determined by getting the minimum $\Delta\left(m,\overline{Y}_{\mathbf{f}}\right)$ through $m\in(1,n-1)$ and the complex $\overline{Y}_{\mathbf{f}}$.

The H parameter method is highly efficient and can apply even for more complicated faults in complex protected networks. It is efficiently used in non-symmetric networks, multi-circuit networks and non-symmetric multi-circuit systems with internal faults

4.1.5 Accurate fault location Algorithms

For a couple of years different researchers in power engineering have worked on various techniques of a proper determination of the distance to fault location in the transmission line. Some of them just considered measured parameters from one end of the transmission line, while others used data from both ends in case of a two-ended transmission line or they used data from all ends in case of transmission lines with more ends. Recall that protective relays are practically single-ended devices thus, their effectiveness is always influenced by different factors as discussed in previous parts of this work.

With the purpose of improving accuracy for existing methods or just getting new improved and more accurate techniques, researchers have developed different algorithms with various advantages and some disadvantages. In the following paragraphs we will compare some of these algorithms.

4.1.5.1 Comparison of some improved fault location algorithms

Researchers in [15] developed an algorithm for fault location using the distributed parameter transmission line model. This was an improvement of an existing algorithm that used raw samples of voltage and current data. The method applied the voltage and current samples to a specific model of the line. The unknown distance to the fault location was then solved in the time-domain. The applied voltage and current data were from one end of the line and a profile of the voltage and current was built along the line. The method of characteristics was used to solve the voltage profile. Criteria functions were computed from the voltage profiles to determine the fault position. Even if the series resistance were used in the line model, the sampling frequency that was used was around 300 kHz, which does not make it suitable for field implementation. That is why in [15], they presented an extension to these fault location methods. The series line resistance, that was previously ignored, was now modelled and data was acquired from both ends of the transmission line synchronously. The voltage and current profile was built as before and the fault position was computed from the profiles alone. The sampling frequency requirements were also quite modest, in the range of 20 kHz. While this is still outside the capability of conventional monitoring equipment, it can be achieved by using special data acquisition hardware.

Researchers in [16] worked on accurate fault-location techniques based on distributed power quality measurement. Their algorithm were based on a so-called Voltage Drop-based Fault Location (VDFL) technique which uses the voltage waveforms provided by remote devices on the power network. This technique is similar to the existing one described in the IEEE guide based on

the line apparent impedance but with innovative differences. The VDFL technique overcomes accuracy problems by using multipoint voltage measurement rather than the one- or two-end voltage and current measurement techniques. Moreover, the use of several power-quality analysers provides plenty of information on distribution system performance such as voltage unbalance, steady-state voltage level and voltage harmonic content, which can be useful for line maintenance and overall system performance. However this approach does not guarantee that all grouped measurements correspond to the same electrical fault or not.

Reference [17] describes an algorithm with a method to determine the distance to fault location in parallel transmission lines taking into account the mutual coupling effects between circuits of the lines by using the data from only one end of the line. The algorithm is based on modifying the impedance method using modal transformation that transforms the coupled equations of the transmission lines into decoupled equations, and thus eliminating mutual effects. This results in an accurate estimation for the distance to fault location

In reference [18] the author worked on ‘’New Accurate Fault location Algorithm for Parallel Transmission Lines.’’ With assumption that the local voltage and current are available this algorithm method fully considers the mutual coupling impedance, mutual coupling admittance and shunt capacitance with a full consideration of symmetrical components for high precision while determining the distance to fault location. The method is independent of the fault resistance, remote infeed, and source impedance and uses the values of the voltage and current from one end of the parallel line. It uses shunt capacitance based on the distributed parameter line model and mutual coupling between lines instead of the lump parameter to improve the fault distance estimation for parallel transmission lines.

Author in reference [19] presents the derivation of the equivalent π-circuit for the zero sequence networks in the double-circuit transmission line, based on the distributed parameter model. The method applies the symmetrical component transformation that result in positive-, negative-, and zero-sequence. The method also takes into account mutual coupling effect for the zero- sequence analysis and the effects of shunt capacitance as well as the ones caused by a long line.

The algorithm developed in [21] presents a method to determine the distance to fault locations in parallel transmission lines without any measurement from the healthy line circuit. The author discusses method for a new one-end fault location algorithm for parallel transmission lines which considers the flow of currents for the zero sequence and uses the relationship between the sequence components of a total fault current relevant for single phase-to ground faults. Consequently the mutual coupling effect under phase-to ground faults is reflected and considered without using the zero sequence current from the healthy line circuit.

5 CASE STUDY: PARAMETER CALCULATIONS, ERROR RANGE DETERMINATION AND DP SETTING DESIGN FOR HV PARALLEL LINE

In this chapter, we calculate parameters for a 40km long 110kV parallel/double circuit transmission line, supplied from one end (single-sided in-feed), whose phase conductors as well as the earth-wire are made of AlFe6 185mm^2. The phases L_{1a}, L_{2a}, L_{3a} and L_{1b}, L_{2b}, L_{3b} are respectively symmetric and the system is supposed to supply a balanced load. The line phase arrangement as well as the distance between different conductors are presented in Fig. 5.1.

We determine the self and mutual impedances, the impedance in symmetrical components and mutual coupling impedance, operating impedance, earth impedance, the range of error on the measured impedance with no consideration of mutual influences between the two lines, and then the distance protection measuring error caused by the effect of mutual coupling impedance, in a system with and without earth-wire for both cases of transposed and non-transposed parallel transmission lines. We specify the residual and mutual compensation factors, and compare and interpret the obtained results.

After the calculations of all necessary parameters and the determination of the error range, we propose the settings for the digital distance protection for effective and reliable protection of the above described transmission line and at the end, we test the proposed settings.

The Matlab program was used in these calculations and the used scripts are enclosed in the appendices of this work.

From Table 2 we have the conductor resistance $R_k = 0.156\,\Omega$/km and the diameter $d = 19{,}20.10^{-3}$ m thus the radius $r = 9.6.10^{-3}$ m. The correction factor $\xi = 0.809$ from Table 1.

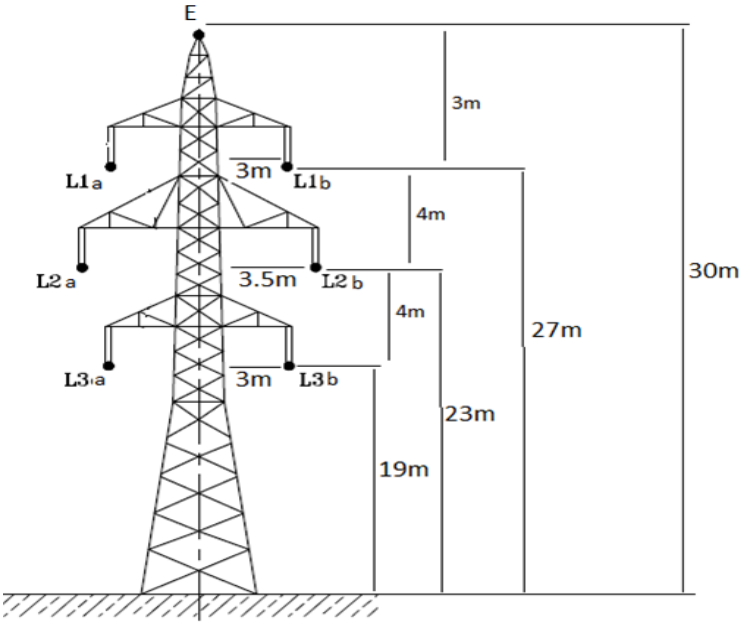

Fig. 5.1 Double-circuit transmission line 110*kV*

5.1 Calculated parameters

1.1.1 Calculated Distances between conductors

Table 5.1 *Calculated distances*

Parameter	Value (m)
$d_{1a2a} = d_{2a3a} = d_{1b2b} = d_{2b3b}$	4.03
$d_{1a3a}=d_{1b3b}$	8
$d_{1a2b} = d_{2a3b} = d_{3a2b} = d_{2a1b}$	7.63
$d_{1a3b}=d_{3a1b}$	10
$d_{1a1b}=d_{3a3b}$	6
d_{2a2b}	7
$d_{E1a}=d_{E1b}$	4.2426
$d_{E2a}=d_{E2b}$	7.826
$d_{E3a}=d_{E3b}$	11.4
d	50.65
d_{E}	7.2337

The distances were calculated directly from the given data about the distance between different conductors. Pythagorean Theorem was often applied.

5.1.1 Calculated Parameters for Non-Transposed line

These parameters were calculated according to the process described in details in the paragraph 3.2 and 3.3 of this work. The matrix impedance modification process allowed us to get parameters of the transmission lines with earth-wire (case I and II). By the process of matrix impedance transformations into symmetrical components we got the positive-, negative- and zero sequences as well as the mutual coupling impedance in zero- and positive-sequence for all the cases. Obtained results are summarized in Table 5.2.

Table 5.2 Non-transposed line calculated parameters

Line with Earth wire (Case I)		**Line with no earth wire (Case II)**	
Impedance, symmetrical components and $\overline{Z}_{0M}$		**Impedance, symmetrical components and $\overline{Z}_{0M}$**	
Parameter	**Value (Ω/km)**	**Parameter**	**Value (Ω/km)**
$\overline{Z}_1$	0.1564+j0.4056	$\overline{Z}_1$	0.156+j0.4067
$\overline{Z}_2$	0.1564+j0.4056	$\overline{Z}_2$	0.156+j0.4067
$\overline{Z}_0$	0.2846+j1.0027	$\overline{Z}_0$	0.3045+j1.3588
$\overline{Z}_{0M}$	0.1286+j0.5194	$\overline{Z}_{0M}$	0.1485+j0.8755
$\overline{Z}_M$	0.0004+j0.0163	$\overline{Z}_M$	0+j0.0175
Phase Operating Impedances		**Phase Operating Impedances**	
Parameter	**Value (Ω/km)**	**Parameter**	**Value (Ω/km)**
$\overline{Z}_{1L1}$	0.1871+j0.3908	$\overline{Z}_{1L1}$	0.1932+j0.4139
$\overline{Z}_{1L2}$	0.1767+j0.3975	$\overline{Z}_{1L2}$	0.156+j0.3923
$\overline{Z}_{1L3}$	0.1055+j0.4281	$\overline{Z}_{1L3}$	0.1188+j0.4139
Phase Actual Impedances		**Phase Actual Impedances**	
Parameter	**Value (Ω)**	**Parameter**	**Value (Ω)**
$\overline{Z}_{1L1t}$	7.4833+j15.631	$\overline{Z}_{1L1t}$	7.73+j16.5541
$\overline{Z}_{1L2t}$	7.0663+j15.8981	$\overline{Z}_{1L2t}$	6.24+j15.6939
$\overline{Z}_{1L3t}$	4.2184+j17.123	$\overline{Z}_{1L3t}$	4.75+j16.5541
Nominal Line Current (kA)		**Nominal Line Current (kA)**	
I_n	3.65	I_n	3.645
Earth Impedance		**Earth Impedance**	
Parameter	**Value (Ω/km)**	**Parameter**	**Value (Ω/km)**
$\overline{Z}_{EL1}$	0.0325+j0.2039	$\overline{Z}_{EL1}$	0.03698+j0.3148
$\overline{Z}_{EL2}$	0.03595+j0.2018	$\overline{Z}_{EL2}$	0.04946+j0.3221
$\overline{Z}_{EL3}$	0.05954+j0.1909	$\overline{Z}_{EL3}$	0.06185+j0.31498
Compensation Factors		**Compensation Factors**	
Parameter	**Value (-)**	**Parameter**	**Value (-)**
$\overline{K}_{E1}$	0.433+j0.1191	$\overline{K}_{E1}$	0.6290+j0.1958
$\overline{K}_{E2}$	0.4327+j0.0978	$\overline{K}_{E2}$	0.7143+j0.1511
$\overline{K}_{E3}$	0.4267-j0.0331	$\overline{K}_{E3}$	0.7029+j0.0500
$\overline{K}_{EM1}$	0.3911+j0.0744	$\overline{K}_{EM1}$	0.6063+j0.1569
$\overline{K}_{EM2}$	0.3913+j0.0635	$\overline{K}_{EM2}$	0.6621+j0.1312
$\overline{K}_{EM3}$	0.3905-j0.0038	$\overline{K}_{EM3}$	0.6583+j0.0665
R_E / R_L	0.2732	R_E / R_L	0.3171
X_E / X_L	0.4907	X_E / X_L	0.7803
R_M / R_L	-0.0593	R_M / R_L	0.3173
X_M / X_L	0.0935	X_M / X_L	0.3842

These residual and mutual compensation factors are very important in improving the accuracy of the distance protection measurements while protecting the parallel and double-circuit lines. They are entered while setting the device and help to avoid the underreach or overreach.

Table 5.3 Error range calculation for non-transposed line

Line with Earth wire		**Line with no earth wire**	
Angle φ		**Angle φ**	
φ_{Line}	69°	φ_{Line}	69°
φ_{K_E}	9°	φ_{K_E}	9°
Error range with no consideration of $\overline{Z}_{0M}$ (%)		**Error range with no consideration of $\overline{Z}_{0M}$ (%)**	
E_1	-3.62	E_1	1.77
E_2	-1.97	E_2	-3.54
E_3	5.58	E_3	1.77
Error due to $\overline{Z}_{0M}$ at the Line Remote End (%)		**Error due to $\overline{Z}_{0M}$ at the Line Remote End (%)**	
ε_1	33.58	ε_1	43.30
ε_2	32.38	ε_2	45.28
ε_3	31.69	ε_3	44.13

These are error ranges in the case of single phase faults. The first ones (E_1 E_2 and E_3) refer to the error caused by the non-symmetry of the line and the fact that in the DP is set the average value of the phase reactance which is not necessarily the actual reactance of the phase. These types of error do not exist in the transposed line. The last ones ($\varepsilon_1, \varepsilon_2$ and ε_3) refer to the errors caused by the effect of mutual coupling impedance in parallel and double-circuit lines. In these cases of non-transposed line it is important to consider this effect in both zero- and positive-sequence system. The graphs in Fig. 5.2 and Fig. 5.3 illustrate the variation of these error ranges with respect to the distance-to-fault location. The impedance measured by the DP D1 located on the faulted line are given by the following expressions for each phase:

Case I:

$$\overline{Z}_{\mathbf{D1L1}} = \frac{x}{l}.(0{,}433\angle 64{,}42° + j0.0163).\left[1 + 0{,}288\angle 6{,}37° \frac{x}{2l - x}\right]$$

$$\overline{Z}_{\mathbf{D1L2}} = \frac{x}{l}.(0{,}435\angle 66{,}03° + j0.0163).\left[1 + 0{,}276\angle 5{,}64° \frac{x}{2l - x}\right]$$

$$\overline{Z}_{\mathbf{D1L3}} = \frac{x}{l}.(0{,}44\angle 76° + j0.0163).\left[1 + 0{,}27\angle 1{,}1° \frac{x}{2l - x}\right]$$

Case II:

$$\overline{Z}_{D1L1} = \frac{x}{l}.(0{,}4568\angle 64{,}98° + j0.0175).\left[1 + 0{,}38\angle 7{,}9° \frac{x}{2l - x}\right]$$

$$\overline{Z}_{D1L2} = \frac{x}{l}.(0{,}422\angle 68° + 0.0175).\left[1 + 0{,}395\angle 6{,}42° \frac{x}{2l - x}\right]$$

$$\overline{Z}_{D1L3} = \frac{x}{l}.0{,}4306\angle 73{,}98°\left[1 + 0{,}385\angle 4{,}29° \frac{x}{2l - x}\right]$$

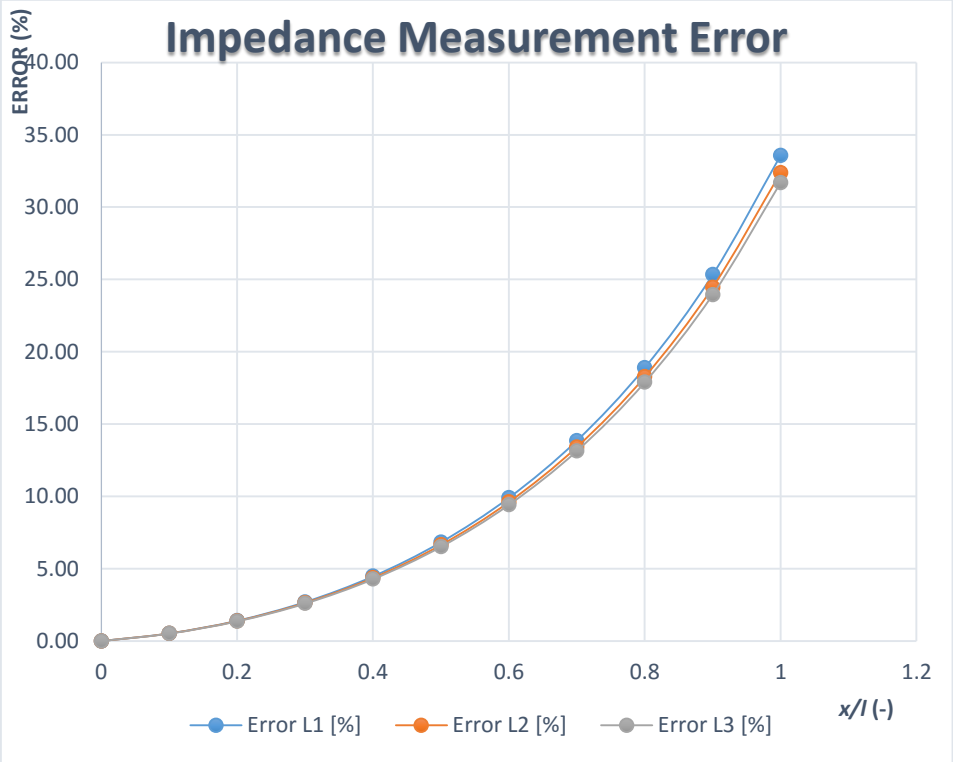

Fig. 5.2 Error range for a non-transposed parallel line with earth-wire

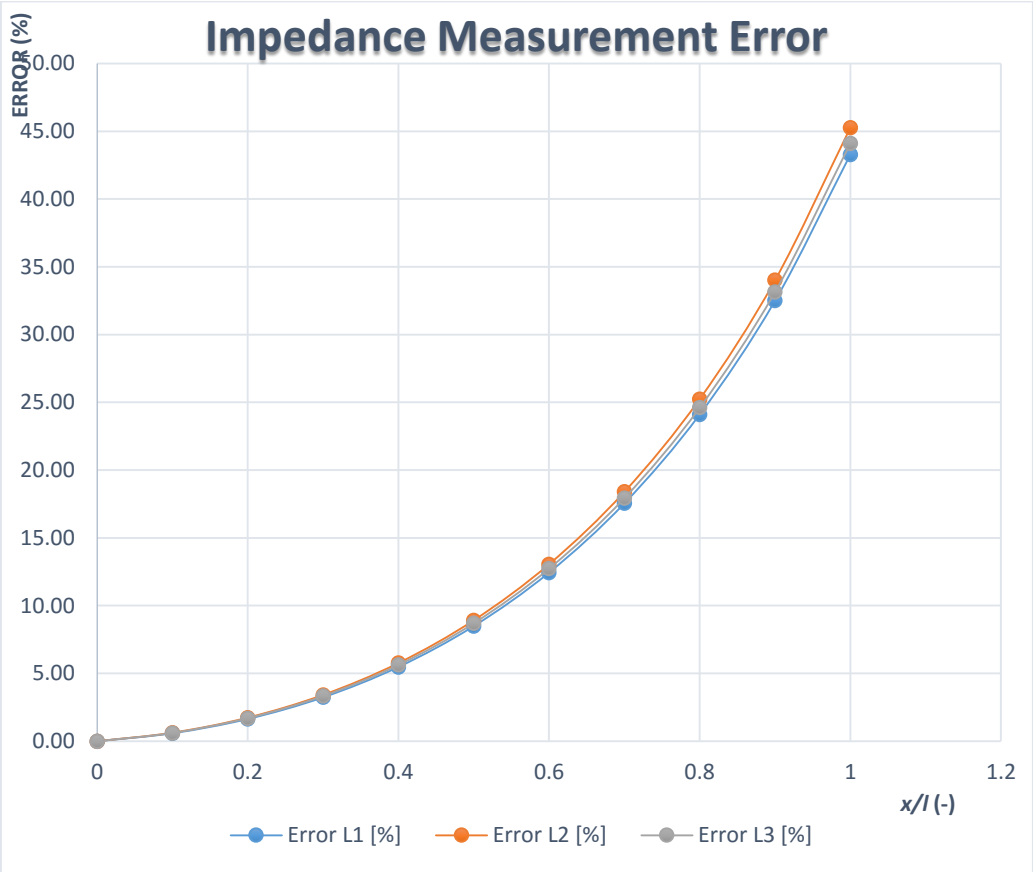

Fig. 5.3 Error range for a non-transposed parallel line without earth-wire

5.1.2 Calculated Parameters for Transposed line

The calculations were done according to the process described in details in paragraph 3.2 and 3.3 of this work.

Table 5.4 transposed line calculated parameters

Line with Earth wire (Case III)		**Line with no earth wire (Case IV)**	
Impedance, symmetrical components and $\overline{Z}_{0M}$		**Impedance, symmetrical components and $\overline{Z}_{0M}$**	
Parameter	**Value (Ω/km)**	**Parameter**	**Value (Ω/km)**
$\overline{Z}_1$	0.156+j0.4067	$\overline{Z}_1$	0.156+j0.4067
$\overline{Z}_2$	0.156+j0.4067	$\overline{Z}_2$	0.156+j0.4067
$\overline{Z}_0$	0.2846+j1.0027	$\overline{Z}_0$	0.3545+j1.3588
$\overline{Z}_{0M}$	0.1286+j0.596	$\overline{Z}_{0M}$	0.1485+j0.9521
Earth Impedance		**Earth Impedance**	
Parameter	**Value (Ω/km)**	**Parameter**	**Value (Ω/km)**
$\overline{Z}_{EL1}=\overline{Z}_{EL2}=\overline{Z}_{EL3}$	0.0429+j0.1987	$\overline{Z}_{EL1}=\overline{Z}_{EL2}=\overline{Z}_{EL3}$	0.0662+j0.3174
Phase Operating Impedances		**Phase Operating Impedances**	
Parameter	**Value in Ω/km**	**Parameter**	**Value in Ω/km**
$\overline{Z}_{1L1}=\overline{Z}_{1L2}=\overline{Z}_{1L3}$	0.156+j0.4067	$\overline{Z}_{1L1}=\overline{Z}_{1L2}=\overline{Z}_{1L3}$	0.156+j0.4067
Phase Actual Impedances		**Phase Actual Impedances**	
Parameter	**Value (Ω)**	**Parameter**	**Value (Ω)**
$\overline{Z}_{1L1t}=\overline{Z}_{1L2t}=\overline{Z}_{1L3t}$	6.24+j16.268	$\overline{Z}_{1L1t}=\overline{Z}_{1L2t}=\overline{Z}_{1L3t}$	6,24+j16.268
Nominal Line Current (kA)		**Nominal Line Current (kA)**	
I_n	3.64	I_n	3.64
Compensation Factors		**Compensation Factors**	
Parameter	**Value (-)**	**Parameter**	**Value (-)**
$\overline{K}_{E1}=\overline{K}_{E2}=\overline{K}_{E3}$	0.4611+j0.0715	$\overline{K}_{E1}=\overline{K}_{E2}=\overline{K}_{E3}$	0.7347+j0.1191
$\overline{K}_{EM1}=\overline{K}_{EM2}=\overline{K}_{EM3}$	0.4611+j0.0715	$\overline{K}_{EM1}=\overline{K}_{EM2}=\overline{K}_{EM3}$	0.7210+j0.1548
R_E / R_L	0.2748	R_E / R_L	0.4241
X_E / X_L	0.4886	X_E / X_L	0.7804
R_M / R_L	-0.0585	R_M / R_L	-0.016
X_M / X_L	0.1552	X_M / X_L	0.447

Angle φ		**Angle φ**	
φ_{Line}	72°	φ_{Line}	74°
φ_{K_E}	8.8°	φ_{K_E}	9.2°
Impedance measured by D1		**Impedance measured by DP1**	
$\overline{Z}_{D1} = \frac{x}{l}.0{,}4356\angle 69° \left[1 + 0{,}3190\angle 6° \frac{x}{2l - x}\right]$		$\overline{Z}_{D1} = \frac{x}{l}.0{,}4356\angle 69° \left[1 + 0{,}4241\angle 8.2° \frac{x}{2l - x}\right]$	
Error at the Line Remote End (%)		**Error at the Line Remote End (%)**	
ε	31.90	ε	42.41

Since the impedance is the same in all the phases of the transposed line, the error range is also the same in all of them. Fig. 5.4 compares the error range caused by the mutual coupling effect in transposed line with earth wire and transposed line without earth-wire.

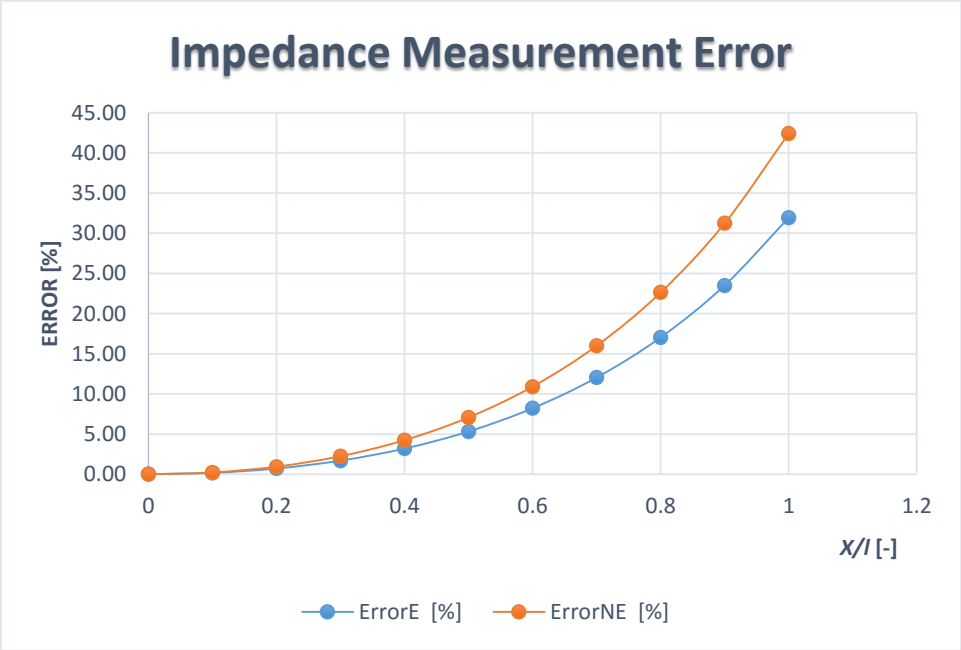

Fig. 5.4 Error range for a transposed parallel line with and without earth-wire

5.1.3 Comparison and Interpretation of the results

In the non-transposed line, the error range is 33.58%, 32.38% and 31.69% respectively in the phase one, phase and phase three of the line with earth-wire whereas it is respectively 43.30%, 45.28% and 44.13% in the line without earth-wire. Clearly the presence of the ground wire contribute to the reduction of the effect of the mutual coupling impedance.

The average values of the calculated phase operating impedances in both cases of the non-transposed parallel line (case I and II), correspond perfectly to the line positive/negative-sequence impedance obtained by the transformation of the line impedance matrix into symmetrical components impedance matrix.

In the case of transposed transmission line (case III and IV), the error range is respectively 31.90%, and 42.41% respectively in the line with earth-wire and the line without earth-wire. Again the earth-wire reduces considerably the error caused by the mutual coupling impedance.

Comparing the transposed and non-transposed line results, we discover that the error in the transposed line with earth-wire is low compared to the one in the non-transposed line with earth-wire. And similarly, the error in the transposed line without earth-wire is less than the one in the non-transposed line without earth-wire. So the transposition of the line contributes in reducing the measuring error and thus improve the measurement accuracy. As it is clearly seen from the result the error in the transposed line with ground-wire is the least.

We again noticed after transformation of the line impedances into symmetrical components in both cases, that the mutual impedances are zero in positive- and negative-sequences and high in zero sequence for the case of the transposed line. But in the case of non-transposed line, these mutual impedances are present and their impact to the impedance measurement is considerable.

5.2 Digital Distance Protection Settings for Accurate Fault Location

In the present paragraphs we propose the setting possibilities of the distance protection for effective and accurate fault location and consequently the appropriate transmission line protection. The setting of the numerical distance protection SIPROTEC 4 7SA6, SIEMENS brand will be designed, in order to protect the HV parallel transmission line calculated in the previous paragraphs of this chapter. The suggested settings apply to the four cases of the computed parallel transmission line i.e. the non-transposed line with earth wire or case one (I), the non-transposed line without earth-wire or case two (II), the transposed one with earth-wire or case three (III), and finally the transposed line without ground wire which is the case four (IV).

5.2.1 Overview on the SIEMENS SIPROTEC 4 7SA6 Distance Protection

The functioning principle of the distance protection SIPROTEC 4 7SA6 is illustrated in Fig. 5.5

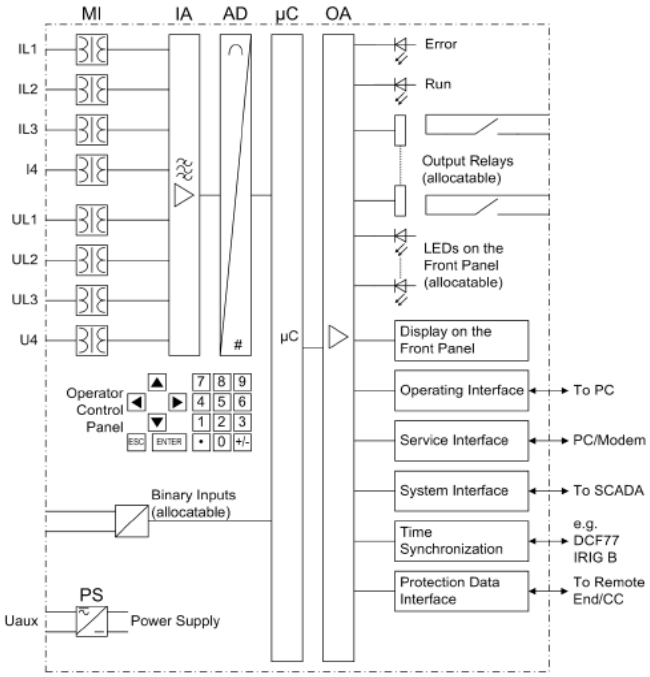

Fig. 5.5 Hardware structure of the DP 7SA6 *[23]*

The measuring input (MI) transforms the values from the instruments transformers to the internal signals for processing. This analogue values are transferred to the input amplifier group (IA) with high resistance termination. This IA is made of filters optimized for measured value processing considering the bandwidth and processing speed. Then the analogue-to-digital converter group (AD), made of converters and memory chips transfers the data to the microcomputer system (µC).

The main function of the µC is to process measured values. In addition, it also executes the actual protection and the control tasks such as: filtering, conditioning and monitoring of measured quantities; monitoring of protection functions, limit values and time sequences; signal control for logical functions; trip and close command decisions, recording messages and fault data for analysis; data storage, real time clock, communication, etc. The information is transmitted through the output amplifier (OA). Binary inputs from the computer system are transferred through the inputs/outputs modules (I/O).The outputs are trip commands and messages for remote signalling of events and states. LEDs and LC indicate what is going on in the device and measured values. Integrated control and numeric keys with LCD enable local communication with the device, facilitating thus the handling and management of configuration and parameter settings.

The serial interface allows the communication with a personal computer (PC) using the DIGSI software program and thus, all device functions can be handled conveniently.

5.2.2 Application of the SIPROTEC 4 7SA6

This device is selective and extremely fast protection for any type of overhead lines and cables such as: single- and multi-ended in-feeds in radial, ring or any kind of meshed systems at any voltage level, in either earthed, compensated or isolated system. It may also be used as time-graded back-up protection for comparison protection schemes, transformers, generators, motors and busbars. The main functions of the SIPROTEC 4 7SA6 include the protection function which is the basic function of the device. Protection of all types of short-circuits as well as earth faults with high fault resistance are provided. In addition it also ensures the multistage overvoltage protection, the undervoltage and frequency protection, the protection against the effect of power swings, thermal overload protection, etc. Using different signal transmission schemes the device can be assisted by teleprotection.

The SIPROTEC 4 7SA6 has a very wide range of functions but in the present work we will be interested only in its functions as a distance protection.

5.2.3 The setting Possibilities for the SIPROTEC 4 7SA6

The PC with the DIGSI operating software is used to enter configuration settings which can be transferred through operator interface on the device front panel or via the service interface. Function parameters and options can be modified via the front panel or PC with the software. For any configuration modification, a level 5 password is required. Normally available protection functions and additional functions are configured as *Enabled* or *disabled*, but some functions have more options. Disabled functions are not executed by the DDP.

5.2.3.1 General settings

In the distance protection SIPROTEC 4 7SA6, the functional scope with available options is configured and set in the functional scope dialog box to meet system requirements. They are clear

and easy to handle. However, some special cases need further explanations. The general and basic settings are illustrated in Table 2.1 in [23].

5.2.3.2 Distance protection 7SA6 settings and Power System Data 1

In Power System Data1 from a PC with the software DIGSI where a dialog box with tabs transformers, power system and breaker will be opened, we enter information about the situation of the power system, some rated data of substations and instrument transformers, polarity and connection of measured quantities, features of the circuit breakers.

- **Polarity of the Current Transformer**

The polarity of the Y-connected transformer is specified in address **201 CT Starpoint**. In our settings, the measuring direction is specified as forward, that is in the line direction and a change in the setting will imply a reversal polarity of the earth current input I_E or I_{EE}. The current transformer polarity for two transformer is illustrated in Fig. 6.1

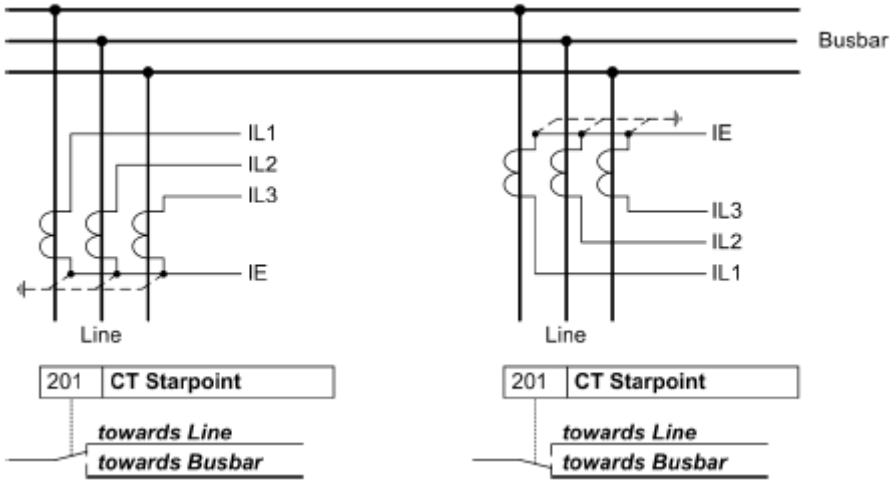

Fig. 5.6 Polarity of current transformer *[23]*

- **Settings of nominal values of the transformer**

Rated values for our instrument transformers are as follows:

VT: $U_1 = 115\text{kV};\ U_2 = 115\text{V}$

CT: $I_1 = 800\text{A};\ 1\text{A}$

These rated values of VT and CT are set respectively in the addresses **203 Unom PRIMARY, 204 Unom SECONDARY, 205 CT PRIMARY** and **206 CT SECONDARY.**

The secondary CT current must meet the rated current of the device, otherwise it will be blocked. This is verified because the nominal current and voltage for the DDP 7SA6 are respectively 1A or 5A and 80V to 125V adjustable.

- **Voltage connection**

The DDP 7SA6 has four measuring inputs for voltage. Three of them are connected to the set of voltage transformers and for the fourth voltage input U_4, we have set in the address 210 **U4 transformer** = **Not connected** because the input U_4 is not required. In this case the factor **Uph/Udelta** is important for it is used to scale measured data and record them.

- **Connection of the Current**

The DDP 7SA6 has four current measurement inputs, three of them are connected to the set of CTs, and the fourth input I_4 is connected to the earth current of the parallel line due to our interest in mutual coupling effect caused by earth currents in parallel lines as well as on impedance compensation of the device, and the fault location.

The address 220 is then set to **I4 transformer =In paral. line** and the address 221 is usually set to **I4/Iph CT=1**. In case the set of CTs on the parallel line has a different transformation ration comparing to the ones on the protected line, the address 220 must be set to: **I4 transformer = In paral. line** and the address 221 **I4/Iph CT= IN paral.line/In prot.line**. The nominal current for our transmission line is 3.64kA.

- **Setting of rated frequency:**

The power system rated frequency is set under the address 230 **Rated Frequency**. It may be set to 50Hz or 60Hz. Therefore our setting will be 50Hz which corresponds to our system frequency.

- **Setting of the System Star-point:**

The correct processing of the earth faults and double earth faults requires the consideration of the way the system star-point is earthed. So, it is to be set in the address 207 **SystemStarpoint = Solid Earthed, Peterson-Coil** or **Isolated**. Here we have set **Solid Earthed.**

- **Setting of phase rotation**

We use the address 235 **PHASE SEQ.** to change the default setting which is L1, L2, L3 for clockwise rotation if the system has a permanent anti-clockwise phase sequence L1, L3, L2. Our system has a clockwise rotation and so is our setting.

- **Setting of the Distance Unit**

In the address 236 **Distance Unit** it is set the distance unit (km or miles) for the fault location indications. Our set distance unit is kilometre (km).

- **Setting the mode of the earth impedance (residual) compensation**

For the accurate measurement of the distance to fault location when an earth fault occurs, the matching of the earth to line impedance is required. Thus, in the address 237 **Format Z0/Z1**, the residual compensation is determined. It is possible to use either the ration **RE/RL, XE/XL** or to enter the complex earth (residual) impedance factor $\overline{K}_0$.

The residual compensation factors R_E / R_L and X_E / X_L are respectively 0.2728 and 0.4903 for the case (I); 0.3169 and 0.7802 for the case (II); 0.275 and 0.4886 for the case (III), and 0.4244 and 0.7804 for case (IV).

- **Setting of Single-pole Tripping on an Earth Fault**

In the address 238 **EarthFltO/C 1p** it is specified whether the earth fault settings of single-pole tripping and blocking in the single-pole dead time are accomplished together for all stages (setting **stages together**) or separately (seting **stages separat.**). We set it to be accomplished separately. This parameter can only be modified with DIGSI under Additional Settings.

- **Setting of Trip Command Duration**

In the address 240 we set 0,03s as minimum trip command duration (**TMin TRIP CMD)**. It applies to all protection and control functions which may issue a trip command. The maximum close command **TMax CLOSE CMD** is set to 0,05s in the address 241 and applies to all close commands issued by the device.

The circuit breaker closing time **T-CB Close** is set to 0,04s in the address 239.

- **Circuit breaker test**

By a tripping and closing command, it is possible to execute a test during operation with the DDP 7SA6. We set the duration of the trip command in the address 242 (**T-CBTest-Dead**) to determine the duration from the end of the trip command until the close command for the test starts. We set it at 0,04s.

The settings of Power system Data 1 are summarized in Table 5.5, in which the addresses with letter A can be changed only with DIGSI, under Additional Settings.

Table 5.5 Power system Data 1 settings

Addres	Parameter	Setting	Comments
201	CT Starpoint	Towards Line	CT Star-point
203	Unom PRIMARY	115 kV	Rated primary voltage
204	Unom SECONDARY	115 V	Rated Secondary voltage (Ph-Ph)
205	CT PRIMARY	800 A	CT rated primary current
206	CT SECONDARY	1A	CT rated secondary current
207	SystemStarpoint	Solid Earthed	System star-point
210	U4 Transformer	Not connected	U_4 voltage transformer
211	Uph / Udelta	1.73	Matching ratio ph-VT To open-delta-VT
220	I4 transformer	I neutral paral. Line	I_4 Current Transformer
230	Rated Frequency	50 Hz	Rated Frequency
235	PHASE SEQ.	L1 L2 L3	Phase Sequence
236	Distance Unit	Km	Distance measurement Unit
237	Format Z0 / Z1	0.2728 ; 0.4903 (I) 0.3169; 0.7802(II) 0.275; 0.4886 (III) 0.4244; 0.7804(IV)	Setting format for zero sequence compensation
238A	EarthFlitO/C 1P	Stages separat.	Earth fault O/C: Setting 1pole
239	T-CB Close	0.04s	Closing (operating) time for BC
240A	TMin TRIP CMD	0.03s	Minimum Trip Command
241A	TMax TRIP CMD	0.05s	Maximum Trip Command
242	T-CBtest-dead	0.04sec	Dead time for CB test-AR

5.2.3.3 System Settings and Power System Data 2

In Power System Data 2 are found settings related to all functions, rather than a given specific protection, monitoring or control function.

The rated primary voltage and current values of the protected transmission line (110kV and 3.64kA) are respectively entered in the addresses 1103 **FullScaleVolt.** and 1104 **FullScaleCurr.**

The line angle is set in the address 1105 **Line Angle**. This angle is determined from the line parameters and is set as 69° for all the cases.

In the address 1211 **Distance angle** the inclination angle of the R section of the DP polygons is specified. Usually the same angle as in address 1105 is set there. Thus we set it to 69° for all cases.

In the address 1107 **P, Q sign**, we set the power flow direction as **not reserved,** because it must correspond to the device polarity as set in the Power System Data 1, i.e. in the forward or line direction, and compared to the polarity of CTs in the address 201.

In the address 1110 the protected line reactance X' is set 0.4056Ω/km for the case (I), and 0,4067Ω/km for the cases (II), (III) and (IV).

And in the address 1111 **Line Length**, we set 40km as the length of the protected line.

- **Zone setting**

We set three zones, zone one, zone two and zone three respectively at 85%, 120% and 240% of the actual line reactance in ohms (Ω). Zones one and two are set in the forward direction and zone three in both directions as illustrated in Table 5.6

Table 5.6 *Zone settings*

	Case I		**Case II,III, IV**		**Set time (ms)**
	R (Ω)	**X(Ω)**	**R(Ω)**	**X(Ω)**	
Zone 1 (85%)	4,2541	11,0323	4,2432	11,0622	50
Zone 2 (120%)	6,006	15,575	5,99	15,6173	120
Zone 3 (240%)	12,012	31,15	11,981	31,236	125

- **Setting of Earth to line impedance ratio**

This setting is very important for the accurate measurement of the distance to fault location when earth faults occur. The realization of this compensation is achieved either by setting the resistance ratio R_E/R_L and reactance ratio X_E/X_L or by entering the complex earth (residual) compensation factor $\overline{K}_0$. This is set in the address 237 **Format Z0/Z1**.

- **Earth Impedance Compensation by Scalar factors R_E/R_L and X_E/X_L**

Ratios R_E/R_L and X_E/X_L are entered in the addresses 1116 to 1119. These earth residual compensation factors were respectively set as 0.2732 and 0.472 for case (I); 0.3173 and 0.7482 for case (II); 0.2748 and 0.4885 for case (III) and 0.4241 and 0.7803 for case (IV). These settings are for the first zone Z1 and are entered in the addresses 1116 **RE/RL(Z1)** and 1117 **XE/XL(Z1)** as the data of the protected line.

- **Earth Compensation with Magnitude and Angle ($\overline{K}_0$ factor)**

In case the complex compensation factor $\overline{K}_0$ is set in the addresses 1120 to 1123, the DDP 7SA6 will need the line angle which is correctly set in the address 1105, to determine the compensation components from $\overline{K}_E$.

The compensation factor K_E, the corresponding angle, and its quadrant are set respectively to 0.3969 with angle of 6.4° in the first quadrant for the case (I), 0.6549 with an angle of 10.56° in the first quadrant for the case (II), 0,467 with angle of 8.8°in the first quadrant for the case (III) and 0.7374 with an angle of 12.12°in the first quadrant for the case (IV).

- **Parallel Line Mutual Impedance**

The mutual coupling factors R_M / R_L and X_M / X_L are set respectively to -0.0676 and 0.077 for case (I), -0.016 and 0.3546 for the case (II), -0.05855 and 0.1552 for the case (III) as well as -0.016 and 0.447 for the case (IV) are respectively entered in the addresses 1126 **RM/XL paralLine** and 1127 **XM/XL paralLine**.

In the address 1128 **RATIO Par.Comp** is set at 60% for the case (I) and (III) with very low ratio and 80% and 85% respectively for the case (II) and the case (IV) with relatively high ratio

- **Current transformer saturation**

The DDP 7SA6 has a saturation detector to determine the measuring errors caused by the saturation of the CTs and introduce the measurement method modification in the distance protection.

In the address 1140 **I-CTsat.Thres** we set the value of 150A as the threshold above which the saturation detector picks up. This parameter can only be altered in DIGSI at **Display Additional Settings**.

- **Circuit Breaker Status**

Different protection functions require information about the CB state for their proper operation.

In the address 1130 the residual current **PoleOpenCurrent** is set at 1A, which will definitely not be exceeded when the circuit breaker pole is open.

This parameter can only be altered in DIGSI at **Display Additional Settings**.

In the address 1131the residual voltage **PoleOpenVoltage**, which will definitely not be exceeded when the circuit breaker pole is open, is set at 45V.

This parameter can only be altered in DIGSI at **Display Additional Settings**.

In the address 1132 the switch-on-to-fault activation (seal-in) time **SI Time all Cl.** is set to 0,08s to determine the activation duration of the enabled protection functions whenever the line is switched on. This time is started by the internal CB switching detection after the information about the line's switching on, or by the CB auxiliary contacts, in case they are connected to the DP through binary input to transmit information that the CB has closed.

This parameter can only be altered in DIGSI at **Display Additional Settings**.

In the address 1134 **Line Closure** we set **CB OR I or M/C** implying that either the currents or the states of the circuit breaker auxiliary contacts are used to determine closure of the CB.

Before each line is detected as switched on, the breaker must be recognized as open for the time of 0,15s as set in the address 1133 **T DELAY SOTF**.

In the address 1135 **Reset Trip CMD** we decide in which situation a trip command is reset. Here we set it as **CurrentOpenPole** and it means that whenever the current is off.

Since the time **SI Time all Cl.** In the address 1132 above is activated following each recognition of the line switching on, **SI Time Man.Cl** of 0,20s is set in the address 1150 as the time following the manual closure in which special influence of the protection functions is activated. This parameter can only be altered in DIGSI at **Display Additional Settings**.

In the address 1136 **OpenPoleDetect.** we define the criteria for operating for the internal open-pole detector by setting **w/ measurement**, to evaluate all available data that indicate single-pole dead time.

In the address 1151 **MAN. CLOSE** we specify the manual closure of the circuit breaker via binary inputs, by setting it as **MAN. CLOSE = w/o Sync-check** because no synchronism check is supposed to be performed with manual closing.

For commands via the integrated control the address 1152 **Man.Clos. Imp.** is set as **NONE** to ensure that the close command via the control will not generate a MANUAL CLOSE impulse for the protection function.

- **Three-pole Coupling Setting**

This is considered because we have set single-pole auto-reclosure command, otherwise tripping is always three-pole. In the address 1155 **3pole coupling** is set to determine whether for any multi-phase pickup there will be a three-pole tripping command or whether only multi-pole tripping decisions will result in a three-pole tripping command. We set it **with TRIP** meaning that the three-pole coupling of the trip output occurs only when more than one pole is tripped. So it is more selective.

In the address 1156 **Trip2phFlt** is set that the protection command a single-pole trip in case of isolated two phase faults when the single-pole tripping is possible. It is possible to specify whether the leading phase (**1pole leading ϕ**) or lagging (**1pole lagging ϕ**) is tripped. In our case we chose to trip the leading phase.

Table 5.7 summarizes the Power System Data 2 settings in which the addresses with letter A can only be changed with DIGSI, under Additional Settings.

Table 5.7 *Power System Data 2 Settings*

Address	Parametr	Settings	Comments
1103	FullScaleVolt.	115 kV	Measurement: Full ScaleVoltage (100%)
1104	FullScaleCurr.	800A	Measurement:Full ScaleCurrent (100%)
1105	Line Angle	69°(I,II); 72°(III) 74°(IV)	Line Angle
1107	P,Q sign	Not reversed	P,Q operational values sign
1110	x‘	0.4056Ω/km (I); 0,4067Ω/km (II) 0.4067Ω/km (III);	x' - Line Reactance per length unit
1111	Line Length	40 km	Line Length
1116	RE/RL (Z1)	0.2732 (I); 0.3173 (II); 0.2748 (III); 0.4241 (IV)	Zero seq. comp. factorRE/RL for Z1
1117	XE/XL (Z1)	0.4598 (I); 0.7344 (II); 0.4885 (III); 0.7803 (IV)	Zero seq. comp. factorXE/XL for Z1
1120	K0 (Z1)	0.3969 (I); 0.6549 (II); 0.467 (III); 0.7374 (IV)	Zero seq. comp. factor K0 for zone Z1
1121	Angle K0 (Z1)	6.4° (I); 10.56° (II); 8.8° (III); 12.12° (IV)	Zero seq. comp. angle forzone Z1
1126	RM/RLParalLine	-0.0676 (I); -0.016 (II); -0.05855 (III); -0.016 (IV)	Mutual Parallel Line compensation ratio RM/RL
1127	XM/XLParalLine	0.077 (I); 0.3546 (II); 0.1552 (III); 0.447 (IV)	Mutual Parallel Line compensation
1128	RATIO Par.Comp	60% (I); 80% (II); 60% (III); 85% (IV)	Neutral current RATIOParallel Line Comp
1130A	PoleOpenCurrent	1A	Pole Open Current
113A	PoleOpenVoltage	45V	Pole OpenVoltageThreshold
1132A	SI Time all Cl.	0.08s	Seal-in Time after ALL
1133A	T DELAY SOTF	0.15s	minimal time for line openbefore SOTF
1134	Line Closure	only with ManCl	Recognition of Line
1135	Reset Trip CMD	CurrentOpenPole	RESET of Trip Command
1136	OpenPoleDetect.	w/ measurement	open pole detector
1140A	I-CTsat. Thres.	30A	CT Saturation Threshold
1150A	SI Time Man.Cl	0.20s	Seal-in Time after MANUAL closures
1151	MAN. CLOSE	w/o Sync-check	Manual CLOSE COMMAND generation
1152	Man.Clos. Imp.	NONE	MANUAL Closure Impulseafter CONTROL
1155	3pole coupling	with TRIP	3 pole coupling
1156A	Trip2phFlt	(1pole leading ϕ)	Trip type with 2phase Faults

5.3 Test and Measurements

The proposed settings in the previous paragraph were used to configure the distance protection Siemens SIPROTEC 7SA610. Using the PC with the software DIGSI and OMICRON we have tested them. In this work we presented as an example, the tests conducted in the transposed line with earth-wire (case III) for single-phase faults. The procedure steps as well as the tests results are given below.

5.3.1 Procedure steps

After the connection of all the devices and their interconnection, we opened the software DIDSI on the PC. We created our new project and decided the mode of operation we wanted to use whether it was online or offline and the serial interface we use between the front and the back. In our new project we opened the dialogue box of Power System data1 and we entered the settings about the power system, transformers and circuit breaker as shown in Fig. 5.7

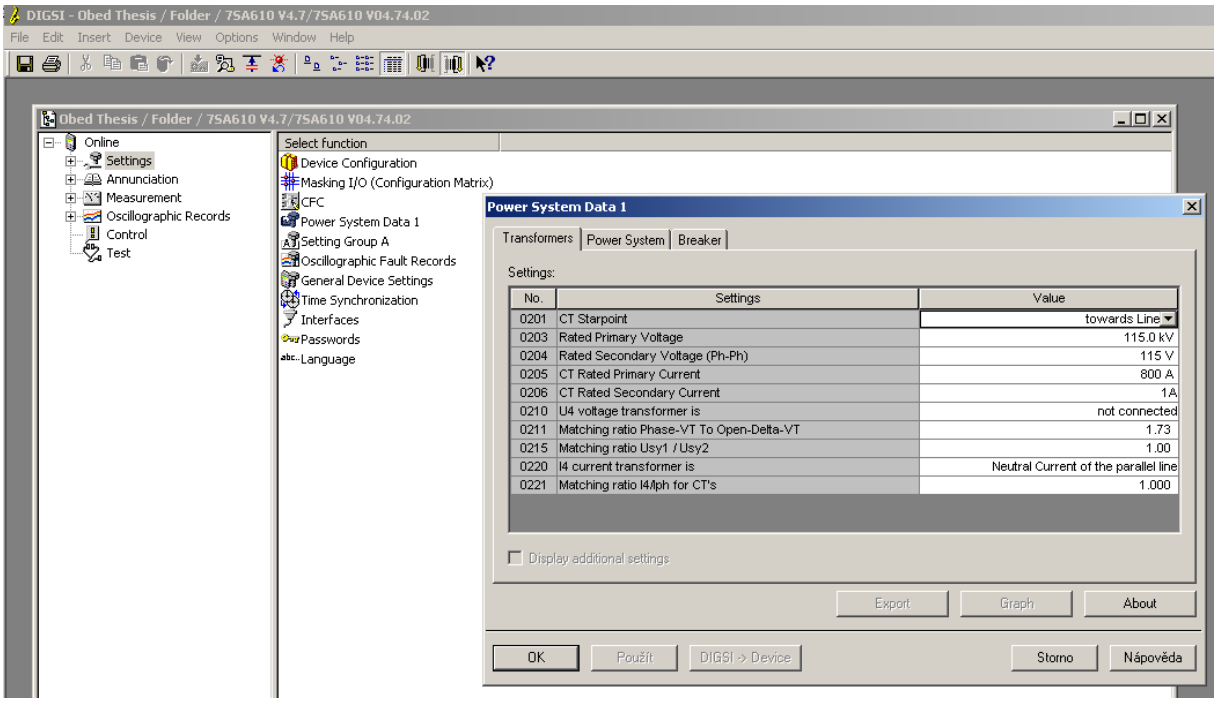

Fig. 5.7 Power System Data 1

After setting the power system data1, we opened the file of Setting Group A where we entered all settings about power system data 2, distance protection general settings and we defined there the distance zones. Fig. 5.2 illustrates this step with an example of setting the power system data 2.

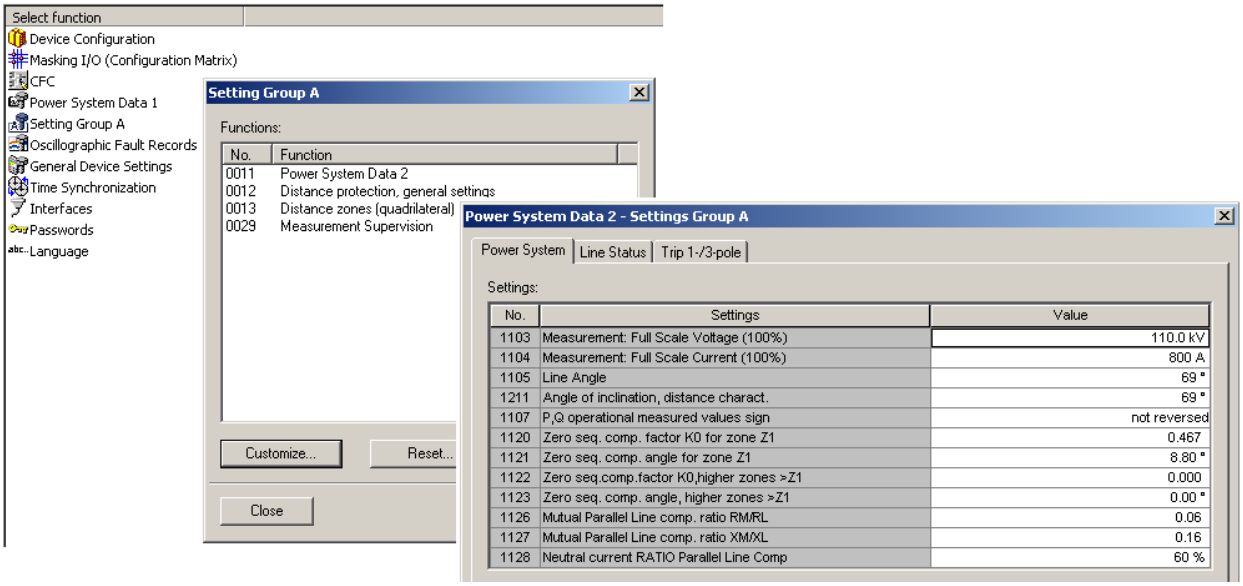

Fig. 5.8 Setting Group A

After entering all settings we sent them to the distance protection through a serial interface connection between the PC and the distance protection and exported them to OMICRON as an XRION file saved in a different folder on the PC. Fig. 5.3 illustrates the process.

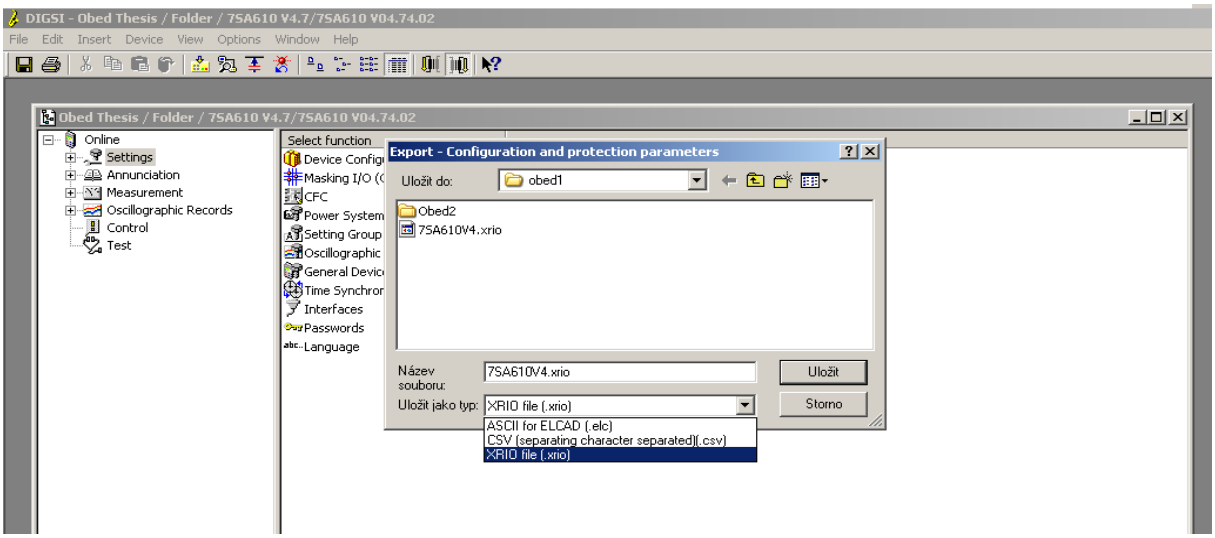

Fig. 5.9 Export-Configuration and Protection Parameters

In the next step we opened OMICRON in the folder Test Universe Start Page on the PC and we went to Distance and then to Advanced Distance. It opened a dialogue box in which we opened the XRIO files and we got the protection zones we had set in the DIGSI, and then we started the tests in different points corresponding to different impedances/lengths. Fig. 5.4 illustrates this process.

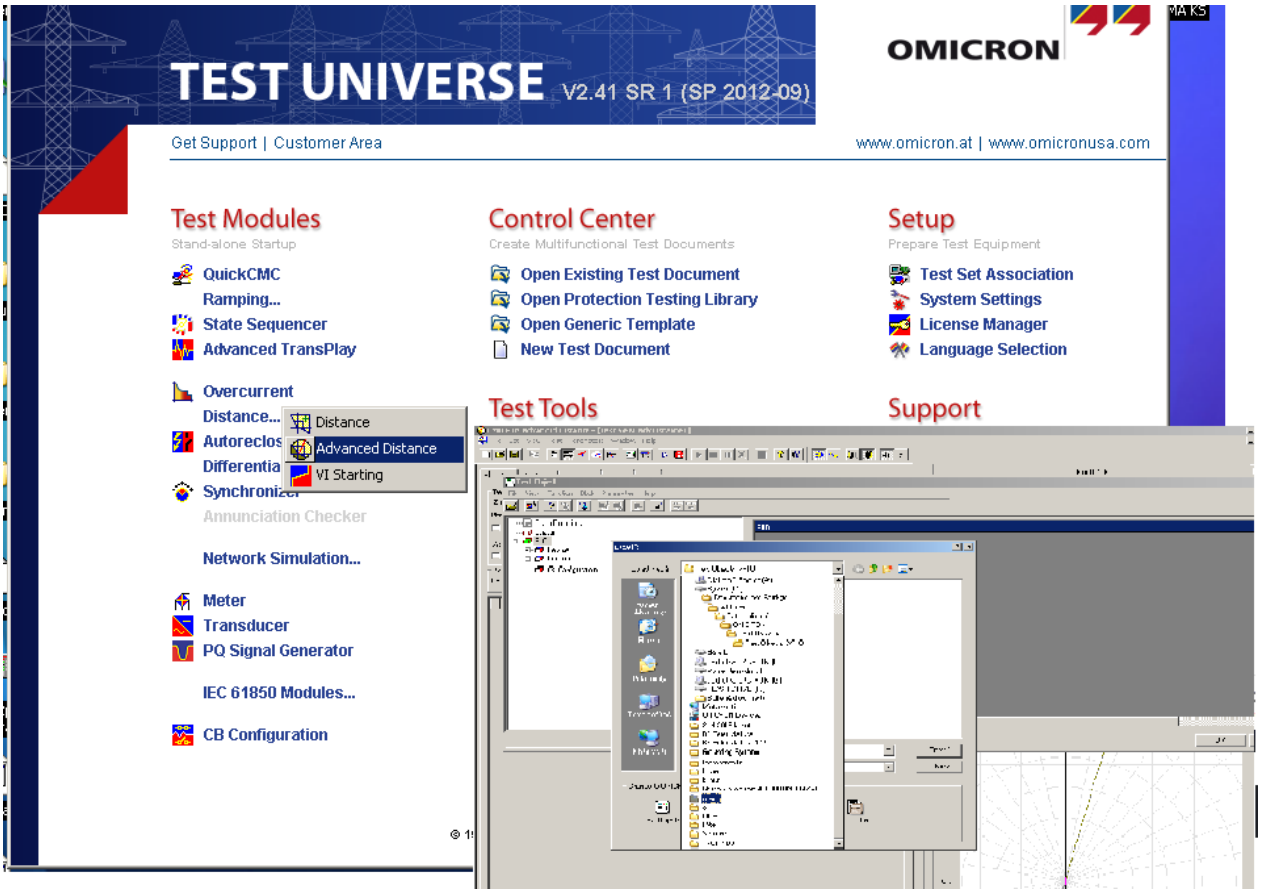

Fig. 5.10 Test Universe OMICRON

5.3.2 Tests Results

The results of the test are summarized in Table 5.8 and shown in Fig. 5.11. The green cross means that the test in that point was successfully conducted and the fault at was correctly cleared while the red one means that the test failed. To any point in zone one and two, the distance protection reacted correctly according to the settings but for some faults in zone three for example the fault number 4 and 18 in Table 5.8, the test failed. This means that the DP was not able to clear them, they may be cleared by other distance protections which have them in their first or second zone.

Even though our testing process has been a success, we faced some technical problems. For example there was a communication problem between the used devices (PC with DIGSI, DP and OMICRON). Most of times we noticed that the entered settings in DIGSI were not perfectly transferred to the DP and exported to OMICRON through the XRIO file, and thus the DP was measuring with wrong settings. To correct that we changed manually the settings in OMICRON to harmonize them with the ones we had set in DIGSI. That can be seen even in our results were the set delay time of 5ms was neglected in the third zone and the DP used the same set time of 120ms as in the second zone. It was also not possible for us to test faults at longer distances near the remote end of the third zone, due to some limitation settings of the DP that we have not yet been able to change. But since research is a continuing process, we will continue to work on that.

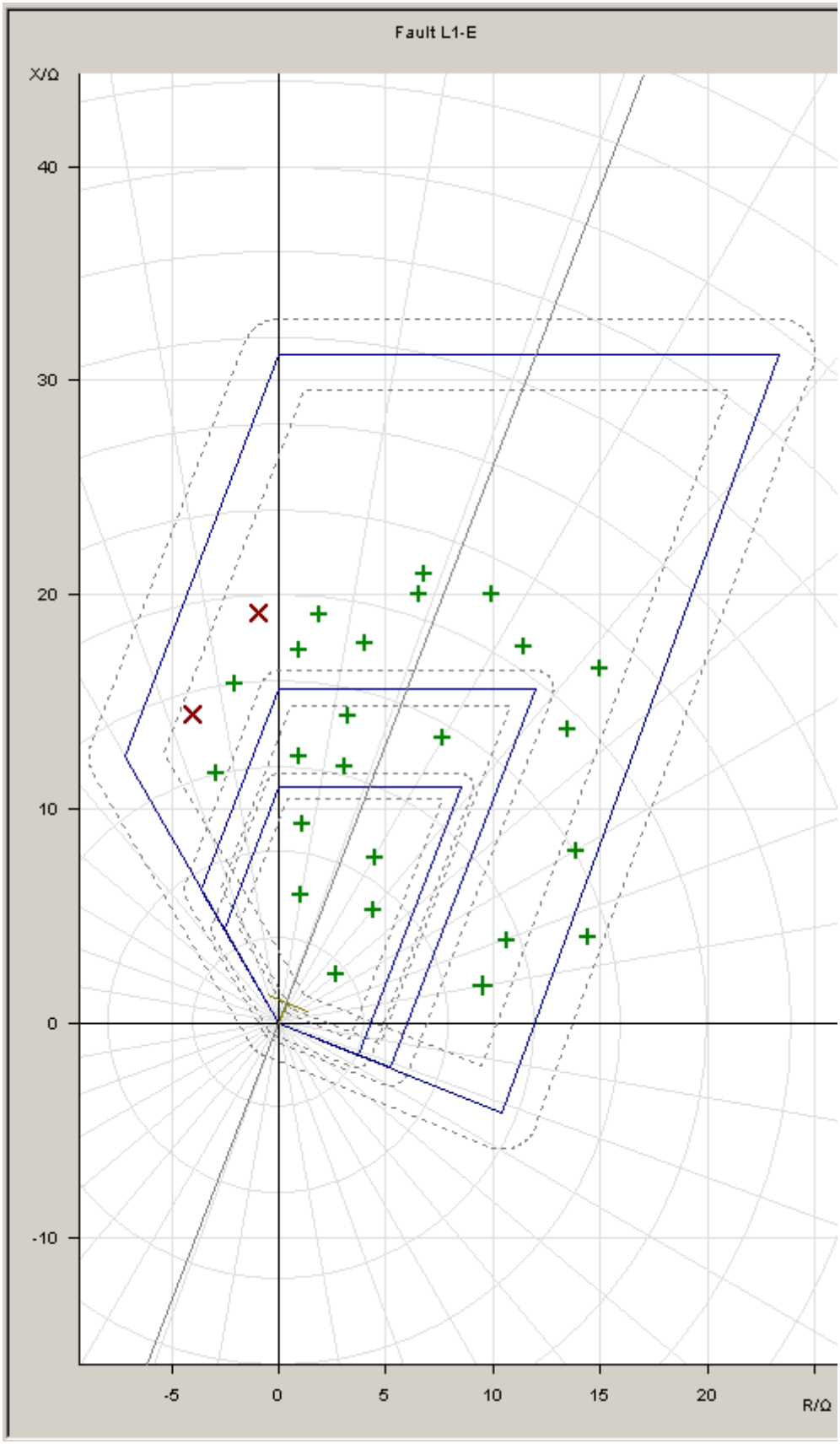

Fig. 5.11 Protection Zones and Tests

Table 5.8 Test Results

	State	|Z|	Phi	%	% of	t nom	t act.	Dev.	t min	t max
1	✚	22.04 Ω	72.07 °	n/a		120.0 ms	184.4 ms	53.67 %	-30.00 ms	270.0 ms
2	✚	21.04 Ω	71.87 °	n/a		120.0 ms	154.2 ms	28.5 %	-30.00 ms	270.0 ms
3	✚	22.33 Ω	63.57 °	n/a		120.0 ms	154.0 ms	28.33 %	-30.00 ms	270.0 ms
4	✖	19.17 Ω	92.83 °	n/a		120.0 ms	no trip		-30.00 ms	270.0 ms
5	✚	19.17 Ω	84.33 °	n/a		120.0 ms	154.5 ms	28.75 %	-30.00 ms	270.0 ms
6	✚	18.18 Ω	77.29 °	n/a		120.0 ms	153.6 ms	28 %	-30.00 ms	270.0 ms
7	✚	19.23 Ω	45.46 °	n/a		120.0 ms	154.2 ms	28.5 %	-30.00 ms	270.0 ms
8	✚	16.00 Ω	30.00 °	n/a		120.0 ms	no trip		-30.00 ms	no trip
9	✚	11.33 Ω	20.00 °	n/a		120.0 ms	154.0 ms	28.33 %	-30.00 ms	270.0 ms
10	✚	14.98 Ω	15.49 °	n/a		no trip	no trip		-30.00 ms	no trip
11	✚	15.35 Ω	60.00 °	n/a		120.0 ms	154.6 ms	28.83 %	-30.00 ms	270.0 ms
12	✚	14.70 Ω	77.29 °	n/a		120.0 ms	154.2 ms	28.5 %	-30.00 ms	270.0 ms
13	✚	17.44 Ω	86.89 °	n/a		120.0 ms	154.5 ms	28.75 %	-30.00 ms	270.0 ms
14	✚	20.97 Ω	56.94 °	n/a		120.0 ms	153.8 ms	28.17 %	-30.00 ms	270.0 ms
15	✚	12.48 Ω	85.65 °	n/a		120.0 ms	153.8 ms	28.17 %	-30.00 ms	270.0 ms
16	✚	12.39 Ω	75.62 °	n/a		120.0 ms	154.1 ms	28.42 %	-30.00 ms	270.0 ms
17	✚	12.00 Ω	104.25 °	n/a		120.0 ms	169.3 ms	41.08 %	-30.00 ms	270.0 ms
18	✖	14.96 Ω	105.51 °	n/a		120.0 ms	no trip		-30.00 ms	270.0 ms
19	✚	8.926 Ω	60.00 °	n/a		50.00 ms	69.40 ms	38.8 %	-100.0 ms	200.0 ms
20	✚	6.863 Ω	50.00 °	n/a		50.00 ms	48.80 ms	-2.4 %	-100.0 ms	200.0 ms
21	✚	6.092 Ω	80.00 °	n/a		50.00 ms	49.50 ms	-1 %	-100.0 ms	200.0 ms
22	✚	3.512 Ω	40.00 °	n/a		50.00 ms	44.10 ms	-11.8 %	-100.0 ms	200.0 ms
23	✚	9.355 Ω	83.22 °	n/a		50.00 ms	63.80 ms	27.6 %	-100.0 ms	200.0 ms
24	✚	16.00 Ω	97.35 °	n/a		120.0 ms	153.9 ms	28.25 %	-30.00 ms	270.0 ms
25	✚	22.33 Ω	47.83 °	n/a		120.0 ms	154.0 ms	28.33 %	-30.00 ms	270.0 ms
26	✚	9.712 Ω	10.00 °	n/a		120.0 ms	154.4 ms	28.67 %	-30.00 ms	270.0 ms

6 CONCLUSION

Distance protection constitutes the basis for network protection in transmission lines as well as interconnected and complex distribution networks, where it ensures reliable services not only as the main protection for the overhead lines and cables but also as backup protections for other parts of the network, such as bus bars, transformers and other feeders. Its functioning principle is based on the measurement and the evaluation of short-circuited loop impedance from the measured voltage and current provided by voltage and current transformers (VTs and CTs) situated at the relay location. This impedance is compared to the pre-set line impedance in the device. Numerical distance protection operates as the most sensitive, rapid and highly selective protecting device and provides considerable economical and technical advantages.

However, when protecting parallel and double-circuit lines, the distance protection faces a number of factors which influence negatively its operation, and thus affect its accurate determination of the measured impedance. This then results in inaccurate distance-to-fault location determination. These factors include the effect of mutual coupling impedance, cross-country faults, a current reversal phenomenon, fault resistance, intermediate in-feed, earthed transformers, T-outgoing feeders as well as the non-symmetry of the line. All of these factors cause the distance relay to over-reach or under-reach.

In order to handle the problem of inaccurate calculation of distance-to-fault location different methods are applied. These methods include the proper adjustment of the relay settings taking into consideration the existence of the fault resistance and the use of adequate distance relay with enough resistive reserve (e.g. distance protection with quadrilateral characteristic); the proper setting of the residual compensation factors, in the distance protection corrects inaccuracy caused by intermediate in-feeds, earthed transformers and T-outgoing feeders. The line transposition avoids the non-symmetry of the line; the use of a more conductive earth-wire and the proper setting of the mutual compensation factor reduce considerably the effect of mutual coupling impedance for parallel and double-circuit lines.

The method of H parameters which uses the Blondel's constant and relies on handling line parameters for a system with lines or line-segments in cascade allows us to determine the actual impedance of the faulted segment, which makes possible to determine the distance-to-fault location accurately. It is also possible to apply one of different available algorithms to solve a specific problem in order to get the accurate operation of the distance protection.

Present research-work deals with the distance protection for parallel and double-circuit HV lines. As the main objectives, we analysed the problems of accurate fault location in this specific type of lines where parameters are no longer homogeneous. We also explored the current state of methods adopted improve locator accuracy. We developed a theory to determine different parameters necessary for designing the line protection and determining the measuring error range. In the case study, we applied the theory to compute the given HV parallel line, proposed its setting design, and used it to configure the distance protection 7SA610 for the effective protection of the line. Finally, we successfully tested the proposed settings using the PC with an appropriate software DIGSI and the OMICRON

The calculations were conducted for four different cases of the given line: the non-transposed line with the earth-wire (case I), the non-transposed line without the earth-wire (case II), the transposed line with the earth-wire (case III) and the transposed line without the earth-wire (case IV). The calculated line impedances in the positive-/negative-sequence system were 0.1564+j0.4056 Ω/km for the case I and 0.156+j0.4067 Ω/km for the rest of the cases. The zero-sequence impedances obtained were 0.2846+j1.0027 Ω/km for the cases I and II, 0.3045+j1.3588 Ω/km for the case III, and 0.3545+j1.3588 for the case IV. The mutual impedance in zero-sequence system were 1286+j0.5194 for the case I, 0.1485+j0.8755 for the case II, 0.1286+j0.596 for the case III, and 0.1485+j0.9521 for the case IV. We found that the mean value of the calculated operating phase impedances in the non-transposed line (case I and II) corresponds perfectly to the respective line impedance in the positive-sequence.

The mutual coupling impedance in the positive and the negative sequence was found equal to zero in the transposed line and only the zero sequence of the mutual coupling impedance was to be considered in further protection calculations. But in the non-transposed line the mutual coupling impedance in the positive-/negative-sequence was 0.0004+j0.0163 Ω/km for the case I and j0.0175 Ω/km for the case II and these impedances were to be considered in the protection calculation, because they have a considerable impact on the DP measured impedance. The modules of residual and mutual compensation factors obtained were respectively 0.4388 and 0.3938 for the case I (mean value), 0.6948 and 0.6529 for the case II (mean value), 0.467 and 0.467 for the case III, and 0.443 and 0.7374 for the case IV. The error range caused by the non-symmetry of the line in different phases for the non-transposed line was E_1 = -3.62%, E_2 = -1.97%, E_3 =5.58% and E_1 =1.77%, E_2 = -3.54% E_3 =1.77% respectively for the case I and the case II. This errors were completely eliminated by the line transposition. The error range caused by the effect of mutual coupling impedance was 33.58%, 32.38%, 31.69% and 43.30%, 45,28%, 44.13 respectively for each phase of the case I and the case II and 31.90% and 42.41% respectively for the cases III and IV.

From these results, it is clear that the transposition of the line eliminates the non-symmetry of the line and improves the accuracy of the line protection. Since the highest error is found in the non-transposed line without the earth wire and the least error in the transposed line with the earth wire, we conclude that the line transposition and the use of a more conductive earth-wire reduce remarkably the effect of mutual coupling impedance and the non-symmetry of the line. This supports the assumption that the line transposition and the more conductive ground-wire restore the balance nature of the system.

The setting of modern numerical distance protections provides the possibility to compensate the effect of mutual coupling impedance, with the possibility of adequate settings of a tripping mode that can handle cross-county faults and current reversal phenomena occurring in parallel and double circuit lines. Therefore, digital distance protection, correctly set and used in a transposed parallel and double circuit line with more conductive earth-wire, can compute correctly the distance-to-fault location, ensuring thus effective and reliable protection to the transmission line.

REFERENCES

[1] Ziegler, G.: Numerical Distance Protection- Principles and Applications, Publicis Publishing, 2011, 378 pages, ISBN 978-3-89578-381-4

[2] Tlustý, J., Kyncl J., Musil, L., Špetlík, J., Švec, J., Hamouz, P., Müller, Z., Müller, M.: Monitorování, řizení a chránění elektrizačních soustav, české vysoké učení technické v Praze, Praha 2011, 255p

[3] Walter, D.: Protective Relay- Theory and Applications, ABB Power T`§D Company Inc, Marcel Dekker, Inc, New York 1994.

[4] Chris, W.: Transmission Line Protection End-to-end Testing series, online available on: https://www.youtube.com/watch?v=s_IrsNHv4aQ

[5] Apostolov, A., Tholomier, D., Sambasivan S., Richards S.: Protection of Double circuit Transmission lines, online available on:

www.pacw.org/fileadmin/doc/DoubleCircuitProtection.pdf

[6] Cherif, M.: Calcul des protections d'une linge de transport électrique THB-220kV,Université de Kasdi Merbah, Mémoire pour le Master académique, Ouargla,2014, 85p

[7] Colin, R., Brian J.: Transmission and Distribution Electrical Engineering Technology & Engineering -2012-1145pages available online on:

https://books.google.cz/books?isbn=0080969127

[8] Christopoulos, C., Wright A.: Electrical Power System Protection**,** Technology & Engineering, Springer-Science+Business Media, B.V, Nottingham UK, 1999 ,599p

[9] Distance Relays, online document, available on

http://www.gegridsolutions.com/Multilin/notes/artsci/art04.pdf

[10] Calero, F.: Mutual Impedance in Parallel Lines – Protective Relaying and Fault Location, Engineering laboratories,Inc, Florida 2015.

[11] Pritchard, C., Hensler,T.:Test and Analysis of Protection Behaviour on Parallel Lines with Mutual Coupling, OMICRON electronics GmbH, 2014.

[12] George E., Mooney J., Tyska W.: Advanced Application Guidelines for Ground Fault Protection, Schweitzer Engineering Laboratories, Inc, Washington, 2001.

[13] Toman, P., Drápela, J., Mišak, S., Orságova J., Paar, M. Topolánek, D.:Provoz distribučních soustav, ČVUT v Praze, Praha, 2011, 264p.

[14] BARTOŠ, P.: Výpočet nastavení distančních ochran v síti 110 kV, Vysoké učení technické v Brně, Fakulta elektrotechniky a komunikačních technologií, Brno 2012. 78p.

[15] Gopalakrishnan, A., Kezunovic, M., McKenna, S., Hamai D.: Fault Location Using the Distributed Parameter Transmission Line Model, IEEE transactions on power delivery, vol. 15, no. 4, october 2000

[16] Tremblay M., Pater R., Zavoda, F., Valiquette, D., Simard, G., Daniel, R. Germain,M., Bergeron,F.: Accurate Fault-Location Technique Based On Distributed Power-Quality

Measurements, Hydro-Québec – Canada 19th International Conference on Electricity Distribution Vienna, 21-24 May 2007, Paper 0615

[17] Kawady, T., Stenzel, J.: A practical Fault Location Approach for Double Circuit Transmission Lines Using Single End Data, IEEE

[18] Chaiwan, P.: New Accurate Fault location Algorithm for Parallel Transmission Lines, University of Kentucky, Lexington, 2011, 97P

[19] Liao, Y.: Equivalent PI Circuit For Zero-Sequence Networks Of Parallel Transmission Lines, Electric Power Components and Systems.

[20] Grainger, j., Stevenson, W.: Power System Analysis, McGraw-Hill, Inc., New York, USA, 1994.

[21] Kawecki, R., Izykowski, J.: Locating faults in parallel transmission lines under lack of measurements from the healthy line circuit, Proceedings of the 95 Universities Power Engineering Conference, v36 UPEC 2001, 36th Universities, Power Engineering Conference, 2001, p 1635-1639.

[22] Hodinka, M., Fecko, Š., Němeček, F.: Přenos a rozvod elektrické energie, SNTL – Nakladatelství technické literatury, n.p. Praha 1989, 323p, ISBN 80 – 03 – 00065 –

[23] SIPROTEC, 7SA6, Manual, online text. Siemens AG, 2013. 762 p. Available on WWW: http://w3.siemens.com/smartgrid/global/en/products-systems-solutions/Protection/distance-protection/Pages/7SA61.aspx

APPENDICIES

Appendix A: Matlab Program Used in Calculations

```
Rk =0.156;
r= 9.6*10^-3;
%distance between different conductors
d1a2a =sqrt(4^2+0.5^2);
d1a3a =4+4;
d3a3b =3+3;
d3a1b =sqrt(8^2+6^2);
d1a2b =sqrt(6.5^2+4^2);
d1a3b =sqrt(8^2+6^2);
d2a1b =sqrt(6.5^2+4^2);
d1a1b =3+3;
d2a3b =sqrt(6.5^2+4^2);
d3a2b =sqrt(6.5^2+4^2);
d2a3a =sqrt(0.5^2+4^2);
d2a2b =3.5+3.5;
dE1a =sqrt(3^2+3^2);
dE2a =sqrt(7^2+3.5^2);
dE3a =sqrt(11^2+3^2);
d=(d1a2a*d1a3a*d2a3a)^(1/3);
dp=(d1a1b*d2a2b*d3a3b)^(1/3);
dpp=(d1a2b*d1a3b*d2a3b)^(1/3);
dE=(dE1a*dE2a*dE3a)^(1/3);
% In the following calculations the notation NaLb (where a=1;2;0 and b=
% 1;2;3) refers to the value of N in the pozitive negative and ero
% sequence for different phases
%Impedance Matrix determination
R1g=0.0495;
k=0.809; % the correcting coefficient
a=-0.5+1i*sqrt(3)/2;
a2=-0.5-1i*sqrt(3)/2;
Dg=796.04;
Z1a1a=Rk+R1g+0.1445i*log10(Dg/(k*r));
Z2a2a=Z1a1a;
Z3a3a=Z1a1a;
Z1b1b=Z1a1a;
Z2b2b=Z1a1a;
Z3b3b=Z1a1a;
ZEE=Z1a1a;
Z1a2a=R1g+0.1445i*log10(Dg/d1a2a);
Z2a1a=Z1a2a;
Z1b2b=Z1a2a;
Z2b1b=Z1a2a;
Z2a3a=Z1a2a;
Z3a2a=Z1a2a;
Z2b3b=Z1a2a;
Z3b2b=Z1a2a;
Z1a3a=R1g+0.1445i*log10(Dg/d1a3a);
Z3a1a=Z1a3a;
Z1b3b=Z1a3a;
Z3b1b=Z1a3a;
Z1a1b=R1g+0.1445i*log10(Dg/d1a1b);
Z1b1a=Z1a1b;
Z3a3b=Z1a1b;
Z3b3a=Z1a1b;
Z2a2b=R1g+0.1445i*log10(Dg/d2a2b);
Z2b2a=Z2a2b;
```

```
Z1a2b=R1g+0.1445i*log10(Dg/d1a2b);
Z2b1a=Z1a2b;
Z1b2a=Z1a2b;
Z2a1b=Z1a2b;
Z2a3b=Z1a2b;
Z3b2a=Z1a2b;
Z2b3a=Z1a2b;
Z3a2b=Z1a2b;
Z1a3b=R1g+0.1445i*log10(Dg/d1a3b);
Z3b1a=Z1a3b;
Z1b3a=Z1a3b;
Z3a1b=Z1a3b;
ZE1a=R1g+0.1445i*log10(Dg/dE1a);
Z1aE=ZE1a;
ZE1b=ZE1a;
Z1bE=ZE1a;
ZE2a=R1g+0.1445i*log10(Dg/dE2a);
Z2aE=ZE2a;
ZE2b=ZE2a;
Z2bE=ZE2a;
ZE3a=R1g+0.1445i*log10(Dg/dE3a);
Z3aE=ZE3a;
ZE3b=ZE3a;
Z3bE=ZE3a;
%Impedance matrix
ImatE=[Z1a1a Z1a2a Z1a3a Z1a1b Z1a2b Z1a3b Z1aE;Z2a1a Z2a2a Z2a3a Z2a1b
    Z2a2b Z2a3b Z2aE;Z3a1a Z3a2a Z3a3a Z3a1b Z3a2b Z3a3b Z3aE;Z1b1a Z1b2a
    Z1b3a Z1b1b Z1b2b Z1b3b Z1bE;Z2b1a Z2b2a Z2b3a Z2b1b Z2b2b Z2b3b
    Z2bE;Z3b1a Z3b2a Z3b3a Z3b1b Z3b2b Z3b3b Z3bE;ZE1a ZE2a ZE3a
    ZE1b ZE2b ZE3b ZEE];
Imat=[Z1a1a Z1a2a Z1a3a Z1a1b Z1a2b Z1a3b;Z2a1a Z2a2a Z2a3a Z2a1b Z2a2b
    Z2a3b;Z3a1a Z3a2a Z3a3a Z3a1b Z3a2b Z3a3b;Z1b1a Z1b2a Z1b3a Z1b1b
    Z1b2b Z1b3b;Z2b1a Z2b2a Z2b3a Z2b1b Z2b2b Z2b3b;Z3b1a Z3b2a
    Z3b3a Z3b1b Z3b2b Z3b3b];
T=[1 1 1 0 0 0;1 -0.5-1i*sqrt(3)/2 -0.5+1i*sqrt(3)/2 0 0 0;
    1 -0.5+1i*sqrt(3)/2 -0.5-1i*sqrt(3)/2 0 0 0;0 0 0 1 1 1;
    0 0 0 1 -0.5-1i*sqrt(3)/2 -0.5+1i*sqrt(3)/2;0 0 0 1 -0.5+1i*sqrt(3)/2
    -0.5-1i*sqrt(3)/2];
Imat012=T\Imat*T;
Di=triu(Imat012);
Diag=tril(Di);
Mut=[Z1a1b Z1a2b Z1a3b;Z2a1b Z2a2b Z2a3b;Z3a1b Z3a2b Z3a3b];
TMut=[1 1 1;1 -0.5-1i*sqrt(3)/2 -0.5+1i*sqrt(3)/2;
    1 -0.5+1i*sqrt(3)/2 -0.5-1i*sqrt(3)/2];
Mut012=TMut\Mut*TMut;
%operating Impedance for each phase:
Ze1a1a =0.2022+0.5775i;
Ze2a2a =0.1984+0.6092i;
Ze3a3a =0.1967+0.6269i;
Ze1a2a =0.044+0.2019i;
Ze1a3a=0.0427+0.1693i;
Ze2a3a=0.0414+0.2261i;
Ze2a1a=Ze1a2a;
Ze3a1a=Ze1a3a;
Ze3a2a=Ze2a3a;
Z1L1= Ze1a1a+a2*Ze1a2a+a*Ze1a3a;
Z1L2= (Ze2a1a+a2*Ze2a2a+a*Ze2a3a)/a2;
Z1L3= (Ze3a1a+a2*Ze3a2a+a*Ze3a3a)/a;
Z1L1ne= Z1a1a+a2*Z1a2a+a*Z1a3a;
Z1L2ne= (Z2a1a+a2*Z2a2a+a*Z2a3a)/a2;
Z1L3ne= (Z3a1a+a2*Z3a2a+a*Z3a3a)/a;
%Modified Matrix Impedance:
```

```
Zaa=[Z1a1a Z1a2a Z1a3a;Z2a1a Z2a2a Z2a3a;Z3a1a Z3a2a Z3a3a];
Zab=[Z1a1b Z1a2b Z1a3b;Z2a1b Z2a2b Z2a3b;Z3a1b Z3a2b Z3a3b];
Zba=[Z1b1a Z1b2a Z1b3a;Z2b1a Z2b2a Z2b3a;Z3b1a Z3b2a Z3b3a];
Zbb=[Z1b1b Z1b2b Z1b3b;Z2b1b Z2b2b Z2b3b;Z3b1b Z3b2b Z3b3b];
ZaE=[Z1aE;Z2aE;Z3aE];
ZbE=[Z1bE;Z2bE;Z3bE];
ZEa=[ZE1a ZE2a ZE3a];
ZEb=[ZE1b ZE2b ZE3b];
ZaaM=Zaa-ZaE/ZEE*ZEa;
ZabM=Zab-ZaE/ZEE*ZEb;
ZbaM=Zba-ZbE/ZEE*ZEa;
ZbbM=Zbb-ZbE/ZEE*ZEb;
ZM=[ZaaM ZabM;ZbaM ZbbM];

%Modified impedance in symmetrical components
ZM012=T\ZM*T;
% Impedance matrix for transoised line
Zt1a1a=Rk+R1g+0.1445i*log10(Dg/(k*r));
Zt2a2a=Zt1a1a;
Zt3a3a=Zt1a1a;
Zt1b1b=Zt1a1a;
Zt2b2b=Zt1a1a;
Zt3b3b=Zt1a1a;
ZtEE=Zt1a1a;
Zt1a2a=R1g+0.1445i*log10(Dg/d);
Zt2a1a=Zt1a2a;
Zt1b2b=Zt1a2a;
Zt2b1b=Zt1a2a;
Zt2a3a=Zt1a2a;
Zt3a2a=Zt1a2a;
Zt2b3b=Zt1a2a;
Zt3b2b=Zt1a2a;
Zt1a3a=R1g+0.1445i*log10(Dg/d);
Zt3a1a=Zt1a3a;
Zt1b3b=Zt1a3a;
Zt3b1b=Zt1a3a;
Zt1a1b=R1g+0.1445i*log10(Dg/d);
Zt1b1a=Zt1a1b;
Zt3a3b=Zt1a1b;
Zt3b3a=Zt1a1b;
Zt2a2b=R1g+0.1445i*log10(Dg/d);
Zt2b2a=Zt2a2b;
Zt1a2b=R1g+0.1445i*log10(Dg/d);
Zt2b1a=Zt1a2b;
Zt1b2a=Zt1a2b;
Zt2a1b=Zt1a2b;
Zt3b2a=Zt1a2b;
Zt2b3a=Zt1a2b;
Zt3a2b=Zt1a2b;
Zt1a3b=R1g+0.1445i*log10(Dg/d);
Zt3b1a=Zt1a3b;
Zt1b3a=Zt1a3b;
Zt3a1b=Zt1a3b;
Zt2a3b=Zt1a3b;
ZtE1a=R1g+0.1445i*log10(Dg/dE);
Zt1aE=ZtE1a;
ZtE1b=ZtE1a;
Zt1bE=ZtE1a;
ZtE2a=R1g+0.1445i*log10(Dg/dE);
Zt2aE=ZtE2a;
ZtE2b=ZtE2a;
Zt2bE=ZtE2a;
```

```
ZtE3a=R1g+0.1445i*log10(Dg/dE);
Zt3aE=ZtE3a;
ZtE3b=ZtE3a;
Zt3bE=ZtE3a;
ImtransE=[Zt1a1a Zt1a2a Zt1a3a Zt1a1b Zt1a2b Zt1a3b Zt1aE;Zt2a1a
    Zt2a2a Zt2a3a Zt2a1b Zt2a2b Zt2a3b Zt2aE;Zt3a1a Zt3a2a Zt3a3a
    Zt3a1b Zt3a2b Zt3a3b Zt3aE;Zt1b1a Zt1b2a Zt1b3a Zt1b1b Zt1b2b
    Zt1b3b Zt1bE;Zt2b1a Zt2b2a Zt2b3a Zt2b1b Zt2b2b Zt2b3b Zt2bE;
    Zt3b1a Zt3b2a Zt3b3a Zt3b1b Zt3b2b Zt3b3b Zt3bE;ZtE1a ZtE2a
    ZtE3a ZtE1b ZtE2b ZtE3b ZtEE];
Imtrans=[Zt1a1a Zt1a2a Zt1a3a Zt1a1b Zt1a2b Zt1a3b;Zt2a1a Zt2a2a
    Zt2a3a Zt2a1b Zt2a2b Zt2a3b;Zt3a1a Zt3a2a Zt3a3a Zt3a1b Zt3a2b
    Zt3a3b;Zt1b1a Zt1b2a Zt1b3a Zt1b1b Zt1b2b Zt1b3b;Zt2b1a Zt2b2a
    Zt2b3a Zt2b1b Zt2b2b Zt2b3b;Zt3b1a Zt3b2a Zt3b3a Zt3b1b
    Zt3b2b Zt3b3b];
Imtrans012=T\Imtrans*T;
%Modified Matrix Impedance for transposed parallel line:
Ztaa=[Zt1a1a Zt1a2a Zt1a3a;Zt2a1a Zt2a2a Zt2a3a;Zt3a1a Zt3a2a Zt3a3a];
Ztab=[Zt1a1b Zt1a2b Zt1a3b;Zt2a1b Zt2a2b Zt2a3b;Zt3a1b Zt3a2b Zt3a3b];
Ztba=[Zt1b1a Zt1b2a Zt1b3a;Zt2b1a Zt2b2a Zt2b3a;Zt3b1a Zt3b2a Zt3b3a];
Ztbb=[Zt1b1b Zt1b2b Zt1b3b;Zt2b1b Zt2b2b Zt2b3b;Zt3b1b Zt3b2b Zt3b3b];
ZtaE=[Zt1aE;Zt2aE;Zt3aE];
ZtbE=[Zt1bE;Zt2bE;Zt3bE];
ZtEa=[ZtE1a ZtE2a ZtE3a];
ZtEb=[ZtE1b ZtE2b ZtE3b];
ZtaaM=Ztaa-ZtaE/ZtEE*ZtEa;
ZtabM=Ztab-ZtaE/ZtEE*ZtEb;
ZtbaM=Ztba-ZtbE/ZtEE*ZtEa;
ZtbbM=Ztbb-ZtbE/ZtEE*ZtEb;
ZtransM=[ZtaaM ZtabM;ZtbaM ZtbbM];
%Modified impedance in symmetrical components
ZtransM012=T\ZtransM*T;
Zop=Rk+1i*0.1445*log10(d*dpp/(k*r*dp));

%Average values

X0L1 = 1.0027;
R0L1=0.2846;
Z0L1 =R0L1+X0L1*1j;
Z0L2 =Z0L1;
Z0L3 =Z0L1;

Z0L1ne =0.3045+1.3588i;
Z0L2ne =Z0L1ne;
Z0L3ne =Z0L1ne;
Z1 =0.1564+0.4056i;
Z1ne= 0.156+0.4067i;

Z0M = 0.1286+0.5194i;
ZEL1 =(Z0L1-Z1L1)/3;
ZEL2 =(Z0L2-Z1L2)/3;
ZEL3 =(Z0L3-Z1L3)/3;
ZEL1ne =(Z0L1ne-Z1L1ne)/3;
ZEL2ne =(Z0L2ne-Z1L2ne)/3;
ZEL3ne =(Z0L3ne-Z1L3ne)/3;
%Measurement Error with no consideration of mutual coupling effect
X1L1= imag(Z1L1);
X1L2=imag(Z1L2);
X1L3=imag(Z1L3);
X1av =(X1L1+X1L2+X1L3)/3;
E1= 100*(X1L1-X1av)/X1av;
```

```
E2= 100*(X1L2-X1av)/X1av;
E3= 100*(X1L3-X1av)/X1av;
%The error due to the mutual coupling effect

%Error due to the mutual coupling while considering the earth wire
%For phase1

l=40; % assumed length of the protected line segment
x =0:2:l;
q= x/l;
Z1L1t= Z1L1*l;
P1= Z0M/(3*Z1L1);
Q1= 1+(ZEL1/Z1L1);
K1=P1/Q1;
ZD1L1=x*Z1L1*(1+K1*x/(2*l-x));
EL1= 100*(ZD1L1-q*Z1L1t)/Z1L1t;
plot(q,EL1);
% For phase 2

Z1L2t= Z1L2*l;
P2= Z0M/(3*Z1L2);
Q2= 1+(ZEL2/Z1L2);
K2= P2/Q2;
ZD1L2=x*Z1L2*(1+K2*x/(2*l-x));
EL2= 100*(ZD1L2-q*Z1L2t)/Z1L2t;
plot(q,EL2);
% For phase 3

Z1L3t= Z1L3*l;
P3= Z0M/(3*Z1L3);
Q3= 1+(ZEL3/Z1L3);
K3 =P3/Q3;
ZD1L3=x*Z1L3*(1+K3*x/(2*l-x));
EL3= 100*(ZD1L3-q*Z1L3t)/Z1L3t;
plot(q,EL3);
%Error due to the mutual coupling while considering the earth wire
%For phase1
Z0Mne = 0.1485+0.8755i;
P1ne= Z0Mne/(3*Z1L1ne);
Q1ne= 1+(ZEL1ne/Z1L1ne);
K1ne = P1ne/Q1ne;
ZD1L1ne=x*Z1L1ne*(1+K1ne*x/(2*l-x));
Z1L1net=Z1L1ne*l;
EL1ne= 100*(ZD1L1-q*Z1L1net)/Z1L1net;
plot(q,EL1ne)
% For phase 2
P2ne= Z0Mne/(3*Z1L2ne);
Q2ne= 1+(ZEL2ne/Z1L2ne);
K2ne = P2ne/Q2ne;
ZD1L2ne=x*Z1L2ne*(1+K2ne*x/(2*l-x));
Z1L2net=Z1L2ne*l;
EL2ne= 100*(ZD1L2ne-q*Z1L2net)/Z1L2net;
plot(q,EL2ne);
% For phase 3
P3ne= Z0Mne/(3*Z1L3ne);
Q3ne= 1+(ZEL3ne/Z1L3ne);
K3ne = P3ne/Q3ne;
ZD1L3ne=q*Z1L3ne*(1+K3ne*x/(2*l-x));
Z1L3net=Z1L3ne*l;
EL3ne= 100*(ZD1L3ne-q*Z1L3net)/Z1L3net;
plot(q,EL3ne);
```

```
% Error range in transposed line
    %For line with earth-wire
Z0t= 0.2846+1.0027i;
Z1t = 0.156+0.4067i;
Z0Mt = 0.1286+0.596i;
ZEt =(Z0t-Z1t)/3;
KEMt= Z0Mt/(3*Z1t);
KEt=ZEt/Z1t;
Qt= 1+KEt;
Kt = KEMt/Qt;
ZD1t=q*Z1t*(1+Kt*x/(2*l-x));
Z1tt=Z1t*l;
Et= 100*(ZD1t-q*Z1tt)/Z1tt;
plot(q,Et);
    %For line with no earth-wire
Z0tne= 0.3545+1.3588i;
Z1tne = 0.156+0.4067i;
Z0Mtne = 0.1485+0.9521i;
ZEtne =(Z0tne-Z1tne)/3;
KEMtne= Z0Mtne/(3*Z1tne);
KEtne = ZEtne/Z1tne;
Qtne= 1+KEtne;
Ktne = KEMtne/Qtne;
ZD1tne=q*Z1tne*(1+Ktne*x/(2*l-x));
Z1tnet=Z1tne*l;
Etne= 100*(ZD1tne-q*Z1tnet)/Z1tnet;
plot(q,Etne);
% Consideration of mutual impedance in postive and negative sequence for
% the non-transpose line with the ground wire.
% Phase one
Zm = 0.0163i;
Ze1 = (Z0L1-Z1L1-Zm)/3;
KeM1 = Z0M/(3*(Z1L1+Zm));
Ke1 = Ze1/(Z1L1+Zm);
Qm1 =1+Ke1;
Km1 =KeM1/Qm1;
ZD1m1 = q*(Z1L1+Zm)*(1+Km1*x/(2*l-x));
E1m1 = 100*(ZD1m1-q*Z1L1t)/Z1L1t;

%Phase two
Ze2 = (Z0L2-Z1L2-Zm)/3;
KeM2 = Z0M/(3*(Z1L2+Zm));
Ke2 = Ze2/(Z1L2+Zm);
Qm2 =1+Ke2;
Km2 =KeM2/Qm2;
ZD1m2 = q*(Z1L2+Zm)*(1+Km2*x/(2*l-x));
E1m2 = 100*(ZD1m2-q*Z1L2t)/Z1L2t;
% Phase three
Ze3 = (Z0L3-Z1L3-Zm)/3;
KeM3 = Z0M/(3*(Z1L3+Zm));
Ke3 = Ze3/(Z1L3+Zm);
Qm3 =1+Ke3;
Km3 =KeM3/Qm3;
ZD1m3 = q*(Z1L3+Zm)*(1+Km3*x/(2*l-x));
E1m3 = 100*(ZD1m3-q*Z1L3t)/Z1L3t;
% Consideration of mutual impedance in postive and negative sequence for
% the non-transpose line without the ground wire.
% Phase one
Zmne = 0.0175i;
Ze1ne = (Z0L1ne-Z1L1ne-Zmne)/3;
KeM1ne = Z0Mne/(3*(Z1L1ne+Zmne));
```

```
Ke1ne = Ze1ne/(Z1L1ne+Zmne);
Qm1ne =1+Ke1ne;
Km1ne =KeM1ne/Qm1ne;
ZD1m1ne = q*(Z1L1ne+Zmne)*(1+Km1ne*x/(2*l-x));
E1m1ne = 100*(ZD1m1ne-q*Z1L1net)/Z1L1net;

%Phase two
Ze2ne = (Z0L2ne-Z1L2ne-Zmne)/3;
KeM2ne = Z0Mne/(3*(Z1L2ne+Zmne));
Ke2ne = Ze2ne/(Z1L2ne+Zmne);
Qm2ne =1+Ke2ne;
Km2ne =KeM2ne/Qm2ne;
ZD1m2ne = q*(Z1L2ne+Zmne)*(1+Km2ne*x/(2*l-x));
E1m2ne = 100*(ZD1m2ne-q*Z1L2net)/Z1L2net;
% Phase three
Ze3ne = (Z0L3ne-Z1L3ne-Zmne)/3;
KeM3ne = Z0Mne/(3*(Z1L3ne+Zmne));
Ke3ne = Ze3ne/(Z1L3ne+Zmne);
Qm3ne =1+Ke3ne;
Km3ne =KeM3ne/Qm3ne;
ZD1m3ne = q*(Z1L3ne+Zmne)*(1+Km3ne*x/(2*l-x));
E1m3ne = 100*(ZD1m3ne-q*Z1L3net)/Z1L3net;
```

Appendix B: Mounting the DP 7SA610

Housing for Panel Flush or Cubicle Mounting

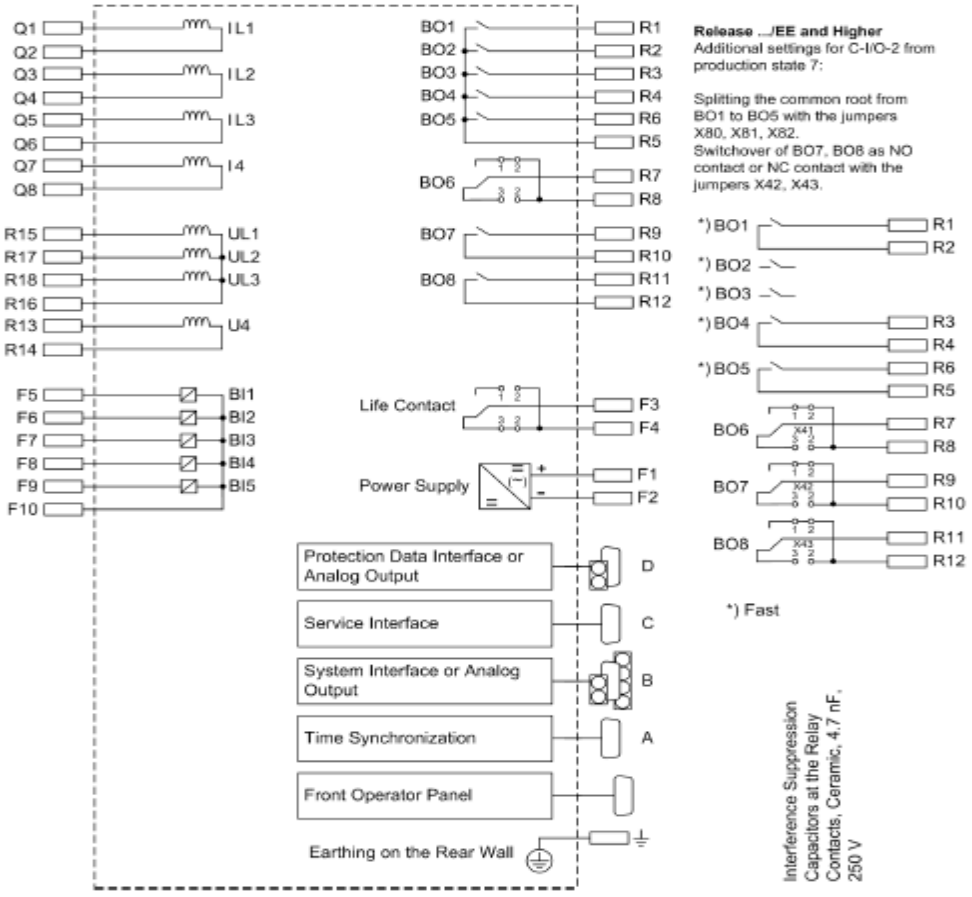

*Fig.B.1 General diagram 7SA610*_*A/J*

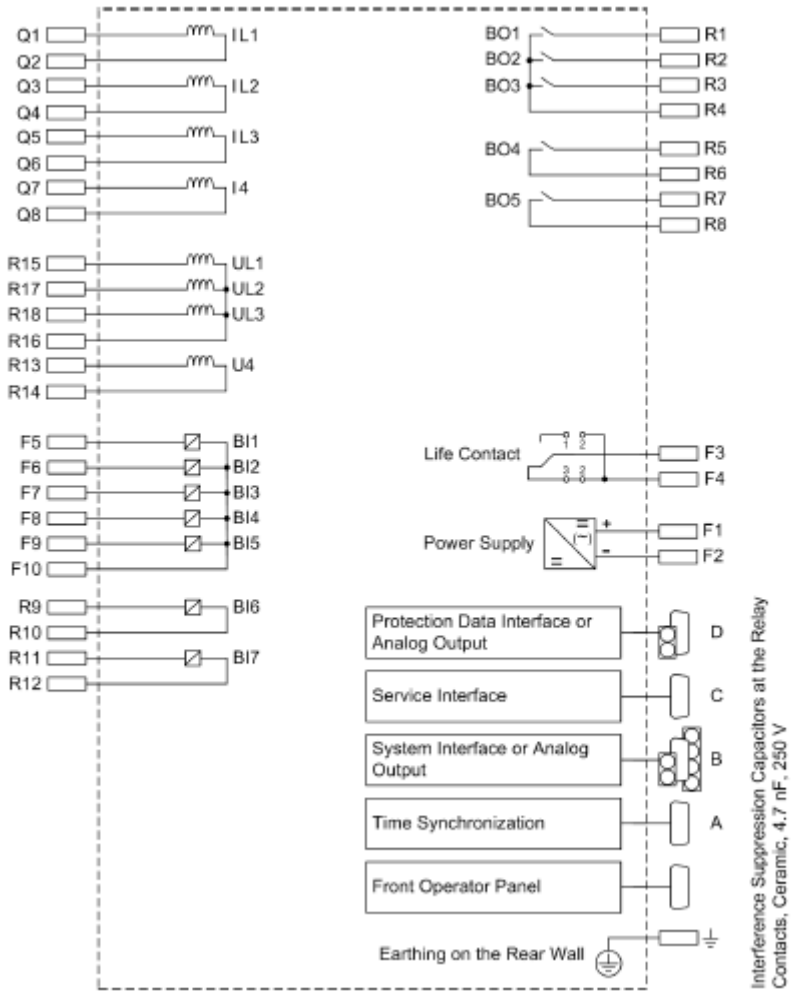

*Fig.B.2 General diagram 7SA610*_*B/K*